

UNIVERSITÁ' DEGLI STUDI DI NAPOLI "FEDERICO II"

FACOLTÀ DI INGEGNERIA

Dipartimento di Ingegneria dei Materiali e della Produzione



**DOTTORATO DI RICERCA IN INGEGNERIA DEI
MATERIALI E DELLE STRUTTURE**

XXIII CICLO

**Study of annealing and orientation effects on
physical properties of PLA based
nanocomposite films**

Scientific committee
Ch.mo Prof. Domenico Acierno
Dott. Pietro Russo

PhD student
Ing. Sara Cammarano

Triennio 2007-2010

Index

Summary	7
Bibliography	10
 Chapter 1 – <i>Introduction</i>	 12
1. Polymer	13
2. Composite	13
3. Nanocomposite	14
3.1 Nanocomposites preparation	16
3.2 Processing conditions effects	18
4. Biodegradable and compostable polymers	20
5. Packaging	23
Bibliography	25
 Chapter 2 – <i>Materials</i>	 28
1. Lactic acid	29
2. Lactic Acid Polymer (PLAS)	31
3. Technology of production of PLAs	32
3.1. Direct Polycondensation (PC)	33
3.2. Ring opening polymerization (ROP)	34
4. Clay and clay minerals	37
4.1. Clay minerals	38
4.2. Sepiolite	43
4.3. Halloysite	44
Bibliography	46

Chapter 3- <i>Properties of PLA-clay annealed nanocomposites: a study on sepiolite and halloysite</i>	48
1. Introduction	49
2. Materials	50
2.1 PLA	50
2.2 Sepiolite	50
2.3 Halloysite	50
3. Experimental Details	50
3.1 Extrusion	50
3.2 Compression moulding	51
3.3 Annealing	52
4. Characterization	52
4.1 SEM	52
4.2 Thermal test	53
4.3 WVTR	53
4.4 Absorption test	54
4.5 Tensile test	54
5. Results and discussion	55
6. Conclusions	72
Bibliography	73
 Chapter 4 - <i>Study on PLA-zeolite and PLA-bentonite composites</i>	 76
1. Materials	77
1.1 PLA2002D	77
1.2 Zeolite	77

1.3 Bentonite	77
2. Preparation and characterization	78
3. Results and discussion	79
4. Conclusion	87
Bibliography	88
 Chapter 5 - <i>PLA-clay oriented film</i>	 90
1. Introduction	91
2. Materials	92
2.1 PLA	92
2.2 Sepiolite	92
2.3 Halloysite	93
3. Method	93
3.1 Preparation of master-batch at 15% of clay	93
3.2 Preparation of PLA-clay composites	93
3.3 Preparation of films	94
3.4 Orientation	94
4. Characterization	94
4.1 Thermal tests	94
4.2 Absorption test	95
4.3 SEM	96
4.4 Birefringence	96

4.5 Tensile tests	96
5. Results and discussion	97
6. Conclusions	107
Bibliography	108
Chapter 6 - <i>Preliminary study of effect of temperature and draw ratio on PLA based film's crystallinity</i>	109
1. Introduction	110
2. Preparation method	111
2.1. Extrusion Conditions	111
2.2. Flat-Film Take-Off Unit CR 72T using conditions	111
2.3. Stretching conditions	111
3. Characterization: Thermal tests	111
4. Comments	114
5. Conclusions	116
Bibliography	116
Chapter 7 - <i>Physical properties of PLA blown films containing halloysite nanotubes</i>	117
1. Materials	118
2. Preparation of PLA/HNT composites	118
3. Characterization	119
3.1 TGA, DSC	119
3.2 Mechanical tests	119

3.3 Rheological Analysis	120
4. Results	120
5. Conclusion	126
Bibliography	127
Chapter 8 - <i>Conclusions</i>	128
Appendix 1 – Instruments description	133

Summary

The aim of this PhD thesis was the production of a compostable material that can be used in food packaging application. Basically, the reasons that induced us to focus our attention on this subject were considerations concerning the impact of plastics on environment.

Research into plastics accelerated during World War II to meet the demand for strong and lightweight materials for military purposes: during that period annual volume of produced plastics tripled. Since the rise of polymeric materials over the second half of 19th century, scientists and researcher focused their attention on the production of plastics more easily processable, cheaper, with improved properties, trying to make the most of polymer very high potential and versatility. The discovery of new technologies, specifically the production of polymer-clay nanocomposites (PCN) by Toyota researchers, more than twenty years ago, was an epoch-making event: since then the number of publications on PCN has rapidly increased thanks to the exceptional opportunity opened by this new field. In PCN only a few wt.-% of silicate is randomly and homogeneously dispersed in the polymer matrix leading to superior properties compared to pristine polymers: tensile strength, tensile modulus, heat distortion temperature and gas barrier property can result strongly modified.

There are, however, environmental issues associated with the production and disposal of plastics: over 200 million tons of plastic are manufactured annually around the world, according to the Society of Plastic Engineers. The huge amount of disposable product available nowadays has the disadvantage of increasing waste because of the improper disposal of these goods by consumers. One of the biggest problems in plastics recycling goals is that conventional plastics are often commingled with organic wastes making it difficult and impractical to recycle the underlying polymer without expensive cleaning and sanitizing procedures. If even a small amount of conventional plastics were to be commingling with organic materials, the entire batch of organic waste is "contaminated" with small bits of plastic that spoil prime-quality compost humus. Composting of mixed organics is a potential strategy for recovering large quantities of waste and it dramatically

increases community recycling goals. Compostable plastics can replace the non-degradable one, making composting a significant tool to divert large amounts of otherwise non recoverable waste from landfills.

Compostable plastics combine the utility of plastics with the ability to completely biodegrade in a compost facility without separating them from organic wastes, enabling composting of a much larger amount of solid waste.

Among this investigation the production of a compostable material usable in food packaging application, an eco-friendly nanocomposite has been investigated. The selected matrix was Polylactic acid (PLA). This polymer, an aliphatic, thermoplastic and biodegradable polyester, produced by processes of fermentation and distillation from starch, mainly corn [1-10], can be easily processed with standard equipment to produce films, fibers or thermoformed containers and it is recognized as GRAS (GRAS, Generally Recognized as Safe), making it particularly suitable for food packaging application. Some PLA properties like flexural properties, heat distortion temperature, impact factor, gas permeability need to be improved.

The effect of degree of crystallinity on mechanical and barrier properties is reported to be strong as a consequence of the crystallites ability to act as points of reinforcement, constraining the amorphous regions domains.

In this study addition of clay, annealing and unidirectional stretching techniques were applied to change PLA crystallinity with the aim of improving its properties.

Introduction of nano-sized clays is widely reported to be an efficient way of improving polymer matrix properties: relatively low amounts (less than 5 wt.-%) of clays, randomly and homogeneously dispersed in the polymer matrix, can improve tensile strength, stiffness, heat distortion temperature and gas barrier properties of the hosting matrix. The filler dispersion can be strongly affected by the type of clay, their pre-treatment and the way in which the polymer the compounding occurs. The nature of polymer-clay interface plays a very important role in the properties of polymer nanocomposites. Being naturally occurring clays generally highly hydrophilic species, they are naturally incompatible with a wide range of polymer types. A huge amount of investigations regards use of organo-modified clays. In this study natural occurring not modified clays characterized by different topologies were used to produce a completely natural material with the aim of giving back to the nature what it gave us. Sepiolite, halloysite, zeolite and bentonite clays were used to

reinforce PLA matrix. The obtained composites underwent annealing treatment or unidirectional orientation.

Stress-induced crystallization, thanks to a wide processing window, has reported to have led to good results. PLA can be oriented during processing like fiber spinning or film stretching in the melted or rubber state, thanks to its semi-crystalline nature. In this study sepiolite and halloysite clay were used to produce nanocomposites that were oriented using solid state unidirectional deformation technique, because fibrous filler have been reported to be more effective to reinforce unidirectional composites [11] and are also suggested to be possible orientation enhancers [12]. Moreover, use of sepiolite or halloysite in this kind of application can be of high interest because of their one dimensional-like shape that, after the applications of uniaxial deformation, can lead to alignment of clay along the polymer direction.

Being amorphous polymers not in thermodynamic equilibrium, annealing above T_g of PLA is reported to be an efficient treatment to increase modulus, tensile strength and to reduce gas permeability, as a consequence of the reduced free volume and increased crystallinity of the polymer. Moreover, addition of clay is reported to lead to higher crystallinity and stiffness enhancement after annealing [13].

Bibliography

- [1] Holten, C.H., Lactic Acid, Properties and Chemistry of Lactic Acid and Derivatives, Verlag Chemie, GmbH, Weinheim/Bergstr., 1971.
- [2] Schopmeyer, H.H., Lactic Acid, in Industrial Fermentations, Underkofler, L. And Hickley, R.J., Eds., Chemical Publishing Co. New York, NY, 1954, chap. 12.
- [3] Cox, G. and Macbean, R., Lactic Acid Recovery and Purification Systems, Research Project Series, No. 29, October, 1976.
- [4] Urayama, H., Kanamori, T., and Kimura, Y., Properties and biodegradability of polymer blends of poly(L-lactides) with different optical purity of the lactate units, *Macromole. Mater. Eng.* 287, 116, 2002.
- [5] Janzen, J., Dorgan, J.R., Knauss, D.M., Hait, S.B., and Limoges, B.R., Fundamental solution and single-chain properties of polylactides, *Macromolecules*, 2003.
- [6] Ikada, Y., Jamshidi, K., Tsuji, H., and Hyon, S.H., Stereocomplex formation between enantiomeric poly(lactides), *Macromolecules* 20, 904, 1987.
- [7] Tsuji, H. and Ikada, Y., Stereocomplex formation between enantiomeric poly(lactic acid)s. XI. Mechanical properties and morphology, *Polymer*, 40, 6699, 1999.
- [8] Tsuji, H. and Ikada, Y., Properties and morphologies of poly(L-lactide): 1. Annealing condition effects on properties and morphologies of poly(L-lactide), *Polymer*, 36, 2709, 1995.
- [9] Fischer, E.W., Sterzel, H.J., and Wegner, G., Investigation of the structure of solution grown crystals of lactide copolymers by means of chemical reactions., *Kolloid Ze. Ze. fuer Polym.*, 251, 980, 1973.
- [10] Kolstad, J.J., Crystallization kinetics of poly(L-lactide-co-meso-lactide, *J. Appl. Polym. Sci.*, 62, 1079, 1996.
- [11] M. Van Es, Polymer-Clay nanocomposites-the importance of particle dimensions, PhD Thesis TU Delft 2001.
- [12] Bilotti E, Deng H, Zhang R, Lu D, Bras W, Fischer H R, Peijs T. Synergistic Reinforcement of Highly Oriented Poly(propylene) Tapes by Sepiolite Nanoclay *Macromol. Mater. Eng.* 2010, 295, 37–47

[13] Long Yu, Hongshen Liu, Fengwei Xie, Ling Chen, Xiaoxi Li .Effect of annealing and orientation on microstructures and mechanical properties of polylactic acid. Polymer Engineering and Science , April, 2008

Chapter 1

Introduction

1 Polymer

Since the rise of polymeric materials over the second half of 19th century, scientists and researcher focused their attention on the production of plastics more easily processable, cheaper and with improved properties.

Polymers have peculiar properties due to their macromolecular nature. Polymeric chains structure, in terms of repetitive unit, molecular mass and interaction between them, determine chemical and physical properties of polymer. Every chemical or physical action changing molecular weight or chemical structure can lead to polymer performances modifications.

Polymer properties can be improved using different techniques. For example, orientation of polymeric chains as well as fillers introduction are reported to strongly improve flame retardancy, thermal, mechanical and permeability properties [1,2].

2 Composites

Composites are defined as multiphase systems consisting of at least two different phases distinguished as a continuous and a dispersed one [3]. The matrix keeps the reinforcement in a set place and it also protects the reinforcement, while the filler is stronger and stiffer, forming a sort of backbone and imparting its special mechanical and physical properties to enhance matrix ones.

It is possible to distinguish two general categories of composites:

- 1) materials made up of a continuous matrix including one or more dispersed phase made up of discrete particles,
- 2) systems made up of one or more continuous phases forming interpenetrating network.

3 Nanocomposites

Nanocomposites are composite materials containing fillers with at least one dimension on the nano scale. In contrast with micro-composites, where the reinforcements have dimensions in the order of micron, nanocomposite properties enhancement is obtained adding smaller amount of filler, enabling easier processability. Advantages deriving from nanocomposites' use may include decreased gas permeability [4-5] and flammability [6], increased strength and heat resistance [7], high modulus [8-9], and increased biodegradability of biodegradable polymers [10]. According to Vaia and Wagner [11] nanocomposites production must balance 4 independent aspects: constituents' selection, fabrication, performance and cost.

Three types of fillers can be defined according to their dimensions:

- 1) three dimensional (isometric) nanoparticles, all dimensions are in the order of nanometres,
- 2) two dimensional nanoparticles (nanotubes or whiskers) ,
- 3) one dimensional (sheet-like) nanoparticles, only one dimension is in the order of nanometres.

Layered silicates are the most used filler since the study published by the Toyota Central Research Laboratories [12-13]. Polymer –layered silicate composites show superior physical and mechanical properties when compared with unfilled matrix. Mechanical properties are further improved if layered silicates are dispersed into polymeric matrix individually. Ray and Okamoto (2003) proposed that nanocomposites increase barrier properties by creating a tortuous path that retards the progress of the gas molecules through the matrix. Clay dispersion at a nanometric level into polymeric matrix increases interfacial surface enabling forces transfer from matrix to reinforcements, improving mechanical properties like young modulus and tenacity [14-20]. Anyway some drawbacks may come from nanofiller addition such as more complex rheological behaviour and an increased opacity.

Depending on components nature and preparation method, PLSN can be classified as [14-21]:

- a) phase separated: having properties comparable with those of conventional composites [22];
- b) Intercalated structures: polymer chain is hosted into silicate's layers in a well ordered multilayer system with alternating polymer/inorganic host layers. Although the space between phyllosilicate layers increases, the order of the structure is maintained;
- c) Exfoliated structures: silicate layers are delaminated and dispersed in a continuous polymer matrix. Insertion of the polymeric chains increases the distance between the sheets of silicates until there is no more interaction between the layers and the order breaks [23].

Intercalate composites are limited miscibility system, while delaminated are complete miscibility systems. Generally a PLSC is partially intercalated and partially exfoliated. The structures obtained depend on the nature and the miscibility of the compounds (matrix and reinforcement).

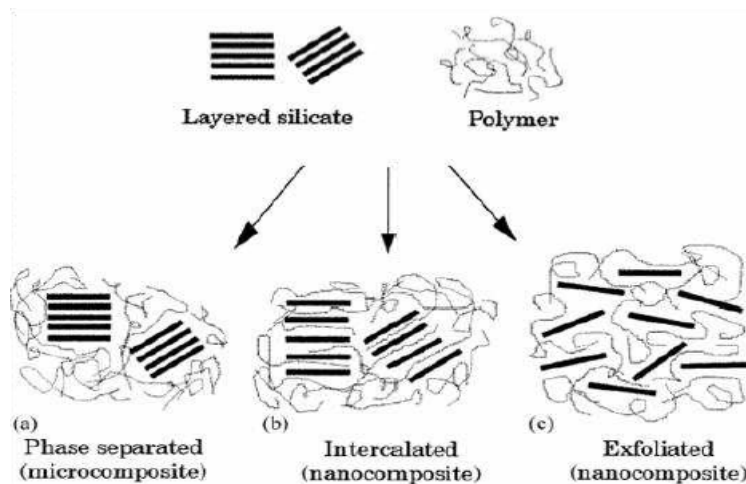


Fig. 1: Scheme of different types of composite arising from the interaction of layered silicates and polymers: (a) phase separated micro composite; (b) intercalated nanocomposite and (c) exfoliated nanocomposite [22]

Exfoliated systems are reported to be more efficient in improving mechanical properties than intercalated structures [24].

When the filler is dispersed at nanometric level into the matrix, nanocomposites show their unique properties thanks to the good interaction between polymer and layered silicate [25].

Interaction of clay into polymer is not a favourite reaction: mixing monomer or polymer with hydrophilic silicate often leads to aggregation. In this case composites are referred as tactoid nanocomposite structure [26].

Organo-modification of clays improves their dispersion into the polymer [27-32] by changing clay's surface behaviour from hydrophilic to hydrophobic and increasing the basal spacing of the layers.

3.1 Nanocomposites preparation

There are several technologies that can be used to prepare nanocomposites. These include in situ polymerization, solution processing and melt compounding. Detailed description of each method are reported in the paragraphs below, with more emphasis on melt compounding, which is the method used in this thesis [16-20]

- a) In-situ polymerization: involves insertion of a suitable monomer between silicate sheets followed by polymerization. Phyllosilicates and monomers are mixed to let the monomer enter into clay's layers, than polymerization reaction is promoted, allowing polymer to grow into clay's galleries. Monomer's polarity is used to intercalate the monomer into the clay. It is the monomer itself to increase the distance between silicate layers: the polymerization of the monomers among the plates of clay separates their layers. During the mixing step, the monomers spread in between the sheets of the clay and they are attracted for the high polarity of the surfaces of clay platelets. Then, the polymerization begins using heating, radiation, catalyst or organic initiator.

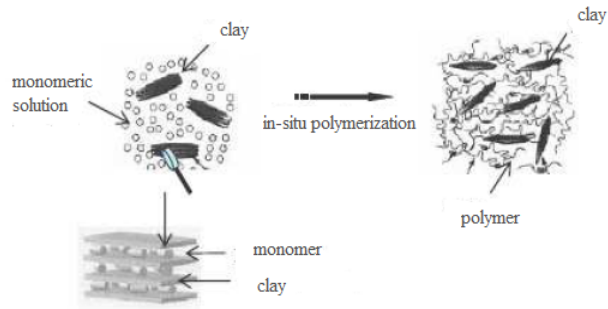


Fig. 2: polymerization in situ [22]

b) Intercalation from solution. Solution processing is based on a solvent system in which the nanoclay is dispersed to form a homogeneous suspension than the polymer is added. In this way, the polymer is exchanged with the solvent previously intercalated. It is necessary to choose a solvent able to solubilise both clay and polymer. When the two solutions are mixed, than solvent evaporate or precipitate adding non miscible solvent enabling layers to be reunited entangling polymer into them and forming an ordered structure. Being forces that take the silicate sheet together weak, it can be exfoliated into single layers using a solvent able to solubilise both polymer and clay.

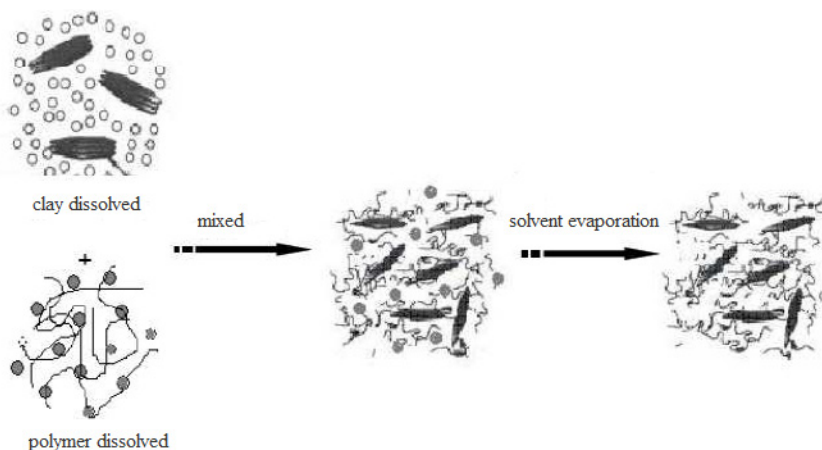


Fig. 3: Solution processing [22]

- c) Melt compounding: in this process clays and polymer are mixed in molten condition. Once the polymer is heated up to T_g , clay is dispersed in it; then clay and polymer are mixed at melt state. If the surface of the clay is enough compatible with the polymer, this one can interfere inside the spaces among the plates of clay and form nanocomposites exfoliated and intercalated. This process is of great interest for the industry because it is possible to use it with conventional technologies as extrusion, which is a cheap and rapid technology. Furthermore the use of harsh organic solvents is not necessary reducing environmental impact and economic cost. In this thesis the nanocomposites have been obtained using this method.

Giannellis et al. demonstrated that it is possible to obtain intercalation of polymeric chains into organo-modified clay by melt blending at temperatures higher than T_g or melting temperature of the hosting matrix. Direct intercalation from melt can be easier using stress shear into a mixing machine. It has been reported that the level of dispersion that can be reached processing polymer and organo-modified clay into an extruder is better than the one obtained without using shear devices (extruder, mixer, ultrasonicator).

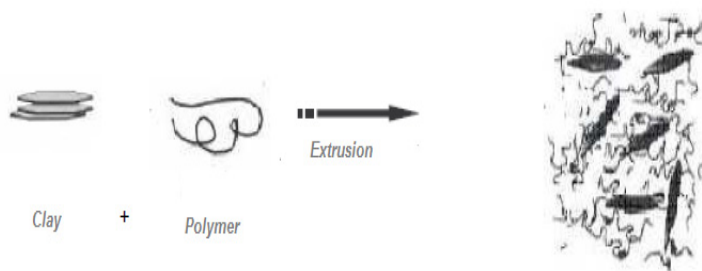


Fig. 4: Melt compounding [22]

3.2 Processing conditions effects

Different **shear devices** (4 roll mill, mixer batch, and extruder) have been studied to define more efficient mixing geometry and optimal flow during exfoliation process. [1, 2, 32] The most efficient way is reported to be double screws extruder, thanks to the superior shear level that can be reached in this dispositive [2, 32]

Residence time and screws geometry have been studied by Paul et al. [32] for nylon 6 reinforced with organo-clays by changing screw lengths, geometry (intermeshing, non intermeshing, different design) and their mutual rotation. The increase of the residence time is reported to positively affect dispersion and delamination. The same effect is achieved by varying the level of the applied shear, but for it is possible to determine the level up to which the dispersion decreases.

Stress shear transmitted to silicate from polymeric chains is directly linked to matrix viscosity. In a recent study [33] three different molecular weights of nylon 6 were processed under the same melt compounding conditions. Structural analysis showed that a mix structure, intercalated and with cluster, is reached for samples that have lower molecular weight; while for higher molecular a completely exfoliated structure is obtained, confirming the importance of this parameter.

Chemist. Three different cases are possible: good compatibility, marginal compatibility and not compatibility. In the first case, the process is completely based on chemistry: it is possible to reach good dispersion with a slight dependence on processing conditions. In the case of marginal compatibility it is possible to reach good dispersion and exfoliation optimizing process conditions. In the case in which there is not compatibility between polymeric matrix and clay the process can be optimized to minimize dimensions of dispersed tactoid, but it is not possible to exfoliate completely the silicate. In this case, it is important to organo-modify clays to make them compatible with matrix using a compatibilizer that must satisfy two requests: 1) being miscible with the matrix 2) having polar functional groups that make it suitable for being intercalated into silicate layers forming hydrogen bond with oxygens present on layers surface.

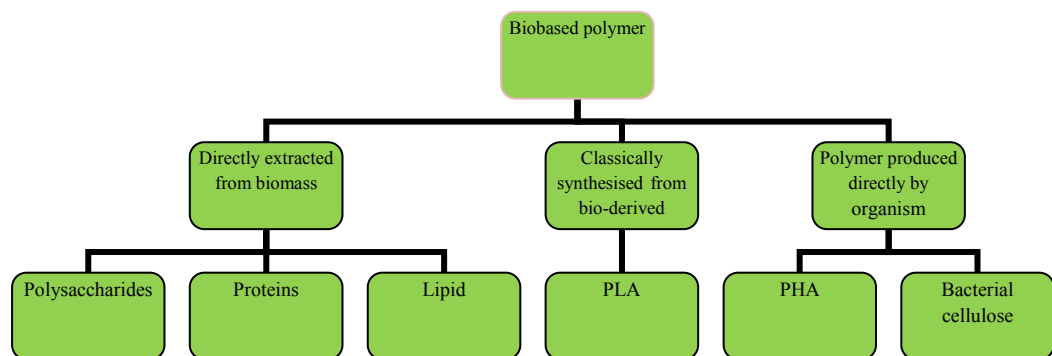
Effect of **organo treatment** on silicate: in absence of good affinity between polymer and silicate, exfoliation is not reported to be reached independently from shear level realized under processing [33-35]. The organic treatment is also reported to be important being effective in reducing cohesion forces, making easier intercalation during process

4 Biodegradable and compostable polymers

According to EN 13432 biopolymers are defined as biodegradable polymers or polymers based on renewable resources.

Polymers from renewable resources (biopolymer) can be classified in 3 categories [36]:

- 1) polymer from natural material (e.g. starch) directly extracted from biomass
- 2) polymer classically synthesised from bio-derived monomer (e.g. PLA)
- 3) polymer produced from genetically modified microorganism or bacteria (e.g. PHBV)



Re-adapted from Van Tuil et al, 2000 [37]

Biodegradable materials are materials that, under the actions of microorganisms, can be converted only in carbon dioxide and water in the environment.

Biodegradation is an enzymatic degradation process. Enzyme speed in transforming a material depends on polymer structure (molecular weight can significantly influence degradation speed); functional group (they can make polymer more or less hydrophilic, making it easier attackable); ramification (it is more difficult to degrade), reticulation (that reducing polymer mobility makes more difficult enzymes introduction into the polymer); surface characteristic (smooth surface are easier attackable by enzymes).

Among the external factors that can influence biodegradability:

Water: bacteria and fungi need humidity to grow

Temperature: generally fungi need temperature in the range of 20/28°C while bacteria in the range of 28/37°C

pH: each organism needs specific pH (acid for fungi, basic for bacteria)

Oxygen: fungi are generally aerobic; while bacteria can be both aerobic and anaerobic

According to the model proposed for plastic material biodegradation, hydrophilic extra cellular enzymes pass from microbial cell to plastic, disaggregating its macromolecule and reducing its dimension in a way to start the endocytosis (mechanism through which the cell is enabled to encompass its cytoplasm). This theory enables to explain the reason because of which plastics, that are generally hydrophobic, are difficult to be biodegraded.

There are three main ways to dispose of waste plastic:

- 1) landfill;
- 2) incineration (burning);
- 3) recycling

Landfill is a convenient method of waste disposal, but it is designed to bury, not to break down rubber. Most plastic cannot be decomposed by micro organism: they will remain buried for thousands of years without rotting.

Incineration is a waste treatment that involves the combustion of organic substances contained in waste materials [38]. The waste is converted into ash (formed by inorganic constituents that can take the form of solid lumps or particulates), flue gas and heat (usable for producing electric power). This waste disposal technique can be dangerous if hazardous materials are not removed before incineration.

Recycling involves processing used material into new products to prevent waste, reduce the consumption of fresh raw materials, and reduce energy usage and air pollution that can be caused from other waste disposal systems such as incineration [39, 40].

Biologic wastes treatment leads to different product:

- 1) Compost if the treatment is aerobic
- 2) Bio-methanation if the treatment is anaerobic

Composting leads to the formation of carbon dioxide, water and compost for agricultural uses; while biomethanation produces biogas (methane and carbon dioxide) and mud, that are later transformed into compost.

Composting can be considered as a recycling technique because the original product is transform into a new usable one (compost) and it is a convenient way to waste disposal especially where landfill sites are limited. Via composting it is possible to let the carbon dioxide, that has been harnessed during corn growing [41], flow back into the atmosphere, closing the carbon dioxide cycle [41].

According to EN13432 a material is compostable if its components are individually compostable. This definition allows to analyze materials components, instead of materials themselves, reducing number of tests.

According to CE n. 62/94 a material is defined as compostable if it is biodegradable; disintegrable; if it has low level of heavy metal; no negative effect on final compost and on compostability process.

Disintegrability and loss of visibility in the final compost means that when samples of the polymer are composted for 3 months with organic waste, mass of material residue must be less than 10%initial one and with dimension lower than 2mm.

5 Packaging

Packaging is defined as a coordinated system of preparing goods for transport, sale and end use. Packaging functions are to contain, protect, preserve, transport, inform and sell [42].

Depending on the level of contact between packaging and product, packaging can be classified as:

- 1) primary: in direct contact with product; it must chemically and physically preserve from environmental factors that can lead to degradation, alteration (humidity, aroma) or loss of quality;
- 2) secondary: used to group together primary packaging and to transmit information to the costumers; it must mechanically protect during transport and storing, give information to the costumer about storage condition, product quality and use (many types of symbols for pack labelling are nationally or internationally standardized, making easy to understand how to handle , store and use the product);
- 3) tertiary: allows an easier shipping of the stuff during transport and handling

Food packaging main function is to protect products against deterioration, to contain the product, to give information to the consumer [43]. The quality of packaged food is directly and strongly dependent on food and packaging material characteristic [44]; as a consequence the choice of packaging materials is very important. Materials used in food packaging are glass, metal, paper and plastic [45]. Properties of plastic make them highly suitable for food packaging [46].

It is possible to classify food packaging materials according to their function:

- 1) Passive food packaging materials: their function is to protect the food from harmful environmental condition;
- 2) Active food packaging materials: along with the protective function, they have the additional aim of enhancing the performance of packaging material extending food shelf life thanks to the addition of antibacterial, antifungal, antioxidant, antimicrobial constituents in the packaging itself [44]. It is also

important to mention that these constituents can be released at request, for example only in presence of basic or acid pH.

As underlined before, packaging aim is also to preserve and in some cases extend product life. Shelf life can be defined as the period of time during which the product undergo to a tolerable quality decrease under defined circumstances. Shelf-life is not necessarily the real life of a product, because its market life can be shorter: after the loss of sensory features costumer loses interest in buying a product that can still be good. It is fundamental to define quality: up to this definition the market life of a product can change. Different attributes can be considered to define quality: the concentration of a component as well as changes in sensorial parameters (increase in unwanted migrant, decrease of vitamins or typical aroma, changes in taste, colour, and smell).

Eco-sustainability, use agricultural surplus, increased value for agricultural products are the reasons that induced scientific community to focus attention on production of bio-based food packaging. Use of bio-based, compostable material obtained from annually renewable resources for food packaging application will satisfy all these important objectives.

Bibliography

- [1] G. Lagaly, *Appl. Clay Sci.*, 1999, 15(1-2), 1–9.
- [2] M. Biswas; S. S. Ray, *Adv. Polym. Sci.*, 2001, 155(1), 167–221.
- [3] H. L. Cox, *Br. J. Appl. Phys.*, 1951, 3, 72–79.
- [4] Messersmith P.B, Giannelis E.P. Synthesis and barrier properties of poly(1-caprolactone)-layered silicate nanocomposites. *J. Polym. Sci, Part A: Polym. Chem.* 33 (1995)1047-57.
- [5] Yano K., Usuki A., Okada A., Kurauchi T., Kamigaito O. Synthesis and properties of polyimide-clay hybrid. *J. Polym. Sci., Part A: Polym. Chem.* 31 (1993) 2493-2498.
- [6] Gilman J.W. Flammability and thermal stability studies of polymer-layered silicate (clay) nanocomposites. *Appl. Clay. Sci.* 15 (1999) 31-49.
- [7] Giannelis E.P. Polymer-layered silicate nanocomposites: synthesis, properties and applications. *Appl. Organomet. Chem.* 12 (1998) 675-680.
- [8] LeBaron P.C., Wang Z., Pinnavaia T.J. Polymer-layered silicate nanocomposites: an overview. *Appl. Clay. Sci.* 15 (1999) 11-29.
- [9] Giannelis E.P. Polymer layered silicate nanocomposites. *Adv. Mater.* 8 (1996) 29-35.
- [10] Sinha Ray S., Yamada K., Okamoto M., Ueda K. New polylactide/layered silicate nanocomposite: a novel biodegradable material. *Nano Lett.* 2 (2002) 1093-1096.
- [11]Wagner, D.; Vaia, R. 2004. Nanocomposites: issues at the interface. *Materials Today*, November, 2004. ISSN:1369 7021 Elsevier Ltd.
- [12] A. Usuki; M. Kawasumi; Y. Kojima; A. Okada; T. Kurauchi; O. Kaminogato, *J. Mater. Res.*, 1993, 8(5),1174–1178.
- [13] A. Usuki; Y. Kojima; M. Kawasumi; A. Okada; Y. Fukushima; T. Kurauchi; O. Kaminogato, *J. Mater. Res.*, 1993, 8(1), 1185–1189.
- [14] T. Lan; P. D. Kaviratna; T. J. Pinnavaia, *Chem. Mater.*, 1994, 6(5), 573–575.
- [15] R. A. Vaia; H. Ishii; E. P. Giannelis, *Chem. Mater.*, 1993, 5(12), 1694–1696.
- [16] M. Alexandre, P. Dubois: Polymer-layered silicate nanocomposites: preparation, properties and uses of new class of materials, *Material science and engineering*, 2000, 28, 1-63.

- [17] T.J. Pinnavaia and G.W. Beall (editors): Polymer-Clay Nanocomposites, 2001, N.Y. John Wiley & Sons Ltd.
- [18] E. P. Giannelis, Polymer-layered Silicate Nanocomposites, *Advanced materials*, vol. 8, 29-35 (1996).
- [19] R. Dagani, Putting the "nano" into composites, *Chemical and Engineering News*, 7/6/1999.
- [20] P. C. LeBaron, T. J. Pinnavaia, Z. Wang; Polymer-Layered Silicate Nanocomposites: an Overview, *Applied Clay Science*, 15 11-29 (1999).
- [21] M. Alexandre; P. Dubois, *Mater. Sci. Eng.*, 2000, 28(1), 1–63.
- [22] Alexandre M., Dubois P. Polymer-layered silicate nanocomposites: preparation, properties and uses of a new class of materials. *Mater. Sci. Eng. Rep.* 28 (2000) 1-63.
- [23] E. P. Giannelis, *Adv. Mater.*, 1996, 8(1), 29–35.
- [24] Jordan, J.; Jacobb, K.; Tannenbaumc, R.; Sharafb, M.; Jasiukd, I. 2005 Experimental trends in polymer nanocomposites. *Materials Science and Engineering A* 393:1–11
- [25] Biswas, M.; Sinha, R. S. 2001. Recent progress in synthesis and evaluation of polymer–montmorillonite nanocomposites. *Adv Polym Sci.* 155:167–221.)
- [26] D. Yebassa; B. Balakishnan; E. Feresenbet; D. Raghavan; P. R. Start; S. D. Hudson, *J. Polym. Sci.: Part*
- [27] R. Krishnamoorti; R. A. Vaia; E. P. Giannelis, *Chem. Mater.*, 1996, 8(8), 1728 1734.
- [28] H. Shi; T. Lan; T. J. Pinnavaia, *Chem. Mater.*, 1996, 8(8), 1584–1587.
- [29] R. A. Vaia; E. P. Giannelis, *Macromolecules*, 1997, 30(25), 7990–7999.
- [30] R. A. Vaia; E. P. Giannelis, *Macromolecules*, 1997, 30(25), 8000–8009.
- [31] A. C. Balazs; C. Singh; E. Zhulina, *Macromolecules*, 1998, 31(23), 8370–8381.
- [32] M. M. Mortland; T. J. Pinnavaia, *Nature*, 1971, 229(18), 75–77.
- [33] T.D. Fornes, P.J. Yoon, H. Keskula, D. R. Paul: Nylon 6 nanocomposites: the effect of matrix molecular weight, *Polymer*, 2001, 42, 9929-9940.
- [34] H.R. Tennis, D.L. Hunter, D. Chang, S. Kim, J.L. White, J.W. Cho, D.R. Paul, *Polymer*, 2001, 42, 9513.
- [35] T. D. Fornes, P. J. Yoon, D.L. Hunter , H. Keskula, D.R. Paul, *Polymer*, 2002, 43, 5915.
- [36] Petersen et al, Implications of Structure and Function for Allergenicity Internet Symposium on Food Allergens 1(3): 95-101 (1999)

- [37] Tuil R. Van, Schennink, G., Beukelaer, H. De, Heemst, J.van and Jaeger, R. (2000). Converting biobased polymers into food packagings. Proceedings of the food biopack conference, Copenhagen 27-29 August 2000, pp 28-30
- [38] Knox, Andrew (February 2005). "An overview of incineration and EFW Technology as applied to the management of municipal solid waste 9MSW". Univeristy of western Ontario. <http://www.oneia.ca/files/EFW0>
- [39] "PM's advisor hails recycling as climate change action" Letsrecycle.com. 2006-11-08. <http://www.letsrecycle.com>
- [40] The Garbage Primer. New York: Lyons & Burford. pp. 35–72.
- [41] Gruber, Pat and O'Brien, Michael, Biopolymer Volume 6, Chapter 8, Polylactides: NatureWorks® PLA, June 2001.
- [42] Soroka (2002) Fundamentals of Packaging Technology, Institute of Packaging Professionals ISBN 1-930268-25-4
- [43] Yam, K.L., Takhistov, P.T., and Miltz, J.2005. Intelligent packaging: concepts and applications. J. Food Sci. 70(1): R1-10.
- [44] Han, J.H. 2005. Innovations in Food Packaging. Elsevier Academic Press, London. 517 p.
- [45] Marsh, Kenneth¹; Bugusu, Betty¹. Source: Journal of Food Science, Volume 72, Number 3, April 2007 , pp. R39-R55(17).
- [46] Jenkins WA, JP Harrington. Packaging food with plastic. Lancaster Technomic Publishing Co. Inc.1991.

Chapter 2

Materials

1 Lactic acid

Lactic acid is an organic acid (2-Hydroxypropanoic acid) which was isolated from milk for the first time in 1780 by Scheele and it was produced commercially for the first time in 1881. Few years after lactic acid was first isolated, its solidification via self- esterification was obtained. Carothers et al. were the first to mention the dimerization of poly-condensed lactic acid into lactide and its polymerization via ring opening in 1932 [1]. At that time PLA's use was not taken into consideration because of its instability to moisture and its high production cost [2]. In 60s attention to PLA arises thanks to its unique characteristic especially for medical applications such as drug delivery systems and sutures [3].

Lactic acid's structure is characterize by the presence of a chiral carbon (Figure 1), thanks to which lactic acid has optical activity.

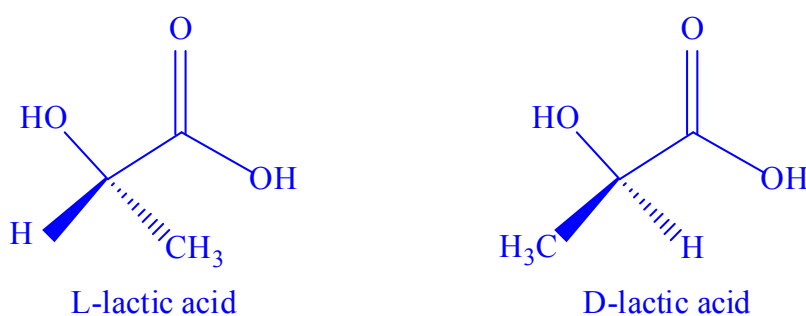


Fig. 1: Chiral form of lactic acid

Enantiomer L (+) is produced by the mammary glands of mammals, while both L and D enantiomer can be produced by bacterial systems. The relationship between the D and L stereoisomers is determined by the specificity of the enzyme. Other carbohydrates, such as maltose, lactose, sucrose can be use as starting material, depending on potential of different bacterial stocks.

Lactic acid's industrial production is obtained mainly thanks to bacterial fermentation. Starch is converted into glucose by enzymatic hydrolysis [4, 5]; than carbon and other elements in this sugar are converted to lactic acid by the action of the enzyme lactate dehydrogenase.

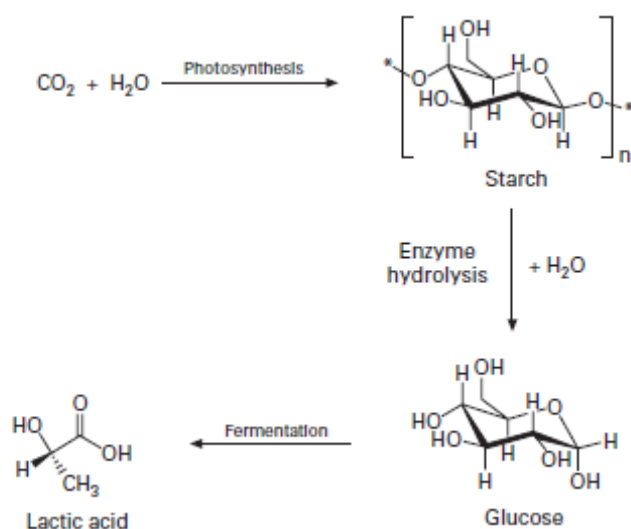


Fig.2: lactic acid formation cycle [6]

Homofermented bacteria, such as genus *Lactobacillus* and *Lactococcus* are among the most used for fermentation. The final product of their fermentation is just lactic acid, using the procedure proposed by Embden-Meyerhof. During the fermentation process is important to control pH, temperature, and in some cases, agitation. Carbon source, complex proteins and other nutrients as nucleotides, amino acids and vitamin B12 are required to allow bacteria to grow and ferment. Generally the commercial fermentation occurs in batch (closed system). To produce lactic acid concentration of 90-99%, it is necessary to start using sugar concentration of 50-10% for a time ranging from 3 to 5 days. To increase the final yield of the process it would be desirable to have high concentration of lactic acid final broth. Important drawbacks deriving from high concentration of lactic acid are increased toxicity and inhibition of bacterial growth. Different methods of neutralization and extraction have been developed to avoid these drawbacks.

The main separation method consists into the addition calcium carbonate or calcium hydroxide to the broth to obtain calcium lactate, which is a soluble salt. Next step is filtration to remove bacterial cells and other insoluble impurities from the final broth. Then the filtrate is evaporated, re-crystallized and acidified with sulphuric acid to obtain raw lactic acid.

2 Lactic acid polymers (PLAS)

Polylactic acid (PLA) is aliphatic, thermoplastic and biodegradable polyester that is produced by processes of fermentation and distillation from starch, mainly corn [7-10].

It is easily processed with standard equipment to produce films, fibers or thermoformed containers. Has property similar to polystyrene (PS).

By controlling percentage of PLA's two stereoisomer during polymerization, PLA properties can be varied: a polymer with high or low molecular weight, characterized by crystalline or amorphous can be obtained. Another important characteristic of PLA is that it is recognized as GRAS (GRAS, Generally Recognised as Safe), making it suitable for food packaging application. Amorphous PLA is soluble in organic solvents, while the crystalline one is soluble in benzene or chlorinated solvents at elevated temperatures. Adequate thermal stability, maintaining the molecular weight and properties, avoiding degradation are fundamental requirements for massive production of PLA. Lactic acid polymers undergo degradation at temperature

above 200°C, because of hydrolysis, cleavage of main chain due to oxidation reactions, trans-esterification and inter-and intra-molecular reformation of lactide. Degradation process is reported to depend on time, temperature, presence of impurities of low molecular weight and concentration of catalysts. Catalysts and oligomers, in fact, reduce the degradation temperature thereby increasing the degree of degradation itself. Moreover they can cause changing in rheological properties of the polymer, a decrease in mechanical properties and the production of smoke during production process. PLA can be degraded by simple hydrolysis of ester bonds without requiring the presence of enzymes to catalyze this reaction. The rate of degradation depends on the size and shape of the article, the ratio of isomers and temperature. Degradation process consists of two different steps:

- 1) hydrolysis of the chain to obtain oligomers with lower molecular weight.

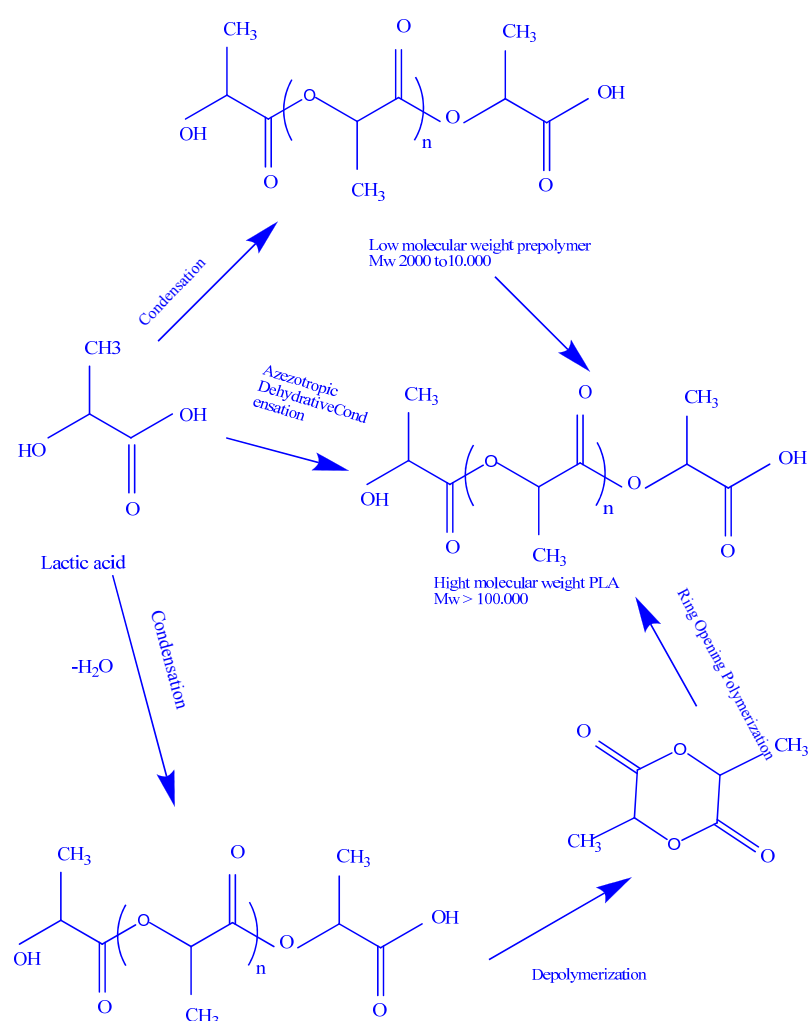
This phase is accelerated by the presence of acids or bases, while its rate is strongly dependent temperature and humidity levels. It has been shown that the reaction auto-catalyzed through the detachment posting of terminal carboxylic groups [11, 12]

2) digestion of products of hydrolysis by microorganisms to obtain carbon dioxide, water and compost.

3 Technology of production of PLAs

PLAs properties are strongly depending on its stereoisomers' ratio. PLA polymers can be synthesized in different ways, their description is reported in Figure 3. Nomenclature of PLAs polymers changes according to PLAs production way. Typically, polymers derived from lactic acid through direct condensation polymerization of lactic acid are called poly (lactic acid); while polymers obtained by ring opening polymerization (ring-opening polymerization, ROP) through intermediaries lactide are called poly (lactide). PLA is a term used to describe both. Polymerization route to poly (lactic acid):

Fig 3: methods to produce high molecular wight PLA



3.1 Direct Polycondensation (PC)

Historically, first polymers based on lactic acid were obtained by direct polycondensation using lactic acid as monomer. In this reaction water is eliminated via condensation using a solvent under high vacuum and high temperature. The final polymer may be composed of a single stereoisomer, a mixture of D- and L-lactic acid in different ratios or lactic acid in combination with other hydroxy acids. A negative aspect of direct polycondensation is that it is an equilibrium reaction, resulting in increased difficulty in the removal of the residual water, limiting final product molecular weight. Therefore only polymers with low or intermediate molecular weight can be produced using condensation reaction. The low molecular weight is due to the presence of impurities. In figure 4 is reported the direct polycondensation process.

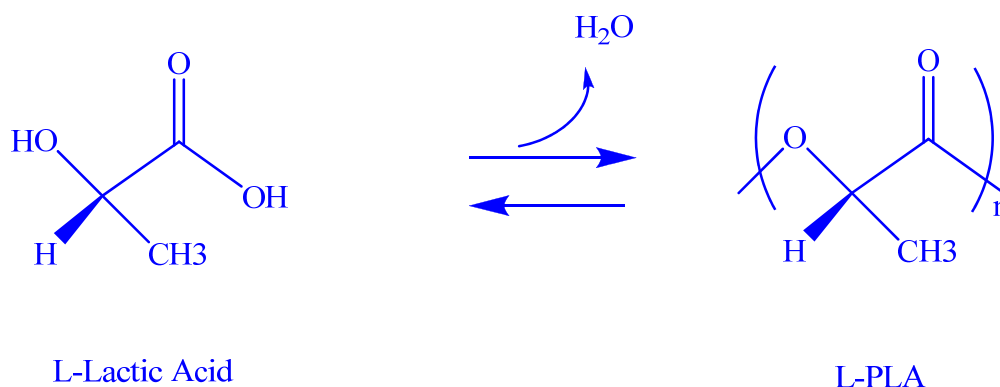


Fig.4: Direct Polycondensation

Different techniques such as the use of adjuvant to promote the esterification (e.g. 2 - trichloromethyl carbonate) or agents that promote the extension of the chain (e.g. Isocyanates, hydrochloric acid) have been used to limit this drawback, leading to an increase in the molecular weight. Obviously this increases the cost and complexity of the process, moreover used agents may not be biodegradable. Other disadvantages of this method are the large size of the reactor required, constant need of regeneration and evaporation of the solvent and the risk of high racemisation.

Recently, Mitsui Toatsu Chemicals has developed a new polycondensation process using azeotropic distillation. They use a solvent that has high boiling temperature to remove water and obtain polymers having high molecular weight, even more than the 300,000 Da [6].

3.2 Ring opening polymerization (ROP)

The second class of polymers derived from lactic acid are obtained by ring opening polymerization of lactide. This kind of reaction was carried out for the first time in 1932 by Carothers [1], but not high molecular weight polymers were obtained up to DuPont in 1954 improved lactide purification techniques. Ring opening polymerization was improved by Cargill Dow. Firstly, it is important to define lactide: it is the cyclic diester (a dimer) of lactic acid. Differently from other hydroxyl acid it cannot form lactone, because its hydroxyl group (-OH) is too close to the carboxyl group (-COOH). In the first phase of the process, water is removed under moderate conditions and without the use of solvent to produce a pre-polymer having low molecular weight. This pre-polymer is then depolymerised using a catalyst to form a mixture of cyclic intermediate dimer (lactide). The mixture is then purified through distillation. The purified lactide is polymerized in a ring opening polymerization without using any solvents, using a catalyst based on tin, producing polylactide grains. Once the polymerization is completed, all remaining monomers are removed by vacuum and re-entered at the top of the process [13]. In figure 5 is reported a representation of ring opening polymerization of PLA:

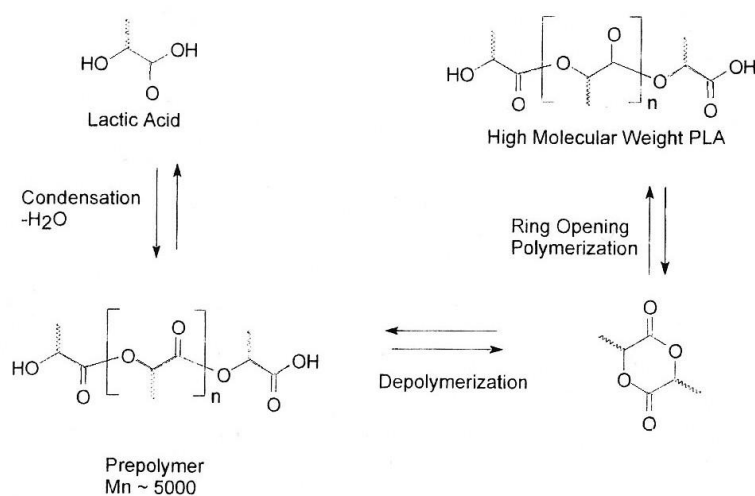


Fig.5: Ring opening polymerization of PLA [5]

By controlling the purity of the lactide a wide range of molecular weights can be produced. Lactic acid chemically synthesized gives rise to a racemic mixture (50% and 50% D L). Instead, lactic acid produced from lactic fermentation is generally made up of 99.5% of isomer L and 0.5% of isomer D [6, 13-15]. Three potential forms can be obtained from the production of cyclic lactide dimer: the D, D lactide (called D lactide), L,L lactide, (called lactide L) and L, D or D, L lactide (called meso-lactide) . In figure 6 is reported a representation of lactide stereoform. Meso-lactide has properties different from the lactide D and L. The lactide D and L are optically active, but not meso-lactide [6, 16].

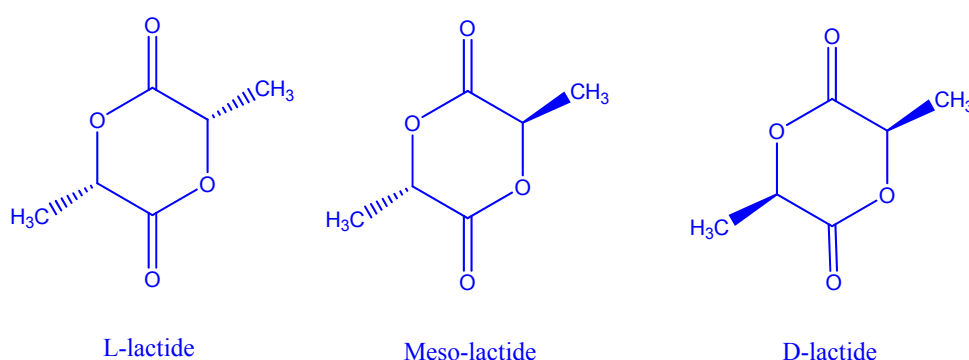


Fig.6: Lactide stereoform

Before the polymerization, lactide stream is divided into flow at low D lactide content and one at high ratio D lactide/meso-lactide. The ring-opening polymerization can produce a family of polymers that differ in the molecular weight distribution and the amount and sequence of D lactide into polymer.. The mechanism involved in the ROP can be either cationic or anion according to the catalytic system that is used. In any case, these processes, because of their high reactivity, often show negative phenomena such as racemisation, transesterification and high levels of impurities. Less reactive catalysts have been studied to overcome these problems and it has been found that PLA at high molecular weight is able to polymerize in the presence of tin, zinc, aluminium or other heavy metals. In particular, zinc and tin (II) lead to polymer characterized by a higher level of purity. Currently tin (II) is the most used thanks to its solubility, low toxicity, high catalytic activity, ability to promote formation of high molecular weight polymers with low racemization (<1%) and being approved by Food and Drug Administration. The

polymerization of lactide using tin (II) consists of a coordination-insertion mechanism: the ring of lactide at the end of the chain is open and two molecules of lactic acid are added. Typical reaction conditions are 180-210°C temperature, concentration of tin (II) of 100-1000 ppm and 2-5 eight hours to reach about 95% conversion. In figure 7 is reported the coordination-insertion mechanism.

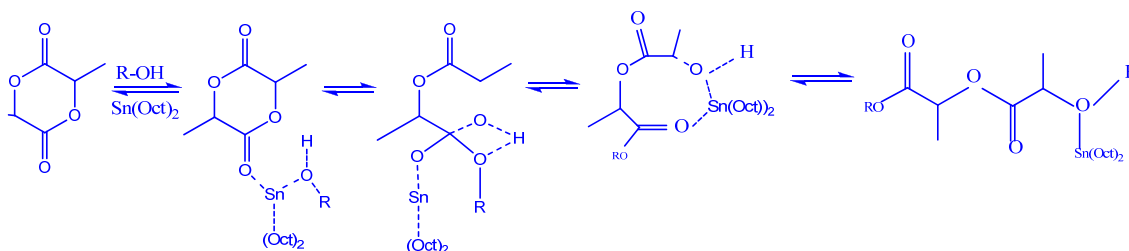


Fig.7: Coordination-insertion mechanism

It has been shown that polymer molecular weight is directly correlated with the amount of hydroxyl impurities, while it is not influenced by carboxylic impurities and catalyst concentration. On the contrary, the degree of polymerization is inhibited by the free carboxylic groups (which bind to the catalyst, reducing its activity); while it is increased by the presence of hydroxyl impurities. Other cyclic monomers can be incorporated in polymers of lactic acid by copolymerization: glycolide and ϵ -caprolactone are among the most used of them.

4 Clay and clay minerals

In the last few years nanotechnology has grown up as an area of research with huge economic and scientific potential. Nano-materials can nowadays be synthesized with great control in respect to their composition, e.g. inorganic, organic, polymeric, biological, as well as structure and function. While there is still much work to be done in the synthesis and characterization of the building blocks, the next challenge of the field is transferring the nano-scale properties of these materials into macro-scale structures. Furthermore, multi-nano-component materials are receiving growing attentions from various disciplines [17].

According to Grim [18, 19] “the term clay implies a natural, earthy, fine-grained material which develops plasticity when mixed with a limited amount of water. By plasticity is meant the property of the moistened material to be deformed under the application of pressure, with the deformed shape being retained when the deforming pressure is removed”.

There are only a few examples of clays that are formed as a consequence of primary igneous or metamorphic environments: the most of them are the result of weathering and secondary sedimentary process [20].

The term clay includes particles $<2\ \mu\text{m}$ in size in geology; while each clay is characterized by its specific morphology. The most of smectite clays present an irregular flake shape with a high aspect ratio, 100-300:1, while kaolinite is usually characterized by hexagonal flake-shaped units with a ratio of areal diameter to thickness of 2-25:1. Attapulgite/sepiolite/palygorskite are fiber-shape clays. Halloysite minerals are characterized by an elongated tubular shape [20]. In figure 8 are reported electron microscope micrographs of different clays.

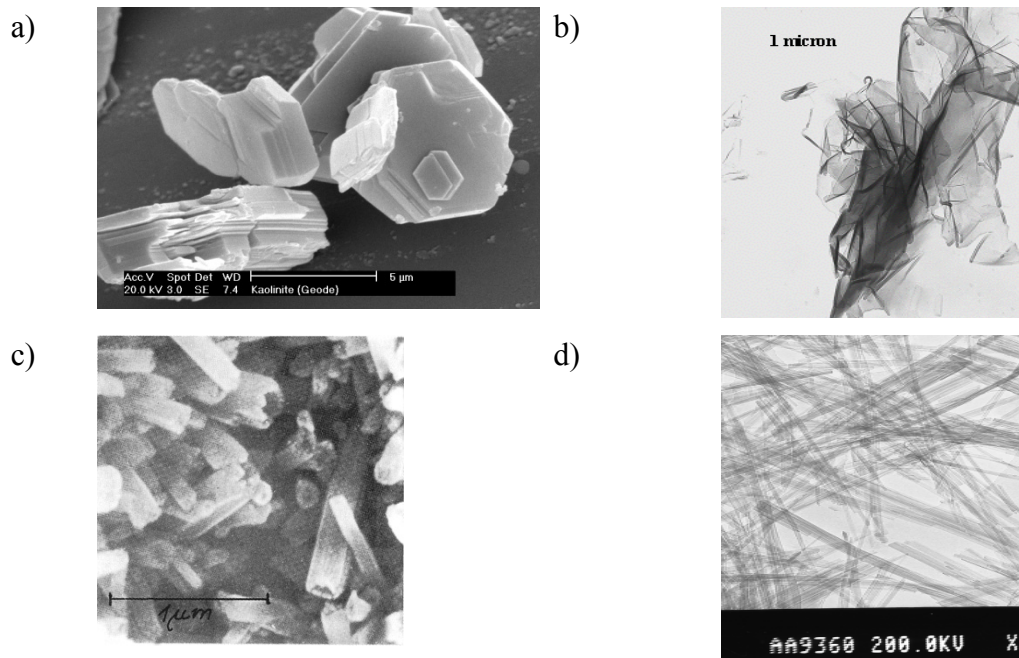


Fig.8: Electron microscope micrographs of different clays: a) kaolinite, b) montmorillonite, c) halloysite and d) sepiolite [4].

The advantage of utilisation of clays in the layer-by-layer assemblies is threefold: 1) the natural abundance of this nano-material resulting in lower cost; 2) their anisotropic sheet-like structure that is of great importance for controlling transport properties through the films; and 3) individual nano-sheets possess exceptional mechanical properties [21].

4.1 Clay minerals

Clay minerals are phyllosilicates (or layered silicate). The phyllosilicates are characterized by tetrahedral and octahedral building units. The structures of the tetrahedral sheets are made up of individual tetrahedrons, in which a silicon atom (or Al^{3+} , Fe^{3+} , etc) is equidistant from four oxygen or hydroxyls in the case their presence is necessary to balance the structure. The arrangement is a hexagonal pattern in which the basal oxygens are linked; while the apical oxygens take part in the adjacent octahedral sheet and they point up/down [20].

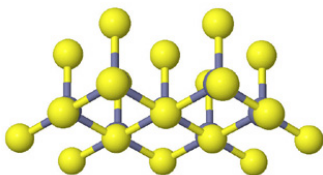


Fig. 9: Tetrahedral sheets [20]

The structure of octahedral sheets is made up of individual octahedrons sharing edges made up of oxygen and hydroxyl anion groups coordinated by cations like Al, Mg, Fe^{3+} and Fe^{2+} , etc [20].

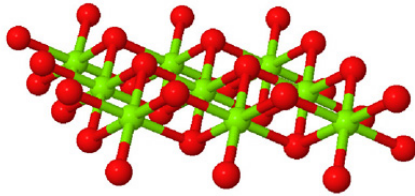


Fig. 10: Octahedral sheet

It is possible to distinguish between di-octahedral or tri-octahedral sheet: they differ because of the valence of the cation: di-octahedral sheet's structure is similar to the minerals Gibbsite $\text{Al}(\text{OH})_3$, while tri-octahedral sheet's structure resemble Brucite $\text{Mg}(\text{OH})_2$. In the case of di-octahedral or Gibbsite-like sheet there is a trivalent cation (i.e. Al^{3+}) and the cation to oxygen ratio is 1:3 to maintain electric neutrality. In this way only 2 out of 3 sites are occupied. It is possible to talk of tri-octahedral or Brucite-like sheet if there is a divalent cation (i.e. Mg^{2+}) occupying the edge sharing hexagonal sheet. In this case the cation to oxygen ratio is 1:2 and every lattice site is filled [20].

The classification of phyllosilicates is based on the way in which the different tetrahedral, di- and tri-octahedral sheets are packed together. The structure of kaolinite is made up of one silica tetrahedral sheet and one alumina octahedral (1:1) sheet combined to form a layer unit characterized by the fact that the apical oxygens of the tetrahedral sheet are also part of the octahedral sheet (Fig. 11 a). Smectite units are made up of two silica tetrahedral sheets with a central alumina octahedral sheet (2:1) (Fig. 11b). The structure of chlorite is characterized by alternating smectite-like layers and tri-octahedral sheets (Fig. 11c).

With the exception of kaolinite, isomorphous substitutions is very common: a cation can be replaced by ions of lower valence (Si^{3+} in the tetrahedral sheet can be replaced by Al^{2+} , while Al^{2+} in the octahedral sheet may be replaced by Li^+ , Mg^{2+} , Fe^{2+} , Fe^{3+} , Zn^{2+} , etc.). Isomorphous substitutions, as well as the presence of vacancies, can induce a negative charged surface of the clays layers [20]. This

negative charged surface is counterbalanced by alkali and alkaline earth cations situated inside the galleries.

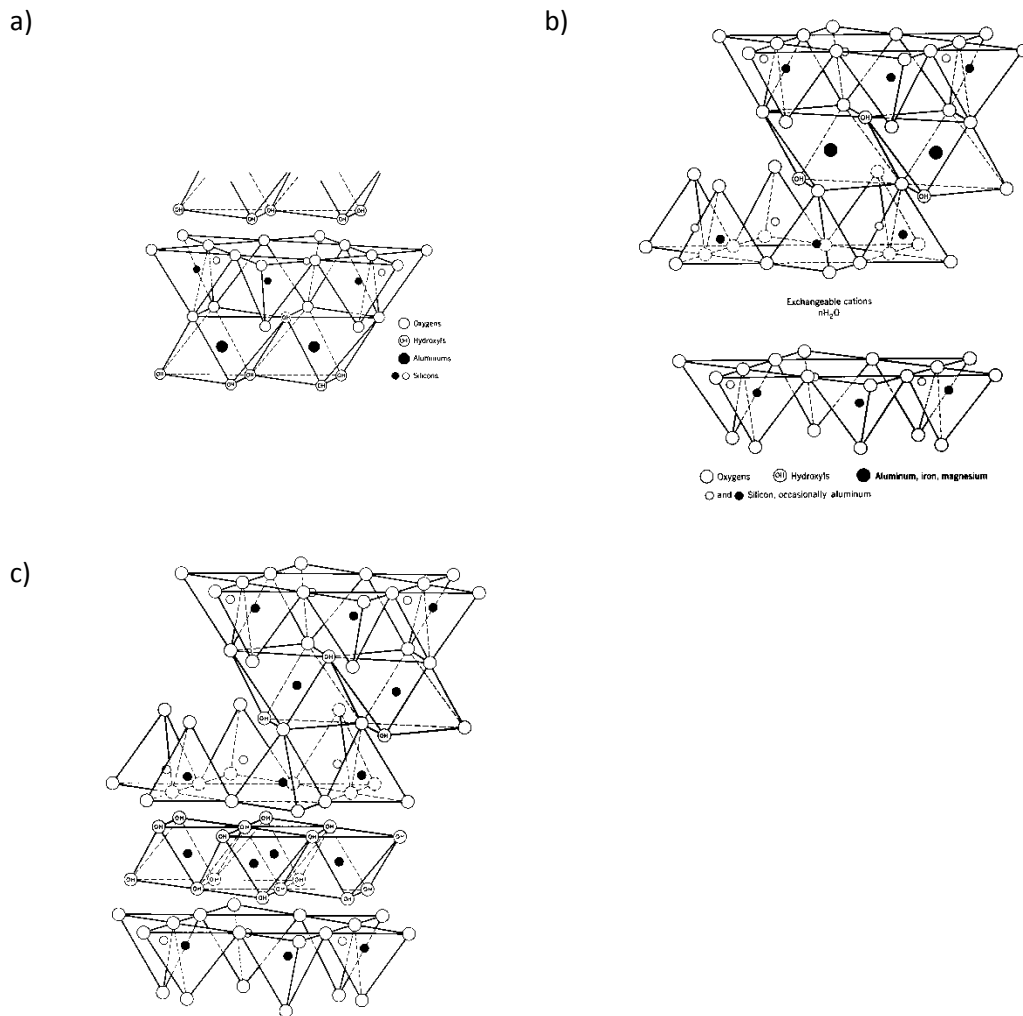


Fig. 11 a, b and c

If the negative charge is located on the surface of silicate layers, as for tetrahedrally substituted layered silicates, the interaction with polymer will be quicker compared with octahedrally substituted material. It is more difficult to exfoliate a structure in presence of interlayer charge, because it creates a bonding between the different layers [4]: in montmorillonite (MMT), on the other hand, the ions are exchangeable and the distance between the layers can increase allowing the material to swell (these

kinds of clays are reported as swelling clay minerals). Two different classifications of clay minerals are presented in Table 1 and 2.

Tab.1: Classification of clay minerals [2].

I.	Amorphous
	Allophane group
II.	Crystalline
A.	Two-layer type (sheet structures composed of units of one layer of silica tetrahedrons and one layer of alumina octahedrons.
1.	Equidimensional
	Kaolinite group
	Kaolinite, Nacrite, etc.
2.	Elongate
	Halloysite group
B.	Three-layer types (sheet structures composed of two layers of silica tetrahedrons and one central di-octahedral or tri-octahedral layer)
1.	Expanding lattice
a.	Equidimensional
	Montmorillonite group
	Montmorillonite, sauconite, etc.
	Vermiculite
b.	Elongate
	Montmorillonite group
	Nontronite, Saponite, hectorite
2.	Nonexpanding lattice
	Illite group
C.	Regular mixed-layer types (ordered stacking of alternate layers of different types)
	Chlorite
D.	Chain-structure type (hornblende-like chains of silica tetrahedrons linked together by octahedral groups of oxygens and hydroxyls containing Al and Mg atoms)
	Attapulgite
	Sepiolite
	Palygorskite

Tab. 2: Classification of phyllosilicate according AIPEA nomenclature committee to the international Mineralogical association [1]

Type	Group	Subgroup	Species
	(x=layer charge)		
2:1	Pyrophyllite-talc	Pyrophyllites	Pyrophyllite
	x~0	Talcs	Talc
	Smectite or montmorillonite-saponite	Diocahedral smectites or montmorillonite	Montmorillonite, beidellite, nontronite
	x~0.5-1	Triocahedral smectites or saponites	Saponite, hectorite, sauconite
	Vermiculite	Diocahedral vermiculite	Diocahedral vermiculite
	x~1-1.5	Triocahedral vermiculite	Triocahedral vermiculite
	Mica	Diocahedral micas	Muscovite, paragonite
	x~2	Triocahedral micas	Biotite, phlogopite
	Brittle mica	Diocahedral brittle micas	Margarite
	x~4	Triocahedral brittle micas	Seybertite, xanthophyllite, brandisite
2:1:1	Chlorite	Diocahedral chlorite	
	x variable	Triocahedral chlorite	Pennine, clinochlore, prochlorite
1:1	Kaolinite-serpentine	Kaolonites	Kaolinite, halloysite
	x~0	Serpentines	Chrysotile, lizardite, antigorite

4.2 Sepiolite

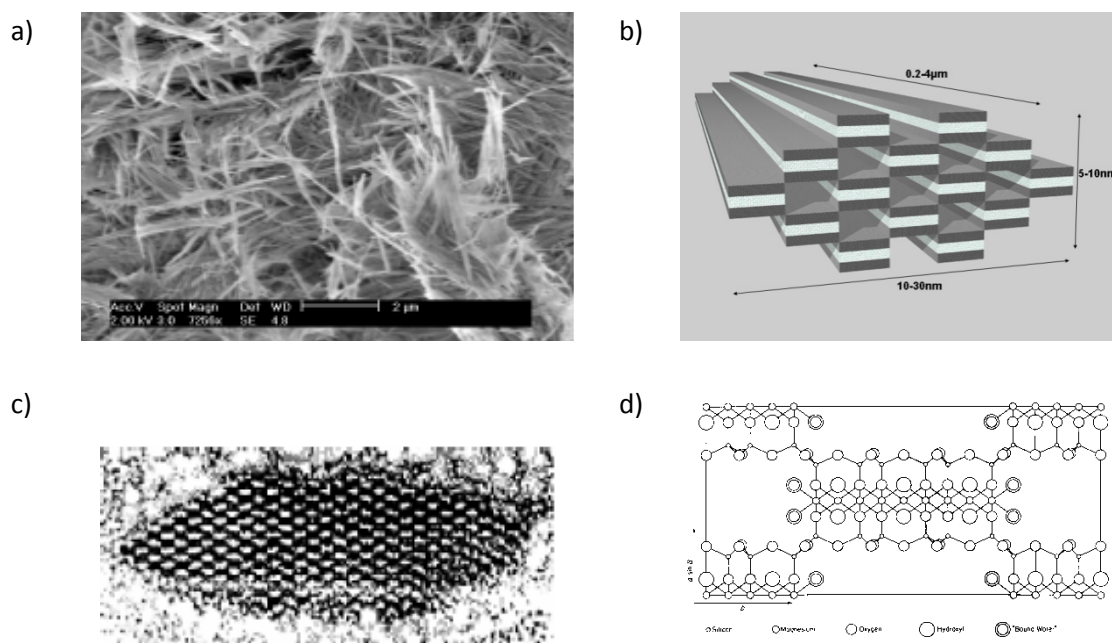
Sepiolite is a hydrated magnesium silicate whose typical formula is $\text{Mg}_4\text{Si}_6\text{O}_{15}(\text{OH})_2 \cdot 6\text{H}_2\text{O}$.

Its name derived from its resemblance of the porous bones of the sepia, because of its fibrous shape. Containing a continuous two-dimensional tetrahedral sheet of composition Si_2O_5 [17, 19], sepiolite is considered as part of the phyllosilicate group also if, differently from other phyllosilicate, it doesn't contained a continuous octahedral sheet as visible from figure 12 d.

Sepiolite is made up of two tetrahedral silica sheets and a central octahedral sheet containing Mg, but continuous only in one direction (c-axis). More blocks are linked together along their longitudinal edges by Si-O-Si bonds creating channels along the c-axis (Fig. 12 b-d) [20]. The presence of covalent link between different blocks makes sepiolite non swellable clay.

Sepiolite is fibre-like clay. The dimensions of the sepiolite fibre vary between 0.2-4 μm in length, 10-30nm in width and 5-10nm in thickness, with open channels of dimensions 3.6 Å x 10.6 Å running along the axis of the particle (Fig. 12.a-b). Sepiolite surface area is about 300 m²/g.

Fig.12a-b



Sepiolite high porosity is explainable in term of its structure: particles are arranged forming loosely packed and porous aggregates with an extensive capillary network which explains the high porosity [20]. Sepiolite has good colloidal properties: if dispersed into a liquid, it will form a structure of randomly intermeshed particles. This structure is stable also in presence of salt concentration, when other clay, such as bentonite, would flocculate. Sepiolite is not considered dangerous for health according to studies conducted by Tolsa [22] and it is even recognized as safe additive for animal feed [23,24].

4.3 Halloysite

Halloysite nanotubes are versatile and economically viable clays that are formed by surface weathering of alumina-silicate minerals and are composed of aluminium, silicon, hydrogen and oxygen [23, 24]. Halloysite was named after the famous Belgian geologist Omalius d'Halloy [8]. As for most natural materials, the size of halloysite particles varies within a range: 1-15 microns of length and 10-150 nm of inner diameter, depending on the deposits [27].

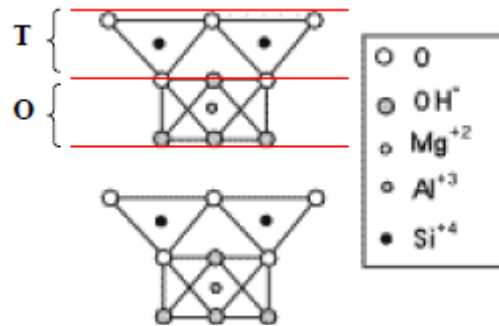
Halloysite is a dioctahedral 1:1 clay miner having a structure $\text{Al}_2\text{Si}_2\text{O}_5(\text{OH})_4\cdot 2\text{H}_2\text{O}$.

Halloysite has the same layer structure as kaolinite, but it differs from it because of the presence of water into the interlayer space. Kaolinite mineral are characterized by Si tetrahedral sheet sharing oxygens with an Al octahedral sheet, while [28] the 1:1 layer of halloysite rolls with the tetrahedral and smaller octahedral sheet.

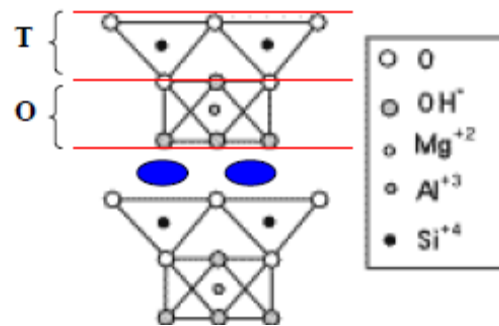
Chemically, the outer and inner surface of the halloysite nanotubes differ because the outer one has properties related to SiO_2 while the inner is similar to Al_2O_3 [26]. The charge (zeta potential) behaviour of the halloysite particles is the results of the combination of mostly negative (at pH 6-7) surface potential of SiO_2 , with a small contribution from de positive Al_2O_3 inner surface [26, 28, 29]. The positive (bellow pH 8.5) charge of the inner lumen allows loading of halloysite nanotubes with negative macromolecules, while, at the same time, the negative charge on the outer surface tries to respell [26]. Halloysite natural shape can be used to entrap in its

structure (both in its inner lumen and within spaces of alumina-silicates shells) a wide range of active agents, such as drugs, nicotinamide adenine dinucleotide (NAD), and marine biocides [24].

Kaolinite



Halloysite



From [30]

Bibliography

- [1] Carothers, H., Dorough, G. L., and Van Natta, F. J., *J. Am. Chem. Soc.*, 54, 761, 1932.
- [2] Lipinsky, E.S. and Sinclair, R.G., *Chem. Eng. Prog.*, 82, 26–32, 1986.
- [3] Nef, J. U., *Liebigs. Ann. Chem.*, 403, 204, 1914;
- [4] Lunt, J., *Polym. Degrad. Stabil.*, 1998, 59, 145.
- [5] D. E. Henton, P Gruber, J Lunt, and J Randall, *Polylactic Acid Technology*
- [6] NatureWorks LLC, <http://www.ingeofibers.com/ingeo/home.asp>
- [7] Holten, C.H., *Lactic Acid, Properties and Chemistry of Lactic Acid and Derivatives*, Verlag Chemie, GmbH, Weinheim/Bergstr., 1971.
- [8] Schopmeyer, H.H., *Lactic Acid*, in *Industrial Fermentations*, Underkofler, L. And Hickley, R.J., Eds., Chemical Publishing Co. New York, NY, 1954, chap. 12.
- [9] Urayama, H., Kanamori, T., and Kimura, Y., *Properties and biodegradability of polymer blends of poly(L-lactides) with different optical purity of the lactate units*, *Macromole. Mater. Eng.* 287, 116, 2002.
- [10] Janzen, J., Dorgan, J.R., Knauss, D.M., Hait, S.B., and Limoges, B.R., *Fundamental solution and single-chain properties of polylactides*, *Macromolecules*, 2003.
- [11] Pitt CG, Gratzl MM, Kimmel GL, Surles J, Schindler A. 1981. Aliphatic polyesters.II. The degradation of poly(DL-lactide), poly(-caprolactone), and their copolymers in vivo. *Biomaterials* 2:215–20.
- [12] Malin M, Hiljanen-Vainio M, Karjalainen T, Seppälä J. 1996. Biodegradable lactone copolymers. II. Hydrolytic study of caprolactone and lactide copolymers. *J Appl Polym Sci* 59:1289–98.
- [13] Ovitt, T.M. and Coates, G.W., *Stereoselective ring-opening polymerization of lactide with a single-site, racemic aluminum alkoxide catalyst: synthesis of stereoblock poly(lactic acid)*, *J. Polym. Sci., Part A: Polym. Chem.*, 38, 4686, 2000.
- [14] Yui, N., Dijkstra, P., and Feijen, J., *Stereo block copolymers of L- and D-lactides*, *Makromol. Chem.*, 191, 487–488, 1990.
- [15] Tsuji, H. and Ikada, Y., *Stereocomplex formation between enantiomeric poly(lactic acid)s. XI. Mechanical properties and morphology*, *Polymer*, 40, 6699, 1999.

- [16] Cox, G. and Macbean, R., Lactic Acid Recovery and Purification Systems, Research Project Series, No. 29, October, 1976.
- [17] D.V. Talapin, ACS Nano 2 (2008) 1097.
- [18] R.E Grim, Clay Mineralogy. 1968, New York: McGraw-Hill.
- [19] R.E. Grim, Applied Clay Mineralogy.1962,New York: McGraw-Hill.
- [20] E. Bilotti, PhD dissertation, 2009
- [21] P.T. Hammond, Adv. Mater. 16 (2004) 1271
- [22] <http://www.hse.gov.uk/lau/lacs/37-2.htm>.
- [23] P. Suárez, M.C. Quintana, and L. Hernández, Determination of bioavailable fluoride from sepiolite by “in vivo” digestibility assays. Food and Chemical Toxicology, 2008. 46(2): p. 490-493.
- [24] <http://www.tolsa.com>.
- [25] E. Hope; J. Kittrick; The American Mineralogist, Jul-Aug 1964, 49, 859-863
- [26] Haq A, Iqbal Y, Riaz Khan M: Historical Development in the classification of kaolin subgroup. J pak Mater Soc 2008; 2(1)
- [27] www.sigmaaldrich.com
- [28] G. Tari, Journal of Colloid and Interface Science, Feb 1999, 210.2, 360-366
- [29] S. Baral, Chemistry of Materials, 1994, 5, 1227-1232
- [30] <http://www.antonio.licciulli.unisalento.it>

Chapter 3

Properties of PLA-clay annealed nanocomposites: a study on sepiolite and halloysite

Properties of PLA-clay annealed nanocomposites: a study on sepiolite and halloysite

1 Introduction

Eco-sustainability, use agricultural surplus, increased value for agricultural products are the reasons that induced scientific community to focus attention on production of bio-based food packaging. Use of bio-based, compostable material obtained from annually renewable resources for food packaging application will satisfy all these important objectives.

In this work, eco-friendly nanocomposites based on PLA have been investigated. Polylactic acid (PLA) is aliphatic, thermoplastic and biodegradable polyester that is produced by processes of fermentation and distillation from starch, mainly corn [1-10]. PLA use can be particularly suitable for application in which packaging, or generally product, recovery is not operable or too complex, such as in the case of agricultural mulching. Another important characteristic of PLA is that it is recognized as GRAS (GRAS, Generally Recognised as Safe), making it suitable for food packaging application, especially in consideration of its compostability: PLA can be thrown away with leftover food.

Two kinds of non organo-modified clay, sepiolite and halloysite, have been investigated and the effect of their different concentration on composites' properties has been analysed in relation to changes that can occur after annealing process.

Annealing on PLA is reported to be an efficient treatment to increase modulus, tensile strength and reduce gas permeability, as a consequence of the reduced free volume of the polymer and increased crystallinity. Moreover, addition of clay is reported to lead to higher crystallinity and young modulus after annealing [11].

Halloysite natural shape can be used to entrap in its structure (either in its inner lumen or within spaces of aluminosilicates shells) a wide range of active agents, such as drugs, nicotinamide adenine dinucleotide (NAD), and marine biocides [12-14].

Sepiolite has been reported to improve mechanical [15-19], rheological [20] and thermal [22] properties

2 Materials

2.1 PLA

PLA2002D, from NatureWorks, was used as matrix. It is specifically designed for extrusion/ thermoforming applications. This PLA has a D content of 4.25%, a residual monomer of 0.3% and a density of 1.24g/cm³.

2.2 Sepiolite

Sepiolite Pangell were supplied by Tolsa (Madrid, Spain). Sepiolite bulk density is 30 g/L and the BET surface area is 320 m²/g. The characteristic average dimensions of the individual sepiolite fibres are 1–2 mm in length and 20–30 nm in diameter. Its aspect ratio is within the range of 100–300.

2.3 Halloysite

Halloysite G produced by Atlas Mining, Nanoclay Technology Division and available from Sigma-Aldrich, was used as reinforce. This material has an average tube diameter of 50 nm and an inner lumen diameter of 15 nm. This halloysite has the following properties: a typical specific surface area of 65 m²/g, a pore volume of ~ 1.25 mL/g, a refractive index of 1.54 and a specific gravity of 2.53 g/cm³.

3 Experimental details

PLA pellets and powders were dried overnight at 80°C before extrusion.

Nominal nanofiller concentration of 0.1, 0.5, 1, 3 and 5%-wt were obtained from master batch at 15% in weight.

3.1 Extrusion

Nanocomposites were prepared via melt compounding using Mini twin-screw extruder DSM Micro 15, a twin screw compounder with a capability of 15 ml.

Both pure PLA, used as reference material, and PLA based composites were processed under nitrogen at 190°C for 5 minutes. Screws speed was set up at 200 rpm.

Nitrogen gas was purged during extrusion in order to reduce PLA's degradation and absorption of humidity from external environment.

Residence time was selected in order to obtain a good dispersion of clays into the PLA matrix: longer time of residence can lead to better dispersion, but it increases the risk of matrix degradation. The choice of the residence time is a compromise between the dispersion and the degradation.

To prepare the samples for further processing, produced polymeric strands were successively pelletized and dried overnight at 80 °C to remove the water absorbed after extrusion.

Pure PLA was produced under same conditions with the purpose to be compared to nanoclay composites.

3.2 Compression moulding

Dried pellets were compression moulded into films with an average thickness of about 100µm using a Platen Hot Press machine.

Every compound was weighed and placed in an aluminium mould of 11x11 cm. The amount of material to put in the square aluminium mould was calculated considering PLA's density of 1 kg/m³ in order to obtain film with the desired thickness.

Process conditions were:

7 min, no pressure applied, 190°C → no pressure was applied in this step to give the pellets time to be completely melted

5 min, 80 bar, 190 °C → temperature was kept at 190°C under a pressure of 80 bar to allow the melted pellets to obtain the desired shape.

80 bar, 40°C → after 5 minutes the samples were cooled until 40°C.

Obtained films were prepared for further characterization cutting them into 3x3 cm square for absorption tests, while for mechanical tests each sample was cut into dog bone using a standard stamp.

3.3 Annealing

Annealing on PLA is reported to be an efficient treatment to increase modulus, tensile strength and reduce gas permeability, as a consequence of the reduced free volume of the polymer and increased crystallinity. For these reasons after compression moulding, pure PLA and PLA based nanocomposites films were annealed at 80°C overnight to study annealing effect on films properties.

4 Characterizations

4.1 SEM

SEM micrographs of nanocomposites were taken to study the dispersion of sepiolite and halloysite in the PLA matrix.

Morphological analyses were carried out using a Jeol JSM-6300F Scanning Electron Microscope (SEM) on gold coated, cold fractured samples. Brittle fracture was obtained after immersion in liquid nitrogen.

4.2 Thermal test

In order to find out thermal properties of nanocomposites, thermal gravimetric analysis (TGA) and differential scanning calorimetry (DSC) are applied.

- TGA

Thermo gravimetric analysis was conducted on a TA Instruments Q500 device. Each specimen was heated from the temperature of 40 to 750°C with a ramp rate of 10°C/min in a nitrogen-filled environment. Average weight of each sample was about 5mg. This test was done in order to study changes in the onset of degradation temperature after nanofiller addition.

- DSC:

DSC tests were performed with a METTLER device. Average weight of each sample was about 3 mg. Samples were heated from room temperature to 230°C at ramp rate of 10°C/min, kept at this temperature for 5minutes to remove the thermal history, cooled at 30°C at the rate of 10°C/min and heat up again to the temperature of 230°C. DSC analysis was performed to obtain information on crystallinity (X_c), glass transition (T_g), melting (T_m) and crystallization (T_c) temperatures of nanocomposites and pure PLA to study the effect of the presence and concentration of clays.

4.3 WVTR

Water vapour permeability was tested on neat PLA and nanocomposite films by means of a ExtraSolution Multiperm equipment, operating at 25 °C and 50% relative humidity (RH).

The instrumental apparatus consists of a double chamber diffusion cell. The film was inserted between the two chambers: water vapour enters the bottom chamber, and a dry nitrogen flux flows in the top chamber. A zirconium oxide sensor detects the vapour diffusion across the film. The exposed area of the film was 50 cm². Collected data were converted in water vapour transmission rate (WVTR) that is the flux of vapour flow between two parallel surfaces under steady conditions at specific temperature and RH. Permeability was calculated multiplying WVTR by film

thickness and diving by water vapour partial pressure in the bottom chamber (that is 11.9 mmHg). All measurements are in duplicate.

4.4 Absorption test

These tests were run to determine the rate of absorption of water by PLA based film during immersion.

Standard designation D 570 was used as a guideline to setup experiment. In this study specimen of each composition were cut into square of 3x3 cm and annealed in an oven at 80°C for 24 hours. Before being tested, specimens were stored into a desiccator at room temperature for 24 hours. During tests specimen were placed into a container filled with distilled water for 24 hours at maintained at room temperature. At the end of each test, specimen surface was wiped off using dry cloth, then immediately weight using an analytic balance capable of reading 0.0001g. After immersion and after checking the weight, each specimen was reconditioned using the initial drying condition, to check the existence of any difference in weight to the presence of water-soluble ingredients.

Percentage increase in weight during immersion was calculated according to the following formula:

$$\text{Increase in weight} = (\text{wet weight} - \text{conditioned weight}) * 100 / \text{conditioned weight}$$

Water absorption was obtained from increase in weight dividing it for each specimen average thickness, according to the following formula:

$$A = \text{Increase in weight} / \text{specimen average thickness}$$

4.5 Tensile test

Tensile tests were conducted to determine tensile strength, Young modulus and elongation at break of the films using a Universal Mechanical Test Frame Instron 5566 equipped with a 1-kN load cell, using a rate of 5mm/min.

Film specimens were cut into dog-bone shape with a length of 43mm.

5 Results and discussion

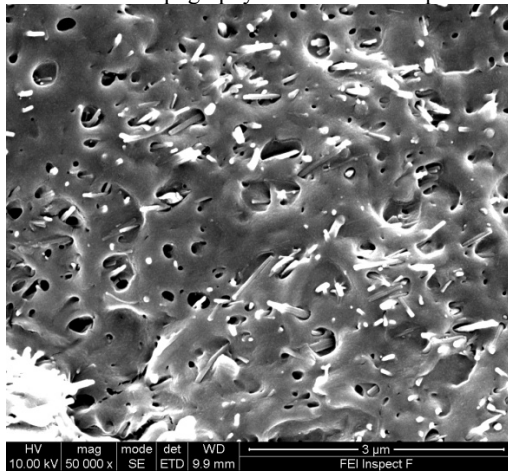
SEM analysis was conducted on PLA based films reinforced with 0.1, 0.5, 1, 3 and 5%wt of sepiolite and halloysite.

Small amount of sepiolite can be well dispersed in PLA by melt compounding; when the concentration of nanofiller increases and reaches 5% wt the quality of the dispersion decrease and micrometric agglomerates of sepiolite starts to appear in the composite, along with region of better dispersion.

The good level of sepiolite dispersion in PLA could be attributed to the good interaction between PLA and sepiolite due to the hydrogen bonding between the carbonyl group of PLA and the hydroxyl group of sepiolite.

Surface topographies of PLA-sepiolite at 5% and 0.1% wt. are reported in pictures 1 and 2 respectively.

Pic.1 SEM topography of PLA+5%sepiolite



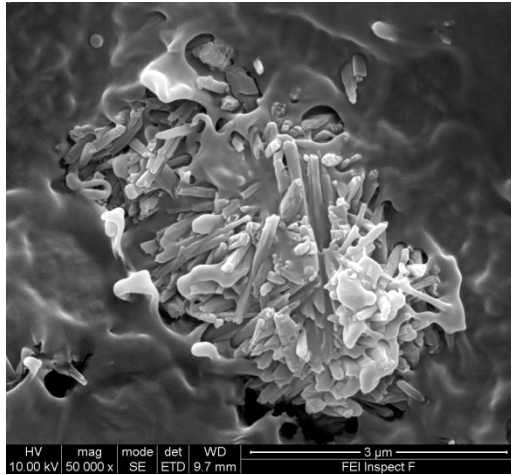
Pic.2 SEM topography of PLA+0.1%sepiolite



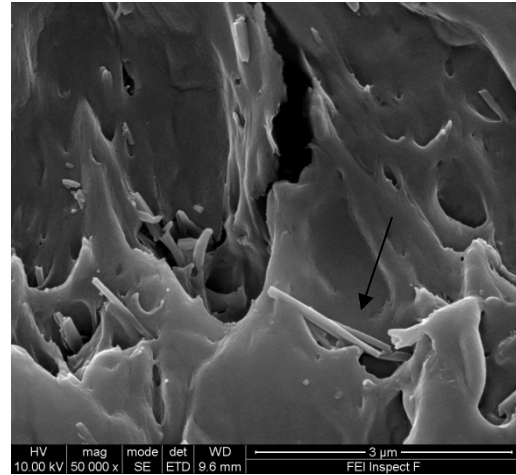
Halloysite–PLA composites showed the presence of agglomerates at percentage of clay higher than 1% as visible in picture 3 in which is reported SEM for PLA-halloysite films at 5% of clay.

Moreover, process conditions lead to halloysite nanotubes break and tube's opening, determining loss of properties, especially in regard to the mechanical one. In picture 4 it is possible to see broken halloysite nanotubes.

Pic.3 SEM topography of PLA+3%halloysite



Pic.4 SEM topography of PLA+1%halloysite



Glass transition, relaxation enthalpy, crystallization and melting temperatures and degree of crystallinity of the polymers are shown for PLA/sepiolite and PLA/halloysite composites after annealing in tables 1 and 2 respectively. The crystallinity was calculated as the difference between the melting and crystallization enthalpies, considering the melting enthalpy of 100% crystalline polylactide as 93.1 J/gm .

Figure 1 and 2 show respectively first DSC scan for sepiolite-PLA and halloysite – PLA composites.

Tab.1: DSC Temperatures for different amount of sepiolite

	annealed			non annealed	
Sample name	T _g (°C)	T _c (°C)	T _m (°C)	X _c (%)	X _c (%)
PLA	57.81	133.27	150.36	18.13	2.7
0.1halloysite-PLA	56.85	134.26	150.84	18.24	2.6
0.5halloysite-PLA	58.19		152.26	23.28	3.5
1halloysite-PLA	57.33		152.35	24.7	4.7
3halloysite-PLA	57.81		151.89	23.24	3.2
5halloysite-PLA	56.77		152.63	20.14	4.3

Tab.2: DSC Temperatures for different amount of sepiolite

	annealed			non annealed	
Sample name	T _g (°C)	T _c (°C)	T _m (°C)	X _c (%)	X _c (%)
PLA	57.81	133.27	150.36	18.13	2.7
0.1sepiolite-PLA	56.67	133.26	150.37	18.32	2.6
0.5sepiolite-PLA	57.25	133.95	150.74	15.11	6.7
1sepiolite-PLA	57.39		152.21	27.08	5.0
3sepiolite-PLA	57.08		150.84	20.61	4.5
5sepiolite-PLA	59.92		152.27	24.47	4.4

Fig 1: PLA-halloysite composite, I DSC scan

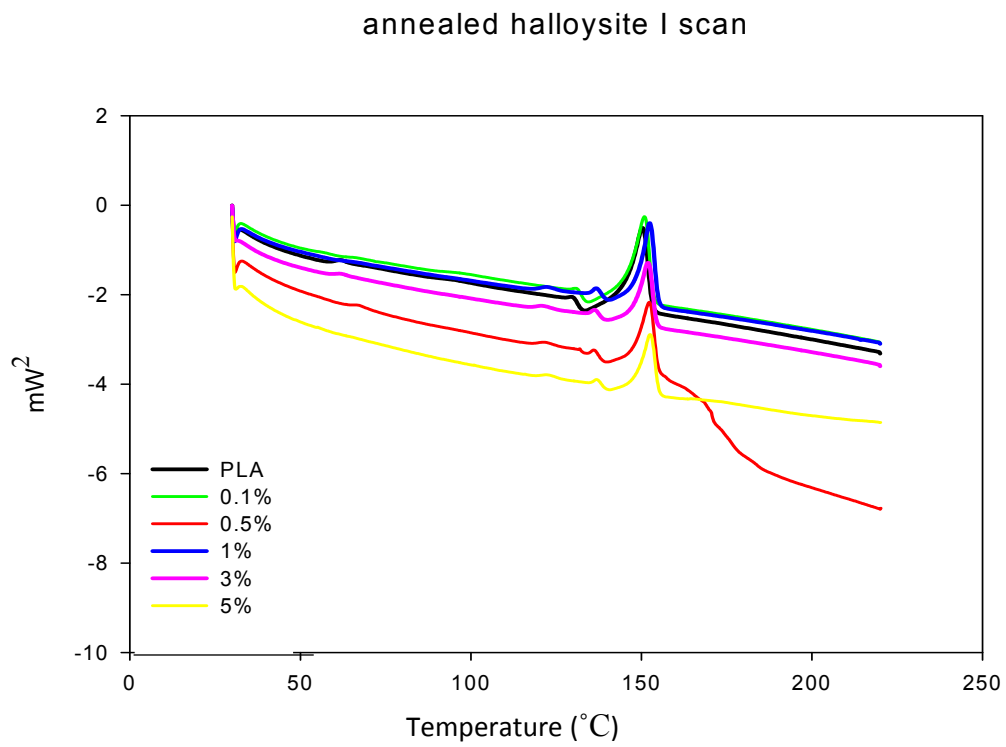
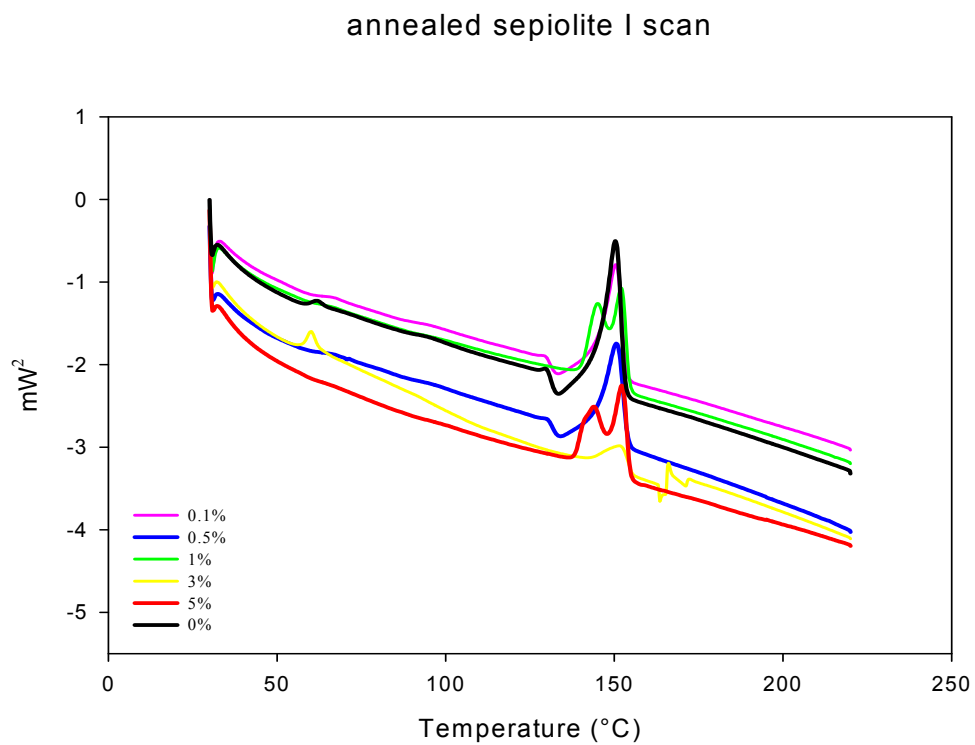
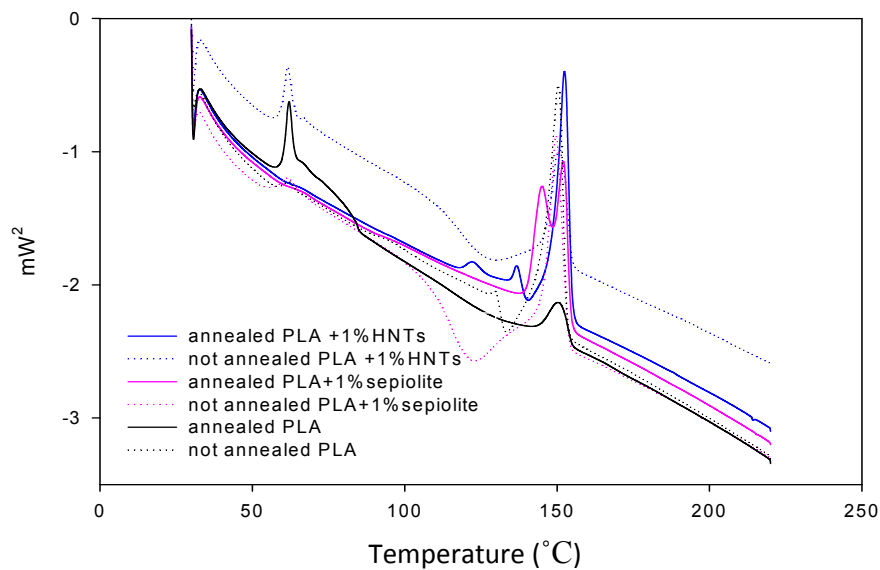


Fig 2: PLA-sepiolite composite, I DSC scan



Amorphous polymer are not in thermodynamic equilibrium at temperature below their T_g and annealing can induce relaxation toward equilibrium of free volume and enthalpy, moreover it can lead to reduction of entropy and internal energy of the polymer. All DSC plots before annealing showed a relaxation peak after glass transition temperature of PLA (that occurred around 57°C), caused by the non equilibrium structure of films. This endothermic peak is called enthalpic or volume relaxation [21]. As a consequence of annealing, annealed samples show a significant decrease of the enthalpy related to the volume relaxation as it is visible from figure 3 in which first DSC scan of annealed and not annealed PLA, 1% sepiolite-PLA and 1%halloysite –PLA halloysite are reported.

Fig 3: annealed and untreated PLA-clay composite, I DSC scan



Present after T_g is another peak which corresponds to a cold crystallization one; the presence of this crystallization peak indicates that extruded and compression moulded samples were semicrystalline.

Generally, the addition of clays is reported to enhance crystallinity and reduce T_c for PLA-based composites as a consequence of clay nucleating effect. In the case of the 2 clays used in this study, there is some evidence of this kind of effect: for both PLA-sepiolite and PLA-halloysite samples crystallinity increased while T_c decreased with clay percentage up to 1%wt of clay. This trend is reported also for not annealed

samples, but it is enhanced by the physical aging process that lead to much higher crystallinity as visible from fig.3 and tab.1 and 2.

After annealing treatment the crystallinity peak diminishes and this is more apparent with the increased amount of clay. Percentages of sepiolite higher than 0.5wt% and percentage of halloysite higher than 0.1wt% of clay don't show this exothermic peak indicating that PLA matrix crystallized during the annealing treatment in presence of clay. The clay therefore may be serving as a nucleating agent for crystallisation of the PLA matrix and its effect is enhanced by the physical aging process that lead to much higher crystallinity and to the disappear of cold crystallization peak.

The annealing treatment itself was found to be able to enhance pure PLA crystallinity of around 570%. This result was expected and it is a consequence of annealing treatment ability in reducing polymer chain free volume.

Calculation of crystallinity level showed that the presence of halloysite in PLA matrix after annealing caused a further increase in the crystallinity up to 1wt% of the clay. At higher concentrations, the crystallinity begins to decline as shown in tab 1 and this could be due to the formation of agglomerates and to a less good dispersion of the clays in the matrix at concentrations of 3wt% and above as shown by SEM analysis.

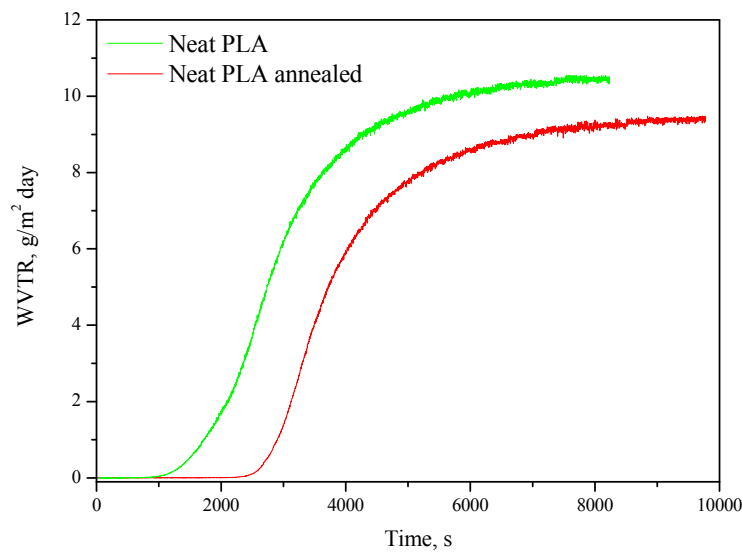
Another interesting phenomenon is the appearance of a double melting peak after annealing the clay-PLA samples of up to 0.5wt% of clay.

PLA double (or bimodal) melting peak has been reported to occur due to the formation of two different crystalline structures [22-24]. The most common polymorphism for PLA is the alpha form which has a pseudo-orthorhombic or pseudo-hexagonal structure [24] and it melts at higher temperature; while beta form can be orthorhombic or triagonal and melt at lower temperature [24]. The double peak is also reported to be due to the reorganization of imperfect crystals formed during cold crystallization of crystals that melt at higher temperature [25].

Annealing effect on crystallinity is widely reported in literature as well as clay nucleating effect [11]. The results presented in this study show that there is a stronger effect of annealing treatment on pure PLA's crystallinity and that it is enhanced by the presence of the clays.

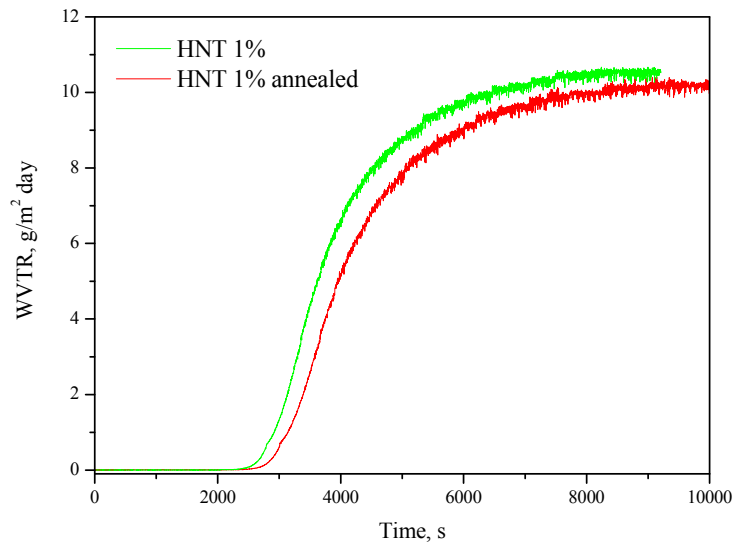
Gas barrier properties are reported to be strongly dependent on shape, presence and dispersion of clays as well as level of crystallinity. Water vapour permeability tests were carried out on MultiPerm equipment, at 25 °C and 50% RH. The following curves (figures 4 and 5) show the experimental flux curves versus time, representing the kinetics of the Water Vapour Transmission Rate. Each curve is the average of the experimental flux curves multiplied by the thickness of the film sample. These tests were carried out only on samples reinforced at 1%wt of each clay. WVTR values should be taken where the permeation curve reaches a steady state. At least two measurements were performed on each sample to ascertain about reproducibility. The latter was found to be rather good in all cases so far. Steady state WVTR value of neat PLA is reduced by approximately 10% after annealing as a consequence of increased crystallinity and reduced free volume induced by annealing treatment. WVTR for both annealed and not annealed PLA are shown in fig 4.

Fig. 4: untreated and annealed PLA, WVTR versus time



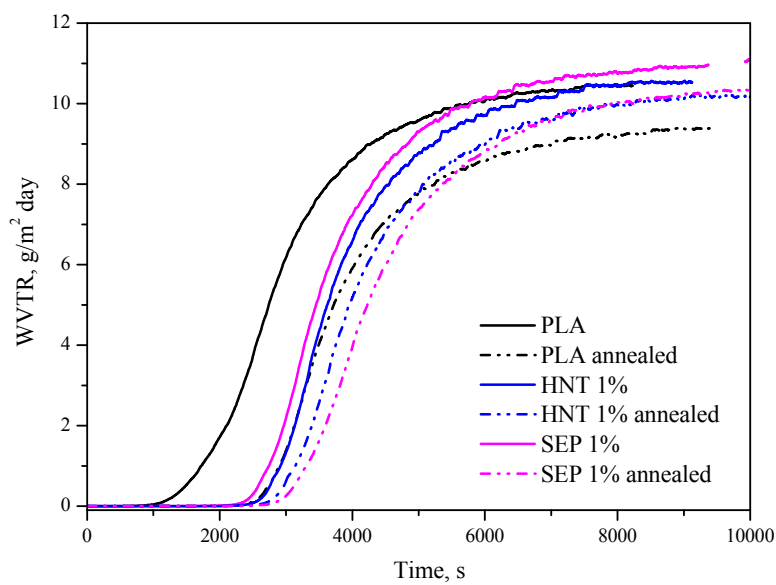
Less significant changes in WVTR are brought about by the annealing of halloysite 1% and sepiolite 1%: respectively increases of 3.8 and 5.5% are reported. In figure 5 is reported as example WVTR for PLA+1%halloysite annealed and not.

Fig. 5: untreated and annealed PLA + 1%hnt, WVTR versus time



In figure 6, WVTR for annealed and not annealed PLA, PLA+1%sepiolite and PLA+ 1%halloysite are reported: it is clear the effect of the presence of clays on lag time, than strongly increase as consequence of increased tortuosity induced by the presence of both the clays.

Fig. 6: untreated and annealed PLA + 1% sepiolite, WVTR versus time



Addition of nanosized fillers caused the time lag (the time during which the WVTR is null) to increase significantly: the presence of the fillers in the polymer decreases diffusion coefficients compared to neat PLA. A decrease in diffusion is related to a more tortuous path for the diffusing gas molecules.

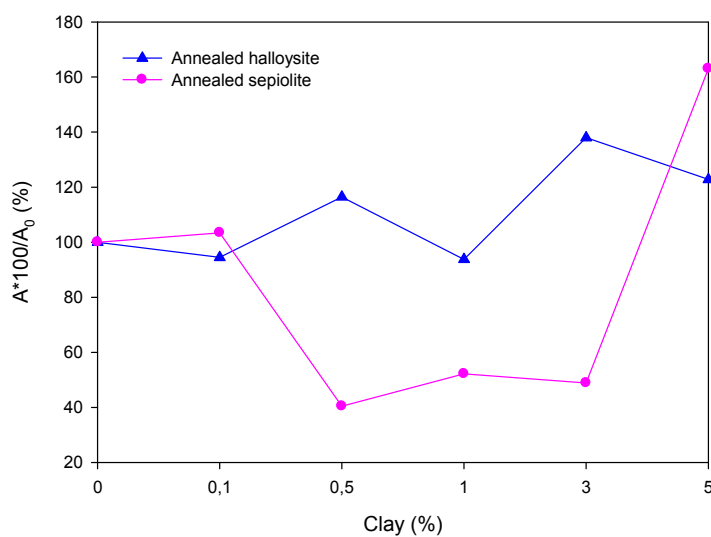
In the following table it is reported a resume of the value of WVTR and permeability for PLA and PLA-clay composites after and post annealing.

Tab.3: WVTR and permeability

Sample	WVTR ($\text{g } 24\text{h}^{-1} \text{ m}^{-2}$)		Permeability ($\text{g } 24\text{h}^{-1} \text{ m}^{-2} \text{ m}^{-6} \text{ mmHg}^{-1}$)	
	untreated	annealed	Untreated	annealed
Neat PLA	10.4	9.3	60,6	54,2
PLA+HNT 1%	10.6	10.2	74,3	71,5
PLA+SEPIOL 1%	10.9	10.3	77,6	73.3

Water absorption tests were run only on annealed samples. Figure7 shows plot of relative absorption versus clay percentage. Relative absorption was calculated normalizing each sepiolite and halloysite composites absorption at pure PLA one.

Fig.7 : A/A_0 versus clay content



PLA-sepiolite composites showed a decrease in the absorption of water with increase of percentage of clay from 0.1% to 3%wt. This reduction in absorption is an effect of the homogeneous dispersion of clay in the composite how is confirmed by a macroscopic analysis and SEM reported in Figure 1. The improvement seems not to be strongly dependent on the increment of crystallinity and the correlation is not linear. At 5%wt of sepiolite clay there is a reverse effect and an increase in water absorption occurs. Possible explanation for this behaviour can be the formation of aggregates due to the decreased dispersion of the clay in PLA that lead to a reduction of the contact surface area between clay and matrix and to the formation of imperfection in the polymer structure.

Halloysite based composites show increase in absorption behaviour also for small amount of reinforcement probably because of the nature and shape of the clay itself characterized by the presence of an internal hole.

Further studies must be conducted to explain the behaviour of both clays to correlate the effect of water absorption property to dispersion or crystallinity effect.

Annealing above T_g is reported to be an efficient treatment to reduce free volume and increase crystallinity and polymer chain relaxation, inducing increases in modulus and strength.

In table 4 and 5 are shows the effects of different amount of sepiolite and halloysite in the matrix on maximum stress, Young's modulus and elongation at break after annealing. In figure 8 the stress-strain curve for PLA - sepiolite samples after annealing are shown.

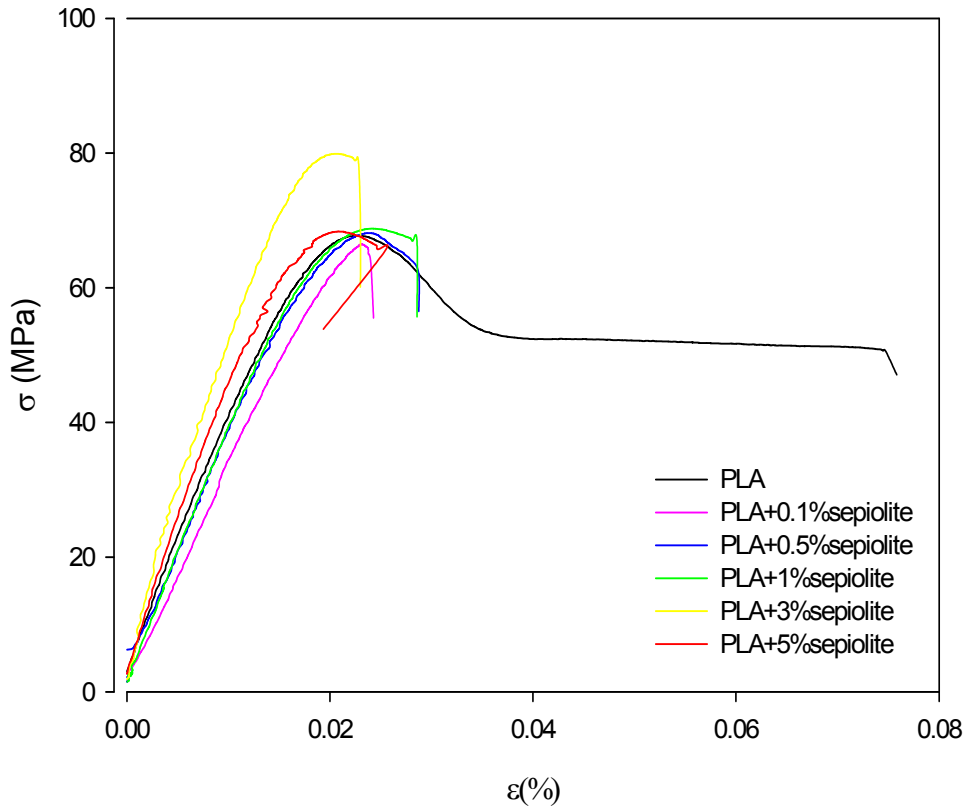
Tab.4: samples name E, σ and ϵ

Sample name	E(GPa)	σ (MPa)	ϵ (%)
PLA not annealed	3.7 \pm 0.1	59.5 \pm 4.8	10.1 \pm 3.5
PLA annealed	3.6 \pm 0.1	69.6 \pm 2.7	5.07 \pm 2.2
0.1 sepiolite annealed	3.6 \pm 0.3	68.6 \pm 4.6	2.7 \pm 0.7
0.5 sepiolite annealed	3.6 \pm 0.1	69.3 \pm 1.4	3.6 \pm 0.4
1 sepiolite annealed	3.7 \pm 0.2	68.3 \pm 0.7	3.4 \pm 0.7
3 sepiolite annealed	3.6 \pm 0.2	71.3 \pm 2.5	3.2 \pm 0.3
5 sepiolite annealed	4 \pm 0.1	66.7 \pm 1.7	2.5 \pm 0.11

Tab.5: samples name E, σ and ϵ

Sample name	E(GPa)	σ (MPa)	ϵ (%)
PLA not annealed	3.7 \pm 0.1	59.5 \pm 4.8	10.1 \pm 3.5
PLA annealed	3.7 \pm 0.1	69.6 \pm 2.7	5.07 \pm 2.2
0.1Halloysite annealed	3.7 \pm 0.3	66.11 \pm 3.6	5.15 \pm 2.1
0.5Halloysite annealed	3.8 \pm 0.4	66.69 \pm 8,3	2.7 \pm 0.4
1 Halloysite annealed	4.0 \pm 0.3	73.8 \pm 7.5	4.2 \pm 1.4
3 Halloysite annealed	3.9 \pm 0.2	69.2 \pm 1.6	2.7 \pm 0.3
5 Halloysite annealed	3.8 \pm 0.2	71.3 \pm 2.5	3.2 \pm 0.3

Fig. 8: Stress-strain curve for PLA - sepiolite samples after annealing



As expected, annealing treatment is efficient in increasing strength: pure PLA strength increased of more than 16%.

Addition of clay was expected to lead to a much more significant increase in both modulus and strength; what was observed in this study, was, instead, an additional increase of around 3% for both clays, leading to the conclusion that annealing treatment is dominant over clay nucleating effect.

Nucleation enhanced crystallinity results in a slight modulus and tensile strength increase; while its effect on elongation is more significant, leading to elongation reduction of more than 70 and 50% for 0.1% wt of respectively sepiolite and halloysite.

Halloysite –PLA samples mechanical properties above a critical wt% start to decrease mainly because of the appearance of agglomerates of clays [26].

Introduction of nanoclay is often reported to be a way of improving polymer thermal stability. Increased thermal stability is attributed both to clay's good thermal stability and to the interaction between clay and polymer [27-30].

Effect of nanoclay in polymeric matrix can be explicated in two different ways: they can create a barrier or they can act as catalytic agent toward the degradation of the polymer. The first effect is more relevant when the wt% of the clay is lower, while the catalytic effect becomes more important at higher percentage of clay content leading to a decrease in polymer thermal stability as reported by Araujo et al [31] and Zhao et al. [32]

Thermogravimetric curves of pure PLA, PLA/Halloysite nanotubes and PLA/sepiolite composites are shown in figures 9 and 10. Onset temperature for calculating the beginning of the degradation process was set at -5% weight lost.

Temperature at the maximum rate of weight loss T_{mwl} 5% weight loss temperatures and residual at 750°C for each type of film are reported in table 6 for sepiolite and in table 7 for halloysite.

Fig.9: PLA/sepiolite Thermogravimetric curve

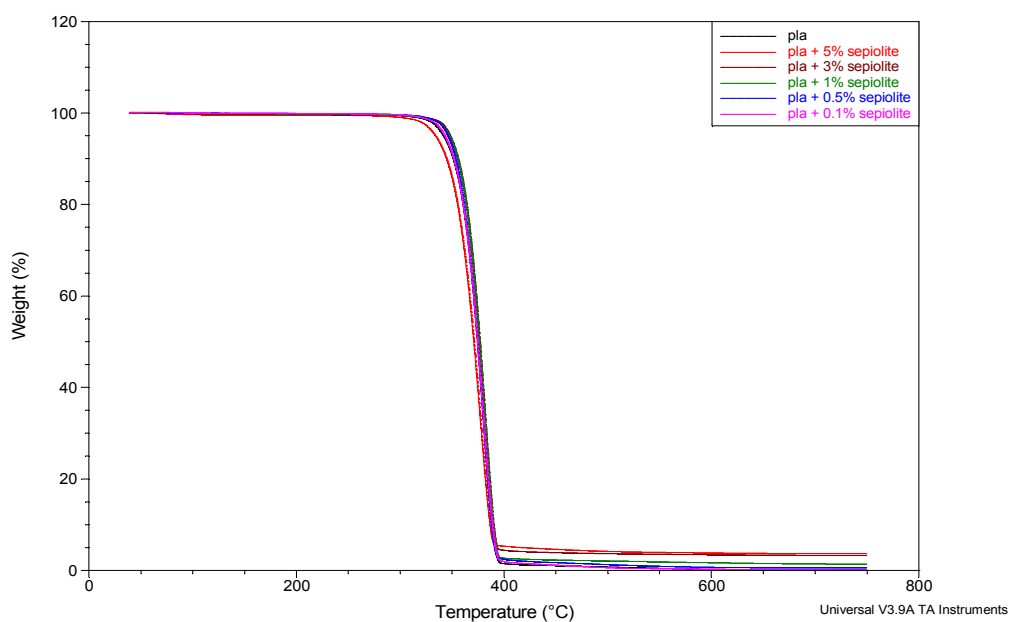
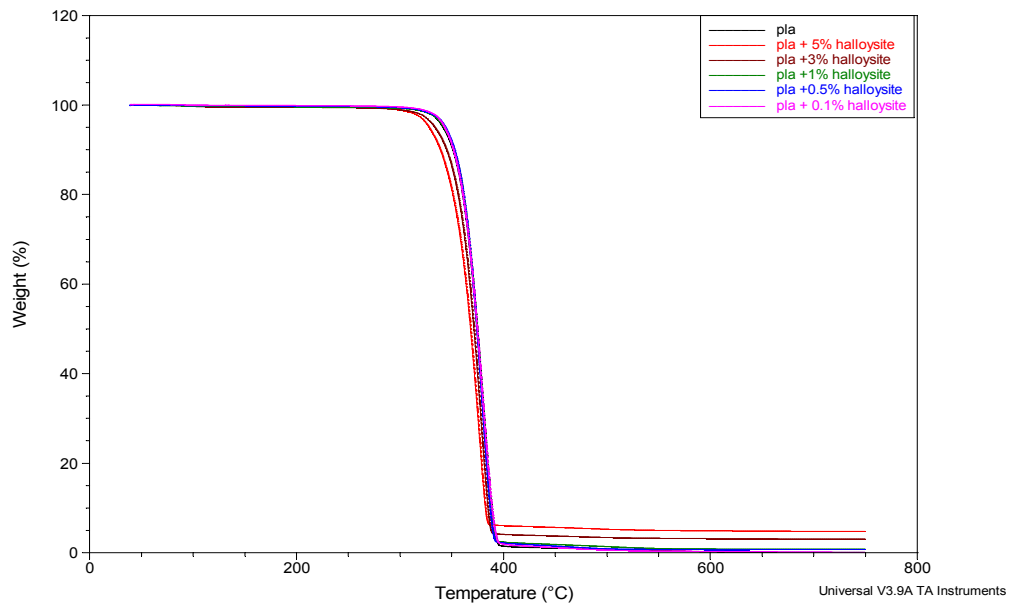


Fig.10: PLA/halloysite Thermogravimetric curve



Tab. 6: TGA Sepiolite

Sample name	T ₅ (°C)	T _{mwl} (°C)	Residual (mg)	Residual - R ₀
PLA	341.6 ± 1.4	379.1 ± 2.1	0.056 = R ₀	0
PLA + 0.1%sepiolite	341.5±1.3	379.4±1.5	0.13	0.074
PLA + 0.5% Sepiolite	345.0 ±1.7	379.1 ± 1.1	0.54	0.48
PLA + 1% Sepiolite	346.9 ± 1.6	379.1 ± 2.0	1.37	1.31
PLA + 3% Sepiolite	347.8 ± 1.9	381.9 ± 2.3	3.21	3.15
PLA + 5% Sepiolite	347.8 ± 1.6	381.0 ± 1.7	5.06	5.00

Tab. 7: TGA Halloysite

Sample name	T ₅ (°C)	T _{mwI} (°C)	Residual (mg)	Residual - R ₀
PLA	341.6 ± 1.4	379.1 ± 2.1	0.056 = R ₀	0
PLA + 0.1% Halloysite	342.3±1.3	380.3±1.5	0.17	0.11
PLA + 0.5% Halloysite	343.1 ± 1.4	389.6 ± 1.3	0.70	0.64
PLA + 1% Halloysite	341.2 ± 1.7	379.1 ± 1.8	0.79	0.73
PLA + 3% Halloysite	327.9 ± 2.0	377.2 ± 2.6	3.01	2.95
PLA + 5% Halloysite	326.9 ± 2.1	375.3 ± 2.5	4.77	4.71

To explain PLA degradation, Kopinke et al. suggested a radical reaction starting with alkyloxigen or acyl-oxygen homolysis, forming carbon monoxide and several types of oxygen-centred and carbon-centred radicals.

The onset of thermal degradation was slight higher for PLA/sepiolite composites than for the neat PLA and it increased with the amount of clay, leading to the maximum increase in thermal stability correspondent to a not relevant increment of 6°C. This behaviour is believed to be due both to the presence of the silicate acting as an insulating barrier and to the labyrinth effect due to the dispersion of clay in nanocomposites: this effect can lead to a delay in the volatilization process; while according to Wu et al.[33] the improved thermal stability can be also ascribed to the ability of clays of reorganize creating a physical barrier on PLA surface. The mechanism governing the increase in thermal stability needs further investigation. Halloysite addiction leads to a decrease in thermal stability that is more pronounced at higher percentage of clay. These results are ascribed to a reduced contact surface between polymeric matrix and clay due to the formation of aggregates as demonstrated by SEM topographies.

There can be translucency only if the average size of the dispersed phase is smaller than visible light's wavelength.

Pictures of PLA-sepiolite and PLA-halloysite composites were taken to show the not significant effect of these two kinds of clays on PLA optical properties at a macroscopical level.

Figures 10 and 11 show sepiolite and halloysite specimen, one specimen per each percentage of clay was used. Transparency decreases with the amount of clay for each kind of clay, but samples remain mainly transparent due both to the good distribution and the small amount of clays introduced in them for percentage of clays lower than 3%. There is a much more evident loss of transparency at 5% of halloysite clay, due to the reported lack of dispersion and formation of aggregates as discovered after SEM tests, but also if samples are cloudier; there is still no problem in reading through the films.

Fig. 10: Translucency of PLA-sepiolite samples

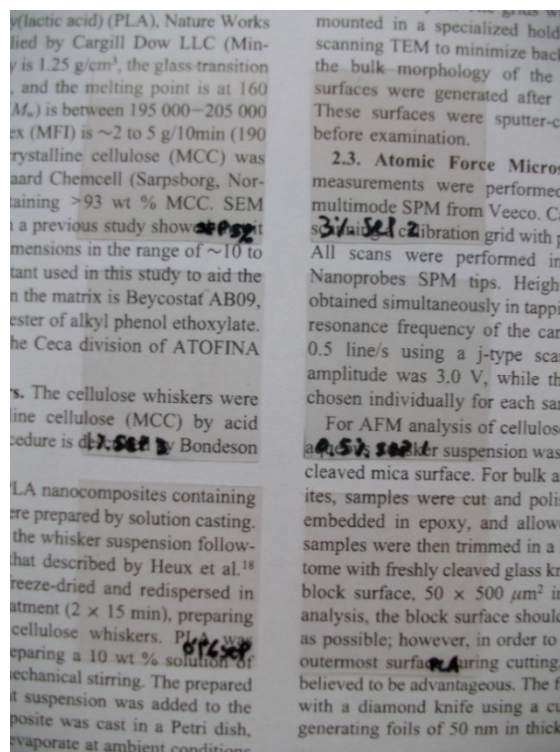
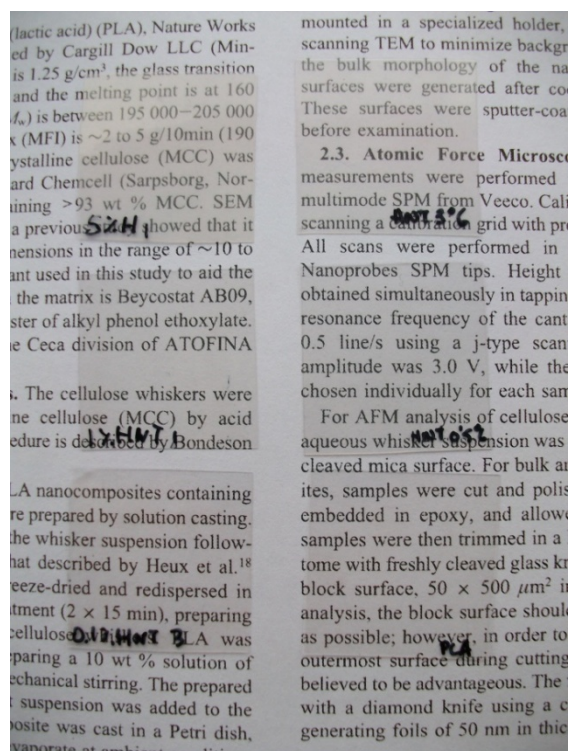


Fig. 11: Translucency of PLA- halloysite samples



6 Conclusions

In this work, it was demonstrated that good dispersion of sepiolite or halloysite clays can be obtained for filler loadings up to 3wt%, especially for sepiolite /PLA composites. This could be attributed to the good interaction between PLA and sepiolite due to the hydrogen bonding between the carbonyl group of PLA and the hydroxyl group of sepiolite. Sepiolite maintained its geometry throughout the processing regime while the halloysite nanotubes fractured during processing.

All samples showed a good transparency with no significant changes with increasing amount of clay, especially for sepiolite.

Absence of crystallization peak after annealing treatment for clay percentage higher than 0.5% showed that the clays serve as nucleating agent and increases in crystallinity with increase in clay concentration confirm this result. Annealing treatment as expected has a strong effect on PLA matrix, leading to a significant increase in crystallinity for both PLA and PLA composites as a consequence of the reduced free volume of the matrix.

Changes in mechanical properties were not significant in the presence of clay. A slight variation of in the Young's and yield strength is obtained after annealing in presence of clay, however, annealing treatment itself leads to a significant enhancement on tensile strength.

Absorption tests showed a significant reduction of water absorption for sepiolite-PLA composite at percentages of 0.5; 1 and 3%, probably thanks to the good dispersion of the clay, while halloysite tubular shape is believed to induce increase in water absorption.

Addition of nanosized fillers caused the time lag to increase significantly: the presence of the fillers in the polymer decreases diffusion coefficients compared to neat PLA by inducing a more tortuous path for the diffusing gas molecules.

Annealing was demonstrated to be an efficient treatment to increase modulus and tensile strength as consequence of reduced free volume and increased crystallinity of the polymeric matrix

Bibliography

- [1] Holten, C.H., Lactic Acid, Properties and Chemistry of Lactic Acid and Derivatives, Verlag Chemie, GmbH, Weinheim/Bergstr., 1971.
- [2] Schopmeyer, H.H., Lactic Acid, in Industrial Fermentations, Underkofler, L. And Hickley, R.J., Eds., Chemical Publishing Co. New York, NY, 1954, chap. 12.
- [3] Cox, G. and Macbean, R., Lactic Acid Recovery and Purification Systems, Research Project Series, No. 29, October, 1976.
- [4] Urayama, H., Kanamori, T., and Kimura, Y., Properties and biodegradability of polymer blends of poly(L-lactides) with different optical purity of the lactate units, *Macromole. Mater. Eng.* 287, 116, 2002.
- [5] Janzen, J., Dorgan, J.R., Knauss, D.M., Hait, S.B., and Limoges, B.R., Fundamental solution and single-chain properties of polylactides, *Macromolecules*, 2003.
- [6] Ikada, Y., Jamshidi, K., Tsuji, H., and Hyon, S.H., Stereocomplex formation between enantiomeric poly(lactides), *Macromolecules* 20, 904, 1987.
- [7] Tsuji, H. and Ikada, Y., Stereocomplex formation between enantiomeric poly(lactic acid)s. XI. Mechanical properties and morphology, *Polymer*, 40, 6699, 1999.
- [8] Tsuji, H. and Ikada, Y., Properties and morphologies of poly(L-lactide): 1. Annealing condition effects on properties and morphologies of poly(L-lactide), *Polymer*, 36, 2709, 1995.
- [9] Fischer, E.W., Sterzel, H.J., and Wegner, G., Investigation of the structure of solution grown crystals of lactide copolymers by means of chemical reactions., *Kolloid Ze. Ze. fuer Polym.*, 251, 980, 1973.
- [10] Kolstad, J.J., Crystallization kinetics of poly(L-lactide-co-meso-lactide, *J. Appl. Polym. Sci.*, 62, 1079, 1996.
- [12] Shchukin D G, Sukhorukov G B, Price R R, Lvov Y M, Halloysite nanotubes as biomimetic nanoreactor. *Small* 1, 510 (2005)
- [13] Nalinkanth G V, Dmitriy M, Vladimir T, Ronald R P, Yuri M L, Organized shells on clay nanotubes for controlled release of macromolecules. *Macromol. Rapid Commun*, 30, 99 (2009)
- [14] Levis S R, Deasy P B, Characterization of Halloysite for use as microtubular drug delivery system. *Int. J. Pharm* 243, 125 (2002)

- [15] J. Ma, E. Bilotti, T. Peijs, J. A. Darr, *Eur. Polym. J.* 2007, 43, 4931.
- [16] E. Bilotti, H. R. Fischer, T. Peijs, *J. Appl. Polym. Sci.* 2008, 107, 1116.
- [17] E. Bilotti, R. Zhang, H. Deng, F. Quero, H. R. Fischer, T. Peijs, *Compos. Sci. Technol.* in press, DOI: 10.1016/j.compscitech.2009.07.016
- [18] H. Fischer, *Mater. Sci. Eng. C* 2003, 23, 763.
- [19] E. Morales, M. C. Ojeda, A. Linares, J. L. Acosta, *Polym. Eng. Sci.* 1992, 32, 769.
- [20] J. L. Acosta, M. C. Ojeda, E. Morales, A. Linares, *J. Appl. Polym. Sci.* 1986, 31, 2351.
- [21] J. L. Acosta, M. C. Ojeda, E. Morales, A. Linares, *J. Appl. Polym. Sci.* 1986, 31, 1869.
- [22] Yuzay I E, Auras R, Selke S. *J. Appl. Polym. Sci.*, Vol. 115, 2262–2270 (2010)
- [22] A. Marcilla, A. Gomez, S. Menargues, R. Ruiz, *Polym. Degrad. Stab.* 2005, 88, 456.
- [23] Yasuniwa M, Sakamo K, Ono Y, Kawahara W, *Polymer* 49 (2008) 1943
- [24] Zhou H, Green TB, Joo L, *Polymer* 47 (2006) 7497.
- [25] Yasuniwa M, Tsubakihara S, Iura K, Ono Y, Dan Y, Takahashi K, *Polymer* 47 (2006) 7554
- [26] Chang J-H, An Yu, Sur GS. *J Polym Sci, Part B: Polym Phys* 2003; 41:94
Chang J-H, An Yu. *J Polym Sci, Part B: Polym Phys* 2002; 40:670
- [27] Wen J, Wilkes GL. *Chem Mater* 1996;8;1667
- [28] Zhu ZK, Yang Y, Wang X, Ke Y, Qi Z. *J Appl Polym Sci* 1999;3:2063
- [29] Petrovic XS, Javni L, Waddong A, Banhegyi GJ. *J Appl Polym Sci* 2000;76:133
- [30] Fisher HR, Gielgens LH, Koster TPM. *Acta Polym* 1999;50:122
- [31] E. M. Araújo, R. Barbosa, A. W. B. Rodrigues, T. J. A. Melo, and E. N. Ito, "Processing and characterization of polyethylene/Brazilian clay nanocomposites," *Materials Science and Engineering A*, vol. 445-446, pp. 141–147, 2007.
- [32] C. Zhao, H. Qin, F. Gong, M. Feng, S. Zhang, and M. Yang, "Mechanical, thermal and flammability properties of polyethylene/clay nanocomposites," *Polymer Degradation and Stability*, vol. 87, no. 1, pp. 183–189, 2005.
- [33] Wu D; Wu L; Zhang M., *Polymer degradation and stability* 91, 3149 2006.

[34]Gilman J, Kashiwagi T, Giannelis E, Manias E, Lomakin S, Lichtenhan J, Jones P., Special publication royal Societe of chemistry 224, 203 1998.

Chapter 4

Study on PLA-zeolite and PLA-bentonite composites

Study on PLA-zeolite and PLA-bentonite composites

1 Materials

1.1 PLA2002D was used as matrix. Its specific are reported chapter 3 in paragraph 2.1.

1.2 Zeolite

The structure of Zeolites is made up of SiO_4 and AlO_4 tetrahedra, forming a network of channels and cavities that gives zeolite its characteristic of ion exchange capacity, reactivity and adsorptivity [1, 2]. Polymer composites containing zeolite have been produced using different kinds of doping agents to change electrical conductivity of polymeric matrix [3, 4]. Furthermore, good antimicrobial properties have been obtained in nanocomposites containing zeolite whose sodium ions were exchanged with silver ions [2, 5] and has also been reported to be used in active food packaging applications [5].

Some studies have underlined the importance of surface treatment of zeolite to obtain a good dispersion in the polymeric matrix [6]; while other studies have shown that surface treatment can lead to pore blockage, causing inferior gas and liquid separation [7].

In this study non-modified zeolite was used.

1.3 Bentonite

Bentonite is an aluminium phyllosilicate consisting mostly of montmorillonite, which is made of tetrahedral silicate sheets linked through a shared oxygen atom to an octahedral sheet [8]. Layered silicates have been used to modify polymers by including them in polymeric chain after the layers are swollen to help introduction of polymeric chain [9, 10, 11]. The composite formed has been reported to have improved mechanical, thermal and barrier properties [12, 13]. The bentonite used in this study was not modified; the clay was not swollen by.

2 Preparation and characterization

PLA-zeolite and PLA-bentonite composites at 0.1, 0.5, 1, 3 and 5 wt % were obtained from master-batch containing 15wt% of the clay according to the procedure described in chapter 3 paragraph 3.1. The master-batches (15% of zeolite or bentonite) were extruded in a mini twin-screw extruder DSM Micro 15 at 190°C, using a screw -speed of 200 rpm for 5 minutes.

The composites at the required clay concentration were prepared from the master-batch via dilution and they were extruded at the same processing conditions used for the masterbatch.

PLA-Zeolite and PLA-Bentonite films were produced via compression moulding according to the procedure reported in chapter 3 paragraph 3.2.

It was not possible prepare zeolite films at percentage of clay higher than 1%-wt. due to high brittleness: films at 3 and 5% of zeolite were recovered completely broken after compression moulding and were unusable for characterisation, especially for mechanical properties.

All the obtained films were annealed at 80°C for 24h to study annealing effect on crystallinity. Both annealed and non-annealed samples were characterized using SEM, TGA, DSC, mechanical and absorption test setup according to the procedures described in chapter 3 paragraph 4.

3 Results and discussion

SEM micrographs of zeolite-PLA and bentonite-PLA composite were taken to observe the dispersion of the clays into PLA matrix. The SEM images for 0.1%-wt zeolite-PLA and 0.1%-wt bentonite-PLA films are reported in figures 1a, 1b and 2a, 2b respectively

Fig.1a, SEM of PLA+0.1wt% zeolite

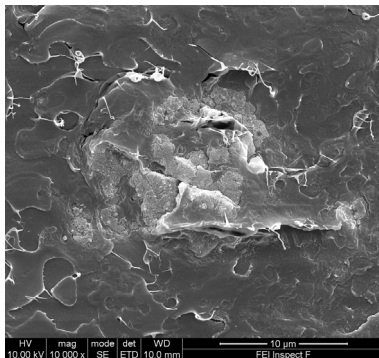


Fig.1b, SEM of PLA+0.1wt% zeolite

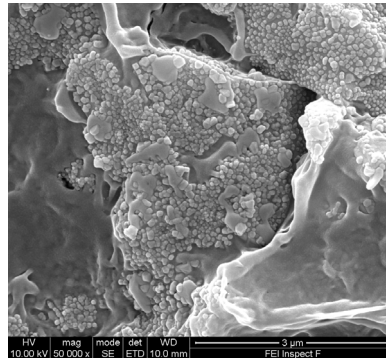


Fig.2a, SEM of PLA+0.1wt% bentonite

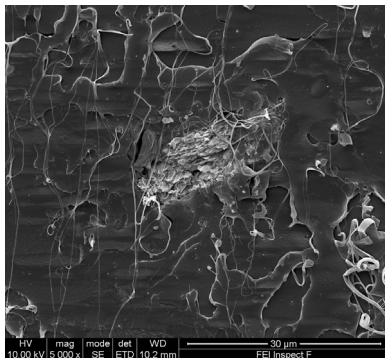
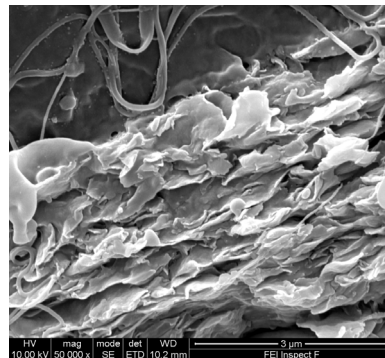


Fig.2b, SEM of PLA+0.1wt% bentonite



From the SEM images it is clear that dispersion of the clay is poor in both types of samples.

Both zeolite and bentonite reinforced composites show the presence of aggregates at the lowest reinforcement percentage of clay. The formation of aggregate at such low

concentration could be attributed to the bad interfacial adhesion between the clays and the PLA matrix due to the use of not modified clay.

Table 1a and 1b report the percentage of crystallinity for annealed and not annealed PLA-zeolite samples from the first scan of DSC; while table 2a and 2b reports the same data for PLA-bentonite composites. Figure 3 show the first DSC scan for annealed PLA-bentonite composites films.

Tab.1a

Samples name	X_c (%)
PLA not annealed	2.7±0.3
0.1%zeolite not annealed	2.5±0.3
0.5%zeolite not annealed	5.1±0.3
1%zeolite not annealed	5.3±0.2

Tab.1b

Samples name	X_c (%)
PLA annealed	18.1±0.6
0.1%zeolite annealed	16.1±0.4
0.5%zeolite annealed	20.8±1.1
1%zeolite annealed	23.7±0.5

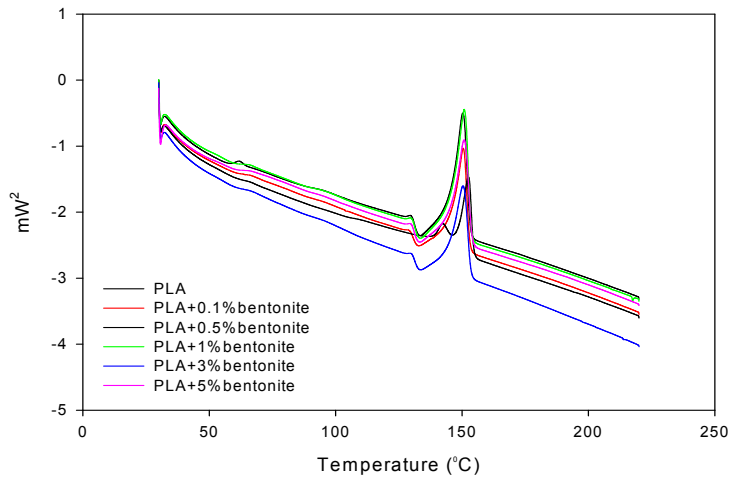
Tab.2a

Samples name	X_c (%)
PLA not annealed	2.7±0.3
0.1%bentonite not annealed	1.4±0.1
0.5% bentonite not annealed	4.3±0.2
1% bentonite not annealed	4.2±0.1
3% bentonite not annealed	7.8±0.3
5% bentonite not annealed	6.3±0.4

Tab.2b

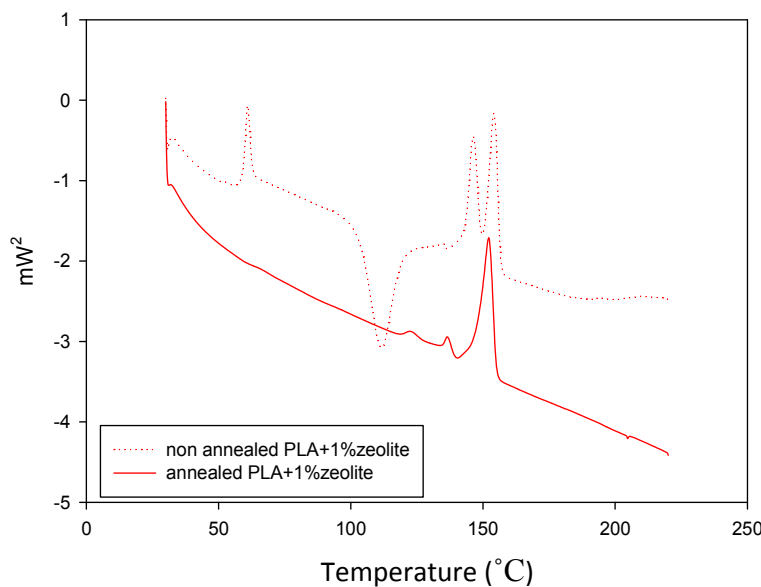
Samples name	X_c (%)
PLA annealed	18.1±0.6
0.1% bentonite annealed	18.8±1.2
0.5%bentonite annealed	17.7±1.8
1% bentonite annealed	17.9±1.3
3% bentonite annealed	15.5±1.3
5% bentonite annealed	16.8±0.7

Fig.3 First DSC scan for annealed bentonite-PLA composites



Generally, the addition of clays is reported to enhance crystallinity and reduce T_c for PLA-based composites as a consequence of clay nucleating effect. In the case of the clays used in this preliminary study, there is some evidence of this kind of effect. PLA-zeolite samples crystallinity increased while T_c decreased with clay percentage. This trend is reported also for not annealed samples, but it is enhanced by the physical aging process that lead to much higher crystallinity. In figure 4, first DSC scan is reported for annealed and not annealed zeolite-PLA composites at 1%wt of clay. PLA-zeolite samples at 1% of clay showed a significantly enhanced crystallinity and the T_c peak after annealing completely disappears.

Fig.4 First DSC scan for annealed and not annealed 1%wt. Zeolite-PLA composites



A similar nucleating effect of zeolites in PLA crystallization has been reported by Yuzay and co-workers [14].

The non-annealed 1% zeolite reinforced samples show an increase in their crystallinity around 96% when compared to non-annealed pure PLA films. Post annealing results showed that 1%zeolite-PLA films compared with pure PLA film had an increment in crystallinity by 30% and could be attributed to the presence of zeolite clay.

Bentonite reinforced samples did not show any significant variation of percentage crystallinity after annealing when compared to pure PLA, leading to hypothesis that these values are due to the annealing effect on PLA matrix itself and not strongly influenced by the presence of the clay. In absence of annealing treatment, the crystallinity increase of around 133% for composites at 5wt% of bentonite.

The annealing treatment on pure PLA enhances the crystallinity of around 570%.

The results of the crystallinity level for non-annealed PLA-bentonite and PLA-zeolite films compared with their annealed counterparts, suggests that the presence of clay can play a more important role in absence of annealing treatment that, otherwise, becomes the principal cause of increased crystallinity.

Both for zeolite and bentonite composites the relaxation peak reported for not annealed samples independently from clay percentage decreased significantly after annealing and then it disappears as a consequence of chain reorganization induced by annealing treatment in presence of clay.

Another interesting phenomenon is the appearance of a double melting peak for both annealed and non annealed PLA-1%zeolite reinforced samples. This bimodal peak was reported also by Yuzay and colleagues [14] and it is reported to be more pronounced as zeolite content was increasing. PLA double (or bimodal) melting peak is reported to be due to the formation of two different crystalline structures [15, 16, 17]. The most common polymorphism for PLA is the alpha form which has a pseudo-orthorhombic or pseudo-hexagonal structure [17], and it melts at higher temperature while beta form can be orthorhombic or triagonal and melt at lower temperature [17].

The double peak is also reported to be due to the reorganization of imperfect crystals formed during cold crystallization of crystals that melt at higher temperature [18].

Annealing effect on crystallinity is widely reported as well as clay nucleating effect [14]. The results presented in this study show that there is a stronger effect of annealing treatment on pure PLA's crystallinity. However, annealing of the clay/PLA composites do not show any significant further increase in crystallinity that could have been caused by the presence of the clay and thus nucleating effect of both zeolite and bentonite is less significant. A possible explanation for the low nucleating effect of both clays on PLA matrix is the lack of dispersion and interfacial adhesion due to the absence of compatibilization between clay and matrix.

Table 3 and 4 shows 1% weight loss temperatures, temperature at the maximum rate of weight losses T_{mwl} and residual material at 750°C for PLA-zeolite and PLA-bentonite films.

Tab.3, 1% weight loss temperatures, temperature at the maximum rate of weight loss T_{mwl} and residual at 750°C (error ± 2 °C)

Samples name	$T_{-1\%}$ (°C)	T_{mwl} (°C)	Residual- R_0 0.056 = R_0
PLA	308.7	379.1	0
0.1%zeolite annealed	306.6	378.7	0.12
0.5%zeolite annealed	267.4	379.3	0.55
1%zeolite annealed	245.1	375.3	0.92

Tab.4, 1% weight loss temperatures, temperature at the maximum rate of weight loss T_{mwl} and residual at 750°C (error ± 3 °C)

Samples name	$T_{-1\%}$ (°C)	T_{mwl} (°C)	Residual- R_0 0.056mg = R_0
PLA	308.7	379.1	0
0.1% bentonite annealed	308.9	379.4	0.08
0.5%bentonite annealed	303.8	380.4	0.45
1% bentonite annealed	291.9	376.3	0.6
3% bentonite annealed	283.5	379.3	2.6
5% bentonite annealed	285.5	382.3	3.3

In both cases the presence of clays acts as a thermal destabilize for composites leading to a lower temperature for the onset of the degradation process.

Ogata et al [19] reported that clay seem to retard the deformation of PLA composites' crystalline structure at low temperature, while they can act as degradation accelerator at higher temperature. Similar results are obtained also in other studies on PLA composites [20].

Figure 5 and 6 show the thermo-gravimetric diagram for all the concentrations of zeolite and bentonite respectively.

Fig.5: Zeolite – PLA thermo-gravimetric diagram

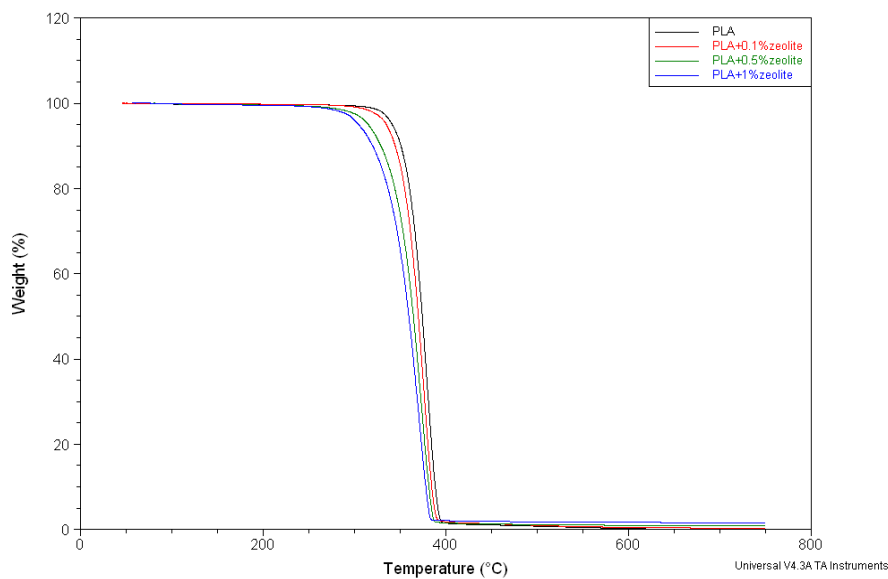
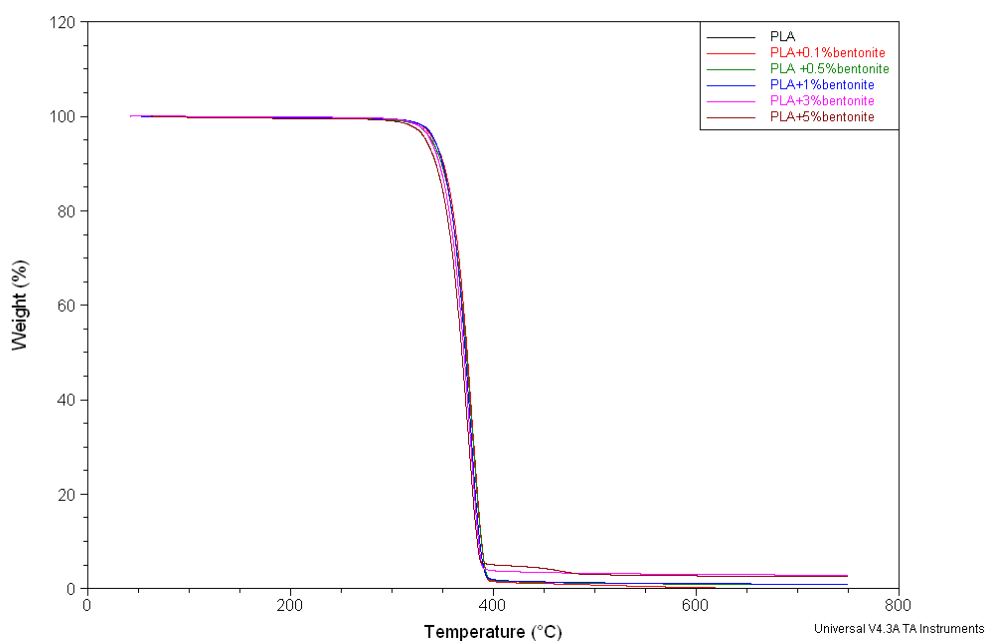


Fig.6: Bentonite – PLA thermo-gravimetric diagram



Mechanical tensile tests were also run, but they are not reported, due to the high dispersion of data caused by the lack of dispersion showed by SEM analysis as reported in fig.1a, 1b and 2a, 2b. Cracks initiate and propagate in areas where the aggregates are present [21]. Both zeolite and bentonite composites break in the regions of the macroscopically visible aggregates and this is independent from the percentage of clay and annealing or non-annealing treatment.

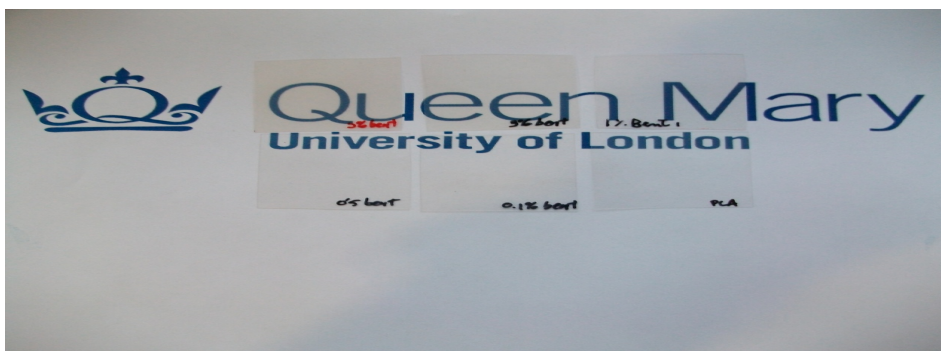
Absorption tests were also done on these samples, but, like in the case of mechanical tests, the obtained results are not reported due to their high dispersion due to the macroscopic defect visible on both zeolite and bentonite films.

To confirm the slight change in optical properties, pictures of zeolite and bentonite films at each concentration were taken and compared with pure PLA films. Looking at the pictures, it is not possible to see the presence of aggregates, but it is clear the lack of dispersion: films at higher percentage of clay were cloudier although there were still no problems in reading through the films. Figures 7 and 8 show samples of zeolite and bentonite respectively.

Fig. 7: Translucency of PLA films containing 0 (pure PLA), 0.1, 0.5 and 1 wt% of zeolite



Fig.8: Translucency of PLA films containing 0 (pure PLA), 0.1, 0.5, 1, 3 and 5 wt% of bentonite



4 Conclusions

Zeolite – PLA and bentonite-PLA composites properties were strongly influenced by the presence of aggregates even for samples at the lowest percentage of reinforcements as showed by SEM analysis. Cracks initiate and propagate in areas where the aggregates are present. Both zeolite and bentonite composites during tensile tests broke in the regions of the macroscopically visible aggregates and this is independent from the percentage of clay and annealing treatment. Composites crystallinity increased while T_c decreased with clay percentage both for zeolite-PLA and bentonite-PLA samples. This trend is reported also for annealed samples, but it is enhanced by the physical aging process that lead to much higher crystallinity. Results related to DSC lead to the hypothesis that annealing treatment can be dominant over clay nucleating ability. Zeolite-PLA and bentonite-PLA composites behavior has been explained in term of lack of dispersion. The formation of aggregates has been attributed to the nature of the clays, their interaction with PLA matrix and interfacial adhesion as a consequence of the absence of compatibilizer between clay and matrix. Natural clay zeolite and bentonite were therefore not considered for further investigations as PLA reinforcing agents.

Bibliography

- [1] Barrer, R. M. Zeolites and Clay Minerals as Sorbents and Molecular Sieves; Academic Press: London, 1978.
- [2] Yang, R. T. Adsorbents: Fundamentals and Applications; Wiley: Hoboken, NJ, 2003
- [3] Chuapradit, C.; Wannatong, L. R.; Chotpattananont, D.; Hiamtup, P.; Sirivat, A.; Schwank, J. Polymer 2005, 46, 947.
- [4] Vitoratos, E.; Sakkopoulos, S.; Dalas, E.; Malkaj, P.; Anestis, C. Curr Appl Phys 2007, 7, 578
- [5] Brody, A.; Strupinsky, E.; Kline, L. Active Packaging for Food Applications; Technomic Publishing Co: Lancaster, PA, 2001
- [6] Mahajan, R.; Koros, W. J. Polym Eng Sci 2002, 42, 1432.
- [7] Moore, T. T.; Koros, W. J. J Mol Struct 2005, 739, 87.
- [8] Zilg C, Dietsche F, Hoffmann B., Macromol.Symp., 169, 65 (2001).
- [9] Rehab A, Salahuddin N., Mater. Sci. Eng., 399, 368 (2005).
- [10] Akelah A, Kelly P, Qutubuddin S., Clay miner, 29, 169 (1994).
- [11] Gultek A, Seckin T, Onal Y, J. Appl. Polym. Sci., 81, 512 (2001).
- [12] Tien Y I, Wei K H, J. Appl. Polym. Sci.,86, 1741 (2002).
- [13] Wanjale S D, Jog J P., J. Appl. Polym. Sci., 90, 3233 (2003).
- [14] Yuzay I E, Auras R, Selke S. J.Appl. Polym Sci,Vol. 115, 2262–2270 (2010)
- [15] Yasuniwa M, Sakamo K, ono Y, Kawahara W, polymer 49 (2008) 1943
- [16] Zhou H, Green TB, Joo L, Polymer 47 (2006) 7497.
- [17] Yasuniwa M, Tsubakihara S, Iura K, ono Y, Dan Y, Takahashi K, Polymer 47 (2006) 7554

- [18] Vink E T H, Rabago K R, Glassnerb D A, Gruber P R, Polym. Degrad.Stab.80 (2003) 403
- [19] Ogata N, Jimenez G, Kawai H, Ogihara T. J Polym Sci, Part B: Polym Phys 1997;35:389
- [20] Jin-Hae Chang, Yeong Uk An, Donghwan Cho and Emmanuel Giannelis, Polym Vol 44, Issue 13 (2003), 3715-3720
- [21]Masenelli-Varlotk, Reynaud E, Vigier G, Varlet J.J Polym Sci, Part B: Polym Phys 2002;40:27

Chapter 5

PLA-clay oriented film

PLA-clay oriented film

1 Introduction

PLA is an environmental friendly material and its use can be particularly suitable for application in which packaging, or generally product, recovery is not operable or too complex, such as in the case of agricultural mulching. PLA compostability makes it the ideal candidate for food packaging application: PLA can be disposed with leftover food.

On the other hand, PLA slow crystallization kinetic is a limiting factor for using it for some application. Stress-induced crystallization, thanks to a wide processing window, has been reported to lead to good results: PLA can be oriented during processing like fiber spinning or film stretching in the melted or rubber state, thanks to its semi-crystalline nature.

Kwolek et al. [1] were the first to successfully find a method to produce stronger and stiffer fiber aligning molecules in the direction of fiber axis. Since then polymer science and industrial research have started focusing their attention on oriented polymer due to the discovery of methods to produce highly oriented polymers [2, 3]. It was commonly recognized since 1930 [2] that if a polymeric chain, such as Polyethylene (PE) was completely extended, it would be extremely stiff in the direction of the chain axis.

Two different methods can be used to obtain fully aligned chain: solution processing or solid state deformation.

The first success was achieved by solid state deformation from Capaccio and Ward [4]: a stretched polymer chain network was obtained by solid state drawing between T_g and T_m .

Kokturk et al. [5] have reported PLA ideal stress-strain behaviour in the temperature range 65-80 °C. They have also referred that, after stretching at high deformation, crystallization and strain hardening lead to uniform thickness as a consequence of a self levelling effect induced by orientation.

Lee et al. [6] have been studying the effect of uniaxial drawing condition on PLLA samples reaching the conclusion that orientation in uniaxial stretched PLLA is

influenced by drawing rate, drawing temperature and draw ratio and that spherulites under drawing can be deformed into new crystal morphologies. They also reported that film shrinkage is linked to crystallinity level and orientation of amorphous phase. Increasing of crystallinity with draw ratio has also been reported by Cicero et al. [7, 8].

In this study sepiolite and halloysite clay were used to produce nanocomposites that were oriented using solid state deformation technique.

Fibrous filler have been reported to be more effective to reinforce unidirectional composites [9]. Use of sepiolite and halloysite in this kind of application can be of high interest because of their one dimensional-like shape that, after the application of uniaxial deformation, can lead to alignment of clay along the polymer creating a 1d polymer reinforced by 1d fillers.

Orientation, creating highly anisotropic structures, is a way to produce high stiffness and strength in polymer [10, 11] and nanoparticles are suggested to be possible orientation enhancers [12].

2 Materials

2.1 PLA

PLA2002D, from NatureWorks, was used as matrix. It is specifically designed for extrusion/ thermoforming applications. This PLA has a D content of 4.25%, a residual monomer of 0.3% and a density of 1.24g/cm³.

2.2 Sepiolite

Sepiolite Pangell were supplied by Tolsa (Madrid, Spain). The characteristic averaged dimensions of the individual sepiolite fibers are 1–2 mm in length and 20–

30 nm in diameter, its BET surface area is 320 m²/g and its aspect ratio is within the range of 100–300.

2.3 Halloysite

Halloysite G produced by Atlas Mining, Nanoclay Technology Division and available from Sigma-Aldrich, was used as reinforce. This material has an average tube diameter of 50 nm and an inner lumen diameter of 15 nm. This halloysite has the following properties: a typical specific surface area of 65 m²/g, a pore volume of ~ 1.25 mL/g, a refractive index of 1.54 and a specific gravity of 2.53 g/cm³

3 Method

Composites at 0.5 and 1%wt. of each clay were prepared from masterbatch at 15% of clays, than diluted at the desiderate percentage and finally extruded using a mono screw extruder with a flat die to produce films.

3.1 Preparation of master-batch at 15% of clay

Master-batch at 15% of sepiolite and halloysite were prepared using a Mini twin-screw extruder DSM Micro 15. Extrusions were performed at 190°C, using screws speed of 40 rpm, setting the residence time at 5 minutes under nitrogen filled atmosphere.

3.2 Preparation of PLA-clay composites

Nanocomposites at 0.5 % and 1%wt. of clay were prepared from master-batch at 15% of clays (respectively sepiolite and halloysite), using a twin screw extruder Collin ZK25 type KNETER attached at a water bath, Collin water-bath teach line. Extrusion profile temperatures, screws speed and feeding speed are reported below.

(150-165-180-190-190-180-180-165) °C, 3kg/h, 35 rpm

3.3 Preparation of films

PLA-sepiolite and PLA –halloysite films at 0.5 and 1% wt. of clays were prepared using a mono screw extruder, Collin E20T, with an attached Flat-Film Take-Off Unit CR 72T flat die with fixed lips fro film from 20 to 1000microm.

Extrusion conditions:

(150-160-180-180-165) °C, 70 rpm

Flat-film take-off unit conditions:

70 °C, 4rpm, 3rpm

3.4 Orientation

A previous study was conducted to determine orientation conditions and it is reported in chapter 6. Films orientation was conducted using Mono-Axial Stretching Units MDO-AT and MDO-BT. The first zone temperature, MDO-AT, was set at 90°C, while the second at 70°C. Draw ratio was set at 2.

4 Characterizations

4.1 Thermal tests:

DSC

DSC tests were conducted using a METTLER device under nitrogen atmosphere according to the following cycle:

5 minutes isothermal at 30°C , dynamic at 10°C /min from 30°C to 180°, 5 min isothermal at 180°C, cooling down to 30°C at 10 °C /min, 5 minutes isothermal at 30 °C than heat up to 180 °C at 10 °C /min.

TG

Thermogravimetric analysis (TGA) was conducted on a TA Instruments Q500 device in the range of temperature 40÷750°C with a ramp rate of 10°C/min in a nitrogen-filled environment

4.2 Absorption tests

These tests were run to determine the rate of absorption of water by PLA based film during immersion.

Standard designation D 570 was used as a guideline to setup experiment, being the dimension of produced specimen a natural limit (specimen maximum width was 2cm). In this study specimen were cut into rectangle of 1.5cm x 4 cm. Before being tested, specimens were stored into a desiccator at room temperature for 24 hours. During tests specimen were placed into a container filled with distilled water for 24 hours at maintained at room temperature. At the end of each test, specimen surface was wiped off using dry cloth, then immediately weight using an analytic balance capable of reading 0.0001g. After immersion and after checking the weight, each specimen was reconditioned using the initial drying condition, to check the existence of any difference in weight to the presence of water-soluble ingredients.

Percentage increase in weight during immersion was calculated according to the following formula:

$$\text{Increase in weight} = (\text{wet weight} - \text{conditioned weight}) * 100 / \text{conditioned weight}$$

Water absorption was obtained from increase in weight dividing it for each specimen average thickness, according to the following formula:

$$A = \text{Increase in weight} / \text{specimen average thickness}$$

4.3 SEM

Morphological analyses were carried out using a Jeol JSM-6300F Scanning Electron Microscope (SEM) on gold coated, cold fractured samples. Brittle fracture was obtained after immersion in liquid nitrogen.

4.4 Birefringence

The polarized light microscope is designed to observe and photograph specimens that are visible due to their optically anisotropic character. The microscope must be equipped with both a polarizer, positioned in the light path somewhere before the specimen, and an analyzer (a second polarizer), placed in the optical pathway between the objective rear aperture and the observation tubes or camera port. Image contrast arises from the interaction of plane-polarized light with a birefringent (or doubly-refracting) specimen to produce two individual wave components that are each polarized in mutually perpendicular planes. Birefringence analyses were carried out using a Leica TCS SP5.

4.5 Tensile tests

Tensile tests were conducted to determine tensile strength, elastic modulus and elongation at break of the films using a Universal Mechanical Test Frame Instron 5566 equipped with a 1-kN load cell, using a rate of 5mm/min.

Film specimens were cut into dog-bone shape with a length of 43mm and an average thickness of 0.10mm.

5 Results and discussion

Thermal tests were run to determine the percentage of crystallinity and how crystallization was influenced both by drawing process and presence of clays. In table 1 are reported: glass transition, relaxation enthalpy, crystallization and melting temperatures and the degree of crystallinity of the polymers at each concentration before and after drawing. Diagram 1 shows X_c (%) versus clay's percentage both for oriented and untreated PLA films.

Tab.1: Sample name, T_g , T_c , T_m (error $\pm 2^\circ\text{C}$) and X_c

Sample name	Draw ratio	T_g ($^\circ\text{C}$)	ΔH_{relax} (Jg^{-1})	T_c ($^\circ\text{C}$)	T_m ($^\circ\text{C}$)	X_c (%)
PLA	1	56.8	8.1	125.5	149.2	3.30 \pm 0.3
PLA	2	59.9	5.4	108.2	146.2	5.75 \pm 0.3
PLA+0.5%sep	1	58.0	7.03	121.1	148.7	3.50 \pm 0.2
PLA+0.5%sep	2	57.1	0.89	86.3	149.5	15.41 \pm 1.0
PLA+1%sep	1	57.9	8.5	128.4	150.1	3.71 \pm 0.5
PLA+1%sep	2	56.9	2.1	86.6	148.9	16.11 \pm 0.2
PLA+0.5%HNT	1	57.8	9.9	113.22	147.4	3.02 \pm 0.8
PLA+0.5%HNT	2	58.2	2.3	88.9	149.9	12.58 \pm 0.7
PLA+1%HNT	1	57.7	6.7	113.72	147.1	3.51 \pm 0.6
PLA+1%HNT	2	57.2	2.4	88.7	149.2	12.24 \pm 0.7

Diagram1: X_c (%) versus clay's percentage both for oriented and untreated films

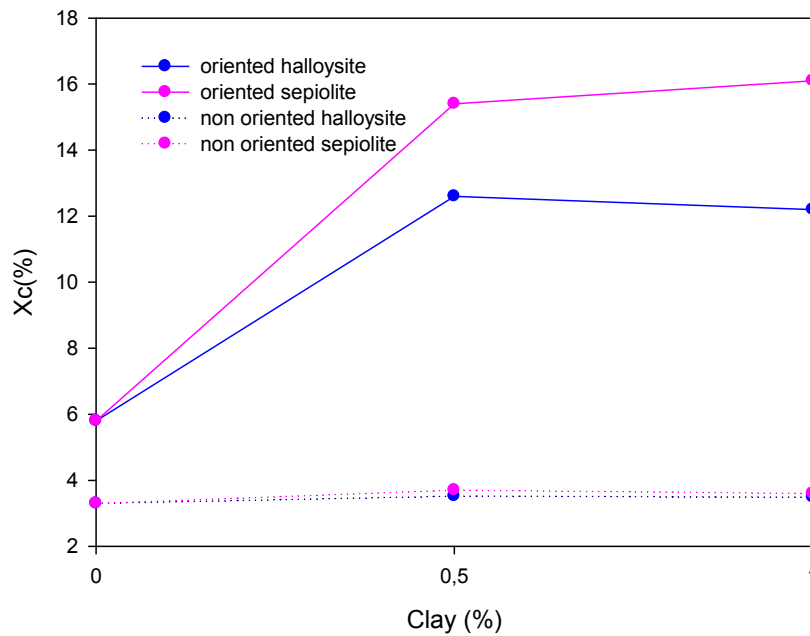
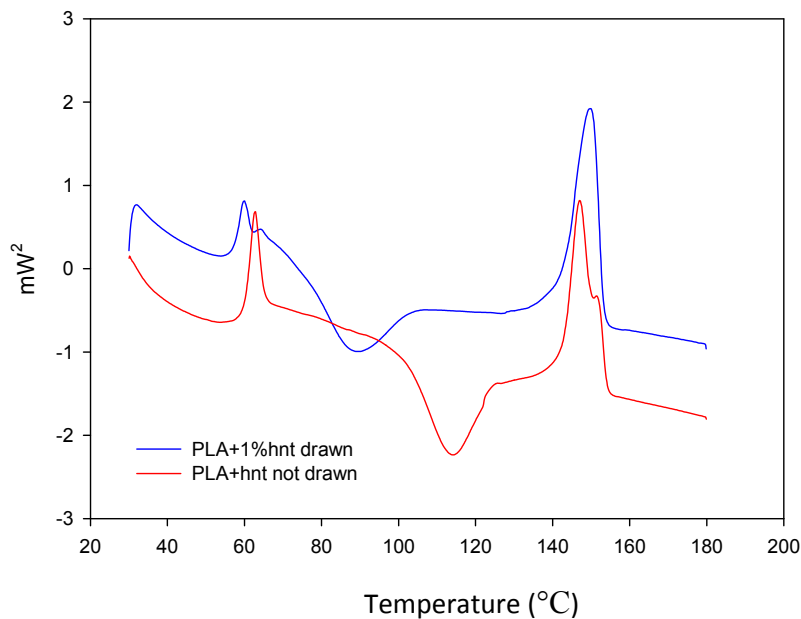


Diagram 1 shows the effect of clays on PLA-composites crystallinity. Not reinforced PLA films after unidirectional stretching show an increase in crystallinity up to 70% due to the effect of orientation. Oriented PLA films have a T_c around 108°C: 17°C lower than the T_c showed by not oriented PLA film, suggesting the obtained orientation of the amorphous phase induced by the unidirectional process. In figure are reported DSC curve for both not oriented PLA and oriented PLA films: the shift of T_c at lower temperatures, as well as the reduction of relaxation enthalpies are visible.

Fig.1: drawn and not drawn PLA first DSC scan.

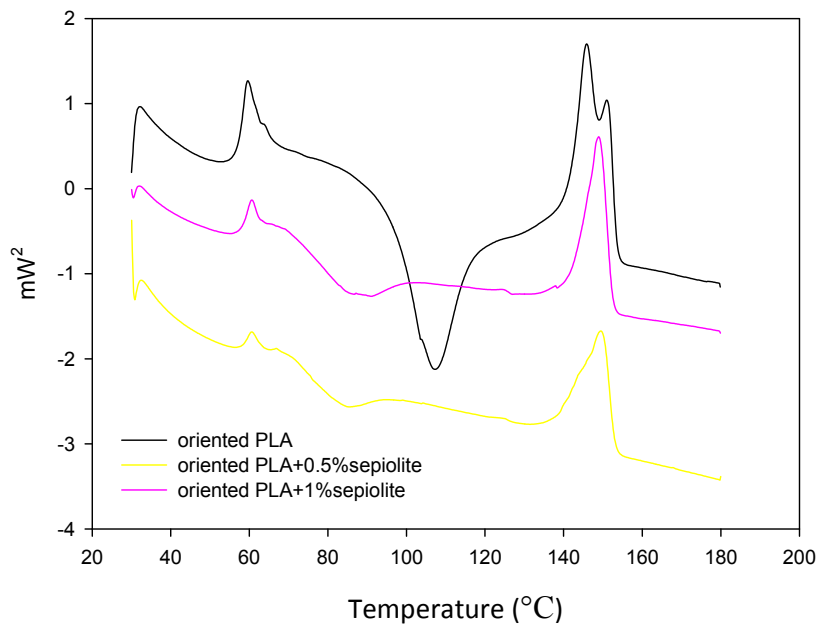


Presence of sepiolite leads to further increase in crystallinity and the reduction of T_c in presence of sepiolite is much more significant, leading to a T_c of 86.3°C for PLA+0.5% sepiolite film: 39°C less than the reported crystallization temperature for not oriented PLA and 22°C less than the reported T_c for oriented PLA films.

The strong effect on crystallinity showed by sepiolite is supposed to be a consequence of both the orientation of PLA macromolecules and alignment of sepiolite fiber that are also able to act as nucleating agent. This hypothesis is reinforced by the strong reduction of cold crystallization registered in presence of sepiolite and a possible explanation for this behaviour is the interaction between the polymer and the clay due to the hydrogen bonding between the carbonyl group of PLA and the hydroxyl group of sepiolite. Evidences of sepiolite alignment in the stretching direction, as well as the same kind of proof for halloysite, are showed in SEM pictures and are reported in pictures 1 (for halloysite) and 2 (for sepiolite).

In figures 2 is showed the DSC curve for PLA-sepiolite films confronted with curve of oriented PLA films.

Fig.2: PLA-sepiolite first DSC scansion



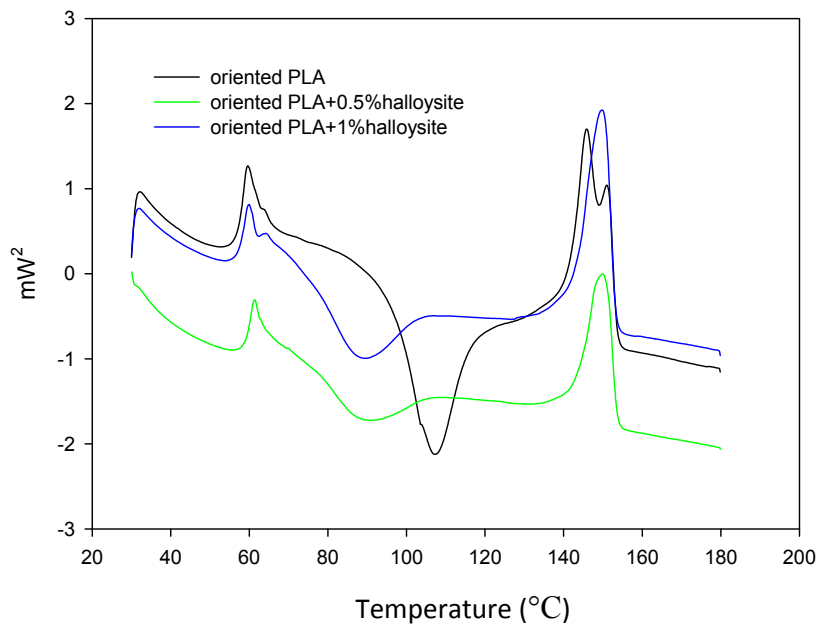
The presence of halloysite nanotubes also induces a reduction of T_c that shift of 20°C both for oriented samples at 0.5% and at 1% of clay.

As underlined before, pure PLA films after orientation show an increasing of crystallinity up to 66 % due to the only process. The addition of halloysite clay itself doesn't lead to a significant change in crystallinity, while, after orientation, the presence of clay influence strongly the crystallization behaviour of samples, enabling to achieve further increasing of crystallinity .

These results are explained in terms of increased fraction of oriented amorphous chains that lead to a reduction of the crystallization temperature.

In figures 3 is showed the DSC curve for PLA-halloysite films confronted with curve of oriented PLA films

Fig.3: PLA-halloysite first DSC scansion



As well as T_c decreases after drawing, also the relaxation enthalpy shows the same behaviour and both results are strongly influenced by the presence of clays. The hypothesis for this behaviour is believed to be the synergetic effect of orientation and clay shape.

Being orientation process used in this chapter a uniaxial orientation and being both sepiolite and halloysite clays characterized by an elongated shape in just one direction, it is likely to explain the enhanced crystallinity as a consequence of the orientation of sepiolite fiber and halloysite nanotubes in the orientation direction.

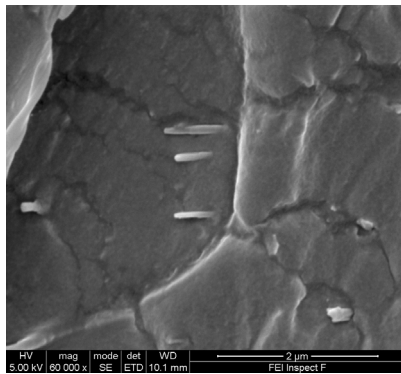
The presence of clay acting as nucleating agent seems to enhance the effect of orientation due to the intrinsic nucleating properties of clay that appears to be increase by the production method.

Comparing results obtained using annealing treatment in this thesis with the results reported in this chapter it is clear the strong effect of the process when combined to the presence of clay, probably due to the shape of used clays. Sepiolite and halloysite

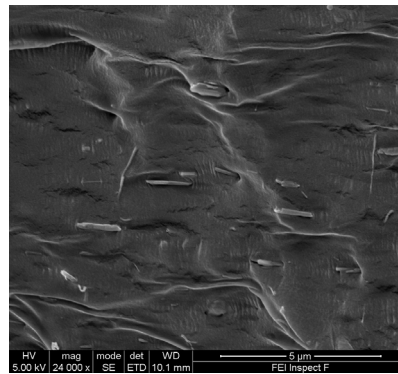
clay, because of their shape seem to be the perfect candidate for unidirectional processing.

In the following pictures, Pic.1 and Pic.2 are respectively reported SEM micrographics of PLA +0.5% sepiolite and PLA+0.5% halloysite. In both cases clays were found to be aligned in the direction of the unidirectional orientation. This fact can be a possible explanation for the increased crystallinity with respect to the unfilled PLA.

Pic.1 oriented PLA+0.5%halloysite



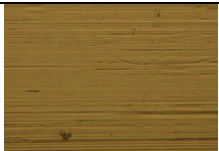

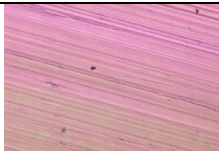

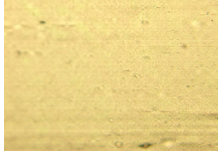







Pic.2 oriented PLA+0.5%sepiolite



Results of birefringence experiments are shown in pictures 3: samples identification and pictures taken at different angles under polarized and unpolarized light are shown. Stress and strain birefringence occurs due to external forces or deformation acting on materials that are not naturally birefringent.

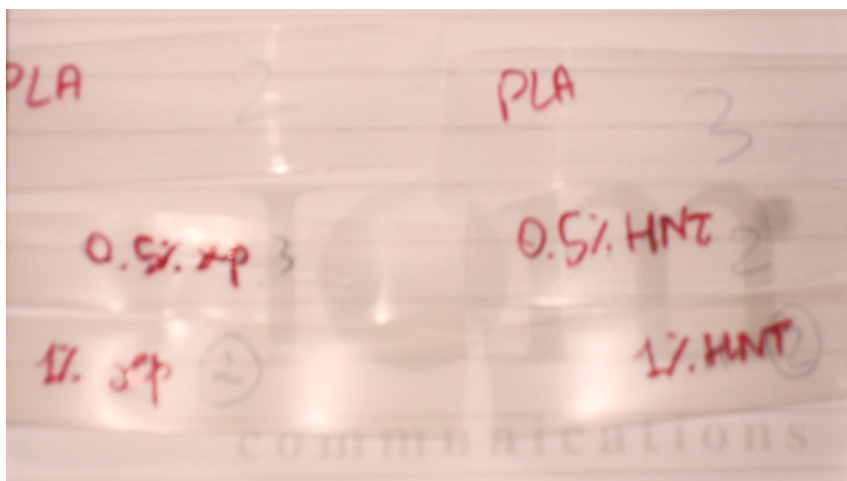
Birefringence is a phenomenon manifested by an asymmetry of properties. Films unidirectional oriented are anisotropic. From pictures 3 it is visible the effect of stretching on PLA films, that results to be oriented in the stretching direction. Presence of clays can lead to the loss of the achieved orientation, but this kind of negative effect was not obtained in the case of the composites analyzed in this study. Both PLA-sepiolite and PLA-halloysite reinforced samples maintained the alignment of the matrix chain in the stretching direction.

Pic.3: samples birefringence

	Polarized light			
Sample/angle	0	0	$\pi/4$	$\pi/2$
PLA				
PLA+0.5%halloysite				
PLA+0.5%sepiolite				

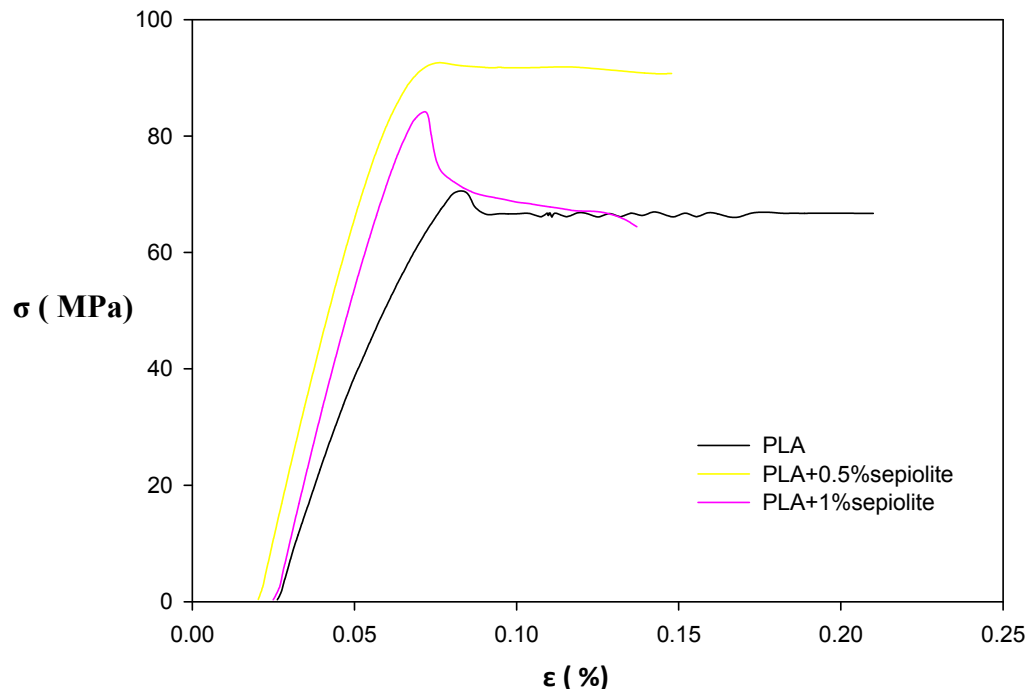
Translucency depends on degree of crystallinity as well as average size of dispersed phase and presence of agglomerates. As visible in picture 4, there is not a significant difference in the degree of transparency between oriented PLA-composites films and pure PLA films (both before and after drawing). Handling samples evidenced the presence of macroscopically visible aggregates that were observed at clay percentages of 0.5% and 1% wt of halloysite and sepiolite respectively: further investigation on the processing method have been planned to eliminate this deficiency.

Pic. 4: Samples translucency



In table 2, 3 and 4 are reported Young modulus and maximum stress for respectively PLA, drawn and not- drawn; drawn PLA-sepiolite samples and drawn PLA – halloysite samples. In figure 4 a typical stress-strain curve is reported.

Fig.4: sepiolite-PLA stress-strain curve



Tab.2: PLA mechanical properties before and after drawing.

Sample name	E (MPa)	σ (MPa)
PLA not drawn	1014 \pm 208	69.2 \pm 4
Drawn PLA	1583 \pm 131	70.0 \pm 3

Tab.3: sepiolite-PLA mechanical properties

Sample name	E (MPa)	σ (MPa)
Drawn PLA	1583 \pm 131	70.0 \pm 3
PLA+0.5sepiolite	1682 \pm 203	94.2 \pm 18
PLA+1%sepiolite	1129 \pm 244	76.1 \pm 5

Tab.4: halloysite - PLA mechanical properties

Sample name	E (MPa)	σ (MPa)
Drawn PLA	1583 \pm 131	70.0 \pm 3
PLA+0.5%halloysite	1018 \pm 324	67.5 \pm 4
PLA+1%halloysite	988 \pm 167	72.3 \pm 5

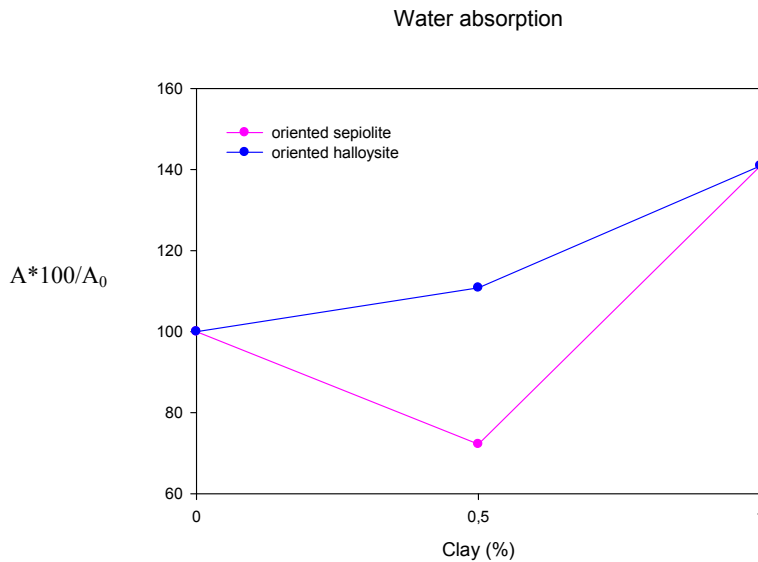
Molecular orientation strongly influences mechanical properties. As expected, the solid-state drawing process changes the mechanical performance of PLA. Young's modulus increases up to 56% for stretched PLA samples, while stress at break remains the same. Young's modulus increases of 6% while strength increase of 34% after drawing and addition of 0.5% of sepiolite. Inclusion of higher percentage of sepiolite leads to a reduction of mechanical properties due to the presence of agglomerates: differently from well dispersed sepiolite, aggregates will act as defect and stress concentration points.

Halloysite – PLA composites don't show significant change in mechanical properties in term of maximum stress, while there is a decrease in modulus that is attribute to the break of halloysite nanotubes during process and to the lack of dispersion, showed by all samples for clay percentage higher that 0.5%.

Stretching of unreinforced PLA increases Young modulus; drawing samples reinforced with 0.5% sepiolite leads to increase also the strength thanks to the presence of the clay that can act as reinforcement and that, as showed in pictures 2 , are aligned in the drawing direction. Enhanced mechanical properties and decrease of crystallization temperature are believed to be consequence of the increased fraction of oriented amorphous chains of PLA after stretching and of the synergetic effect induced by the aligned sepiolite clay.

Absorption tests were run to determine the effect of orientation, presence of clay and crystallinity on water absorption properties. Diagram 2 shows the ratio A/A_0 versus clay content, where A_0 is water absorption for non reinforced PLA

Fig. 4: A/A_0 versus clay content



Presence of halloysite results in increased water absorption: 0.5%wt of clay leads to an increment of around 10%; while at 1%wt of clay, the increase is more significant, corresponding to 40% more. A possible explanation for increased absorption is the nature/shape of the clay itself because of the presence of its internal hole and its lack of dispersion.

In the case of sepiolite, the presence of 0.5% of clay leads to a 30% decrease in the water absorption; while the trend is inverted when the amount of clay increases to 1%, leading to an increase corresponding to 40% more. The reduced absorption is believed to be an effect of the homogeneous dispersion of sepiolite, leading also to a significant increment in the crystallinity. On the other hand, the increased absorption in the presence of sepiolite at 1%wt can be related to the formation of clay aggregates.

Thermo gravimetric analysis was run to determine if the nominal and the actual amount of clays were consistent and whatever there were changes in the thermal stability on PLA after the addition of clays. It was found, like in the case of samples produced according to the procedure described in Chapter 3, that there were no

significant changes in the thermal stability of the composites if compared with the unreinforced material. The level of consistence of the nominal and the actual amount of clays in the composites were found to be very high.

6 Conclusions

Orientation increased PLA crystallinity and tensile strength. Stretching above T_g turned out in increased crystallization and chain relaxation, which resulted in increased modulus. DSC revealed that orientation also affected the chain relaxation of the amorphous PLA, resulting in

- 1) increased crystallinity as consequence of increased fraction of oriented amorphous chains;
- 2) reduction of the crystallization temperature.

Sepiolite addition leads to better mechanical properties and increased crystallinity thanks to the synergetic effect of alignment of sepiolite fibres that are also able to act as nucleating agent probably because of the interaction between the polymer and the clay due to the hydrogen bonding between the carbonyl group of PLA and the hydroxyl group of sepiolite. Percentages of clay higher than 1% led to the formation of aggregates that, acting as defect and stress concentration points, induce both reduction of mechanical properties and increase of water absorption.

Addition of halloysite leads to increased crystallinity, while mechanical and water absorption properties are strongly influenced by halloysite nanotubes rupture during process and formation of aggregates inducing increased water absorption and decreased mechanical properties.

Bibliography

- [1] Kwolek S.L MPW, Schaefgen JR, Gulrich LW *Macromolecules* 1977; 10:1390-1396
- [2]Peijs T, Jacobs MJN and Lemstra PJ. High performance polyethylene fibres. In Chou TW, Kelly A and Zweben C, editors.*Comprehensive composites*, Vol.1.Oxford: Elsevier science publisher Ltd, 2000.pp263-302
- [3] Ward IM. *Plastic, rubbers and composites* 2004;33:189-194
- [4] Capaccio G and Ward IM. *Nature-physics science* 1973;234(130):143-143
- [5]. Kokturk, G., Serhatkulu, T.F., Cakmak, M., and Piskin, E., Evolution of phase behavior and orientation in uniaxially deformed polylactic acid films, *Polym. Eng. Sci.*, 42, 1619, 2002.
- [6]. Lee, J.K., Lee, K.H., and Jin, B.S., Structure development and biodegradability of uniaxially stretched poly(L-lactide), *Eur. Polym. J.*, 37, 907, 2001.
- [7] Cicero, J.A., Dorgan, J.R., Garrett, J., Runt, J., and Lin, J.S., Effects of molecular architecture on two-step, melt-spun poly(lactic acid) fibers, *J. Appl. Polym. Sci.*,86, 2839, 2002.
- [8] Cicero, J.A., Dorgan, J.R., Janzen, J., Garrett, J., Runt, J., and Lin, J.S., Supramolecular morphology of two-step, melt-spun poly(lactic acid) fibers, *J. Appl. Polym. Sci.*, 86, 2828, 2002.
- [9] M. Van Es, *Polymer-Clay nanocomposites-the importance of particle dimensions*, PhD Thesis TU Delft 2001.
- [10] I. M. Ward, *Structure and properties of oriented polymers*, Chapman & Hall, London 1997.
- [11] T. Peijs, M. J. N. Jacobs, P. J. Lemstra, *Comprehensive Composites*, Vol. 1, T.-W. Chou, A. Kelly, C. Zweben, Eds., Elsevier Science, Oxford 2000, p. 263.
- [12] Bilotti E, Deng H, Zhang R, Lu D, Bras W, Fischer H R, Peijs T. Synergistic Reinforcement of Highly Oriented Poly(propylene) Tapes by Sepiolite Nanoclay *Macromol. Mater. Eng.* 2010, 295, 37–47

Chapter 6

Preliminary study of effect of temperature and draw ratio on PLA based film's crystallinity

Influence of different temperatures and draw ratios on PLA based film's crystallinity.

1 Introduction

A preliminary study on effects of different temperatures and draw ratio on PLA based film's crystallinity has been conducted in order to select the operative production condition for PLA-clay unidirectional stretched composites preparation.

Lee et coll. [1] have been studied effect of uniaxial drawing condition on PLLA samples reaching the conclusion that orientation in uniaxial stretched PLLA is influenced by drawing rate, drawing temperature and draw ratio and that spherulites under drawing can be deformed into new crystal morphologies.

The aim of this study is to produce PLA based films usable in food packaging application. Having PLA poor barrier properties, one of the biggest challenges of this thesis is to find a way of improving them.

It is generally recognize that orientation has a strong influence on gas barrier properties, thanks to the changed crystallinity level.

On the other side, it is important to remember that costumers like to see the product they are buying, especially when it is a food product, to be ensured about the food quality.

For this reason, level of transparency of PLA film played a significant role in the choice of drawing conditions.

The two criteria reported were used to select the operative production conditions: percentage of crystallinity and film transparency.

2 Preparation methods

PLA films were prepared extruding PLA pellets, dried overnight at 80°C, using extruder E20T Collin flat die connected to Flat-Film Take-Off Unit CR 72T. Produced films were immediately stretched using a Mono-Axial Stretching Units MDO-AT and MDO-BT. Extrusion and stretching conditions are reported below.

2.1 Extrusion Conditions:

Profile temperature (°C) as read from the feeder to the die: 150-160-180-180-165

Extrusion screw speed: 70 rpm

2.2 Flat-Film Take-Off Unit CR 72T using conditions:

Rolls temperature: 70 °C

Rolls speed: 3rpm

Collecting speed: 4rpm

2.3 Stretching conditions:

Different drawing conditions and draw ratio were used to study both the effect of temperature and draw ratio on PLA crystallinity. Used stretching conditions are reported in table 1.

3 Characterization: Thermal tests

PLA films produced under different conditions were tested using DSC METTLER to determine the percentage of the crystalline content.

In table 1 are reported sample name and crystallinity, while in picture 1 and 2 it is possible to see the different level of transparency of PLA based films changing temperatures and draw ratio.

Table 1: sample ID, drawing condition, X_c (%)

Sample name	Temperature Units MDO-BT (°C)	Temperature Units MDO-AT (°C)	Draw ratio	X_c (%)
70/90 1	70	90	1	11.22
70/90 2	70	90	2	24.11
70/90 3	70	90	3	30.37
90/70 1	90	70	1	3.15
90/70 2	90	70	2	6.13
90/70 3	90	70	3	31.09
90/70 3.5	90	70	3.5	33.34
90/80 1	90	80	1	3.22
90/80 2	90	80	2	31.70
100/70 1	100	70	1	3.17
100/70 2	100	70	2	30.83
100/70 3	100	70	3	32.57
100/70 3.5	100	70	3.5	33.51
100/70 4	100	70	4	33.94

Fig. 1: level of transparency as function of DR and temperature

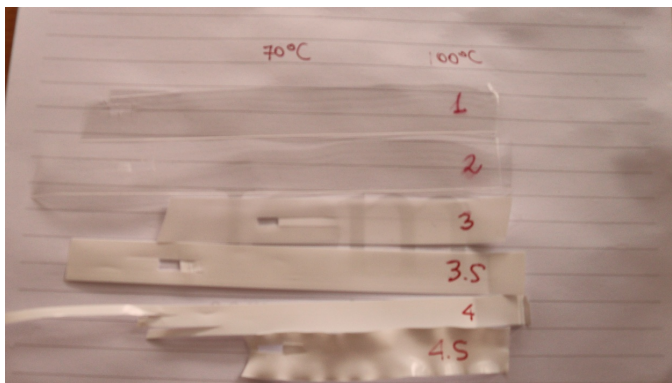
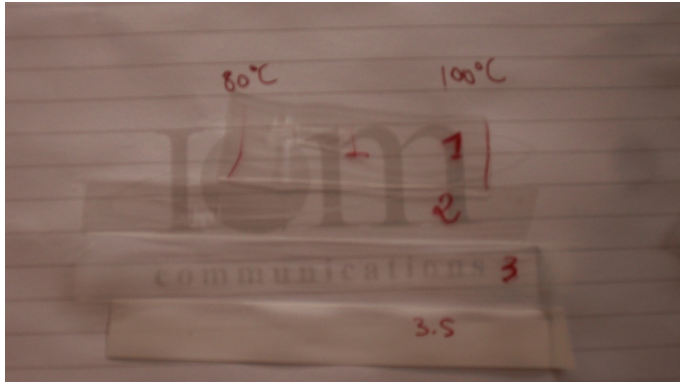
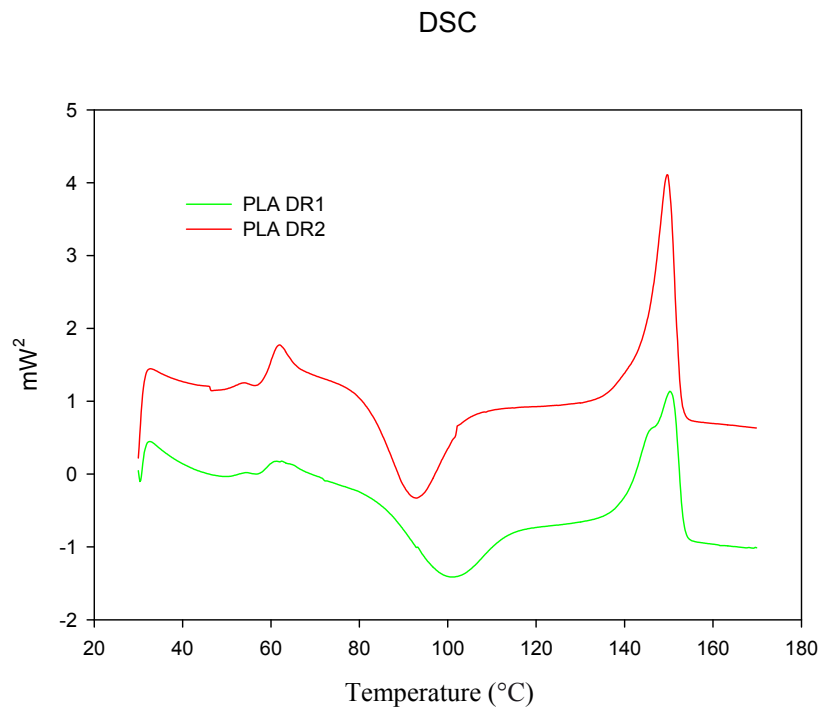


Fig. 2: level of transparency as function of DR and temperature



In figure 3 is reported DSC curve for not stretched PLA and PLA stretched using a draw ratio of 2 using a temperature of 70 °C for Units MDO-AT and a temperature of 90°C for Units MDO-BT.

Fig. 3: DSC diagram for PLA stretched at DR=1 and DR=2



4 Comments

The choice of final drawing conditions was done on the basis of increased crystallinity and film transparency: all films prepared in chapter 5 were produced using a draw ratio of 2 and setting the temperature at 70°C for the first roll and 90°C for the second.

In any case, draw ratios higher than 3 lead to the loss of transparency. Being the aim of this thesis the production of material for food packaging, the loss of transparency has been considered as a negative effect of the orientation and all opaque samples were discarded.

Samples prepared using 70 °C for MDO-BT and 90°C for MDO-AT presented discontinuity in the transparency of the material and they were not considered for further investigation because of the lack of reproducibility of tests run on them.

Samples prepared using 80 °C for MDO-AT and 100°C for MDO-BT as well as samples produced using 70 °C for MDO-AT and 100°C for MDO-BT were not considered for further uses because of difficulties in producing under these conditions due to the higher temperatures involve in the process.

T_g values remain unvaried independently from the drawing temperature and draw ratio.

It was also noticed that increasing the draw ratio the cold crystallization peak shifts to lower temperature and for draw ratio higher than 3 it disappears because of the increase fraction of oriented amorphous chains.

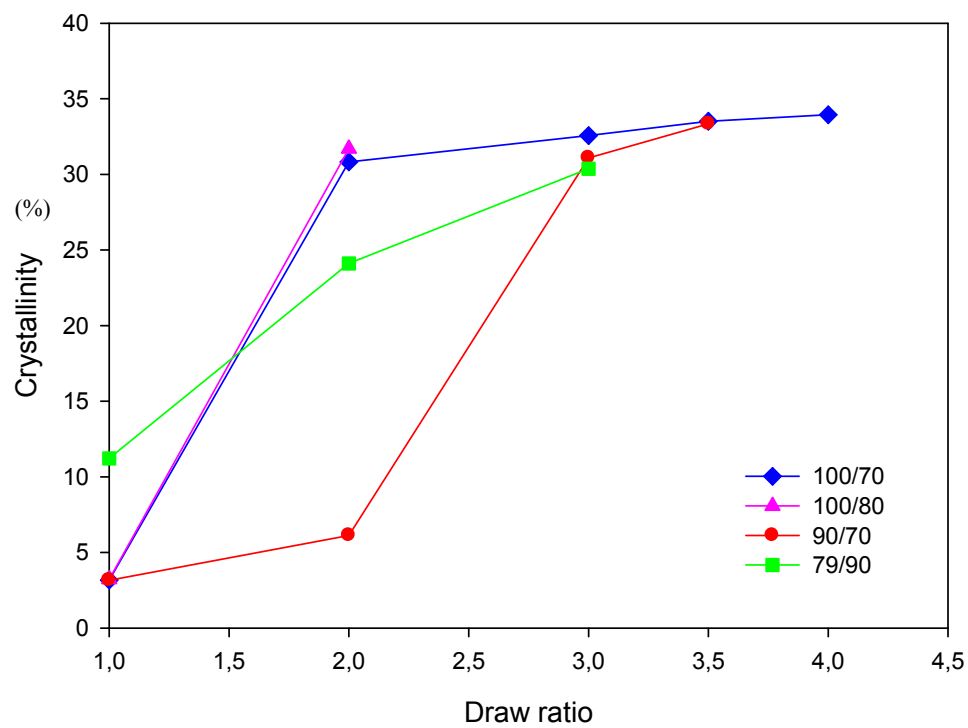
Chosen temperatures of production were 70 °C for MDO-AT and 90°C for MDO-BT due both to the easiness of production and to the high homogeneity of produced samples.

Considering the different percentage of crystallinity achieved and the correspondent transparency, the final choice was done in favour of samples produced at a draw ratio of 2: for this draw ratio produced films are still transparent and the percentage of crystallinity has increase of about 100%.

In figure 4 is reported percentage crystallinity versus draw ratio for all the four used temperature conditions. In each case, increased draw ratio leads to increased

crystallinity. Temperature effect is stronger at lower draw ratio: at draw ratio higher than 3 it is possible to notice a levelling out of the obtained percentage value of crystallinity.

Fig. 4: crystallinity versus draw ratio



5 Conclusions

A preliminary study on effects of different temperatures and draw ratio on PLA based film's crystallinity was conducted in order to select the operative production condition for PLA-clay unidirectional stretched composites preparation. PLA crystallinity percentage was affected by both temperature and draw ratio conditions. PLA crystallinity level was found to increase with draw ratio, while T_c decreased until it disappears for draw ratio bigger than 3 as a consequence of the increased fraction of oriented amorphous phase. Effect of temperature was found to affect PLA crystallinity especially at low draw ratio: at draw ratio higher than 3 it is possible to notice a levelling out of the obtained percentage value of crystallinity that have a limit around 30% of crystallinity.

Bibliography

[1] Lee, J.K., Lee, K.H., and Jin, B.S., Structure development and biodegradability of uniaxially stretched poly(L-lactide), *Eur. Polym. J.*, 37, 907, 2001.

Chapter 7

Physical properties of PLA blown films containing halloysite nanotubes

Physical properties of PLA blown films containing halloysite nanotubes

1 Materials

PLA2002D was used as matrix and halloysite from sigma Aldrich was used as reinforcement. Their specifics are reported in chapter 3.

2 Preparation of PLA/HNT composites

PLA-halloysite composites at 0.5, 1 and 3 wt % were obtained from master-batch containing 15wt% of the clay. PLA pellets and powders were dried overnight at 80°C before extrusion. Nanocomposites were prepared via melt compounding using a twin extruder Polylab Haake ptw 24/40 with an attached cooling bath.

After extrusion, pure PLA and PLA/HNTs composites were dried again overnight at 80°C to remove moisture absorbed during the pelletizing process, then they were extruded in a COLLIN single screw extruder coupled with COLLIN TEACH LINE BL50T. Pure PLA was produced under the same conditions with the purposed to be compared with nanoclay composites.

Extrusion and film blowing conditions are reported below:

Extrusion conditions:

Temperature profile (°C): 140 -150-155-160-175-175-160-160-160

Screw speed (rpm) = 60

Feed rate (rpm) = 30

Film blowing conditions:

Profile temperature (°C): 165-180-180-200-210

Screw speed (rpm): 20

Nip rolls speed (rpm): 7.2

Blow-up ratio (BUR) was set at 2 controlling the air pressure in the bubble, allowing the production of a bubble of an average film thickness of 0.030mm. In table 1 samples name and description are reported.

Tab.1: Samples name and description

ID	Amount of clay (%)	Preparation process
neat PLA	0	None
0%HPLA	0	Extruded
0.5%HPLA	0.5	Extruded
1%HPLA	1	Extruded
3% HPLA	3	Extruded

3 Characterizations

3.1 TGA and DSC were run according to the procedures described in chapter 3 paragraph 4.

3.2 Mechanical tests

Tensile tests were conducted either in the take up either in the radial direction to analyze the influence of the biaxial orientation on mechanical properties of PLA/HNTs films. Specimen with planar dimensions of 80x10 mm² and a gauge length of 50.0mm were tested at room temperature using a strain rate of 5mm/min. At least five samples were tested for each type of films.

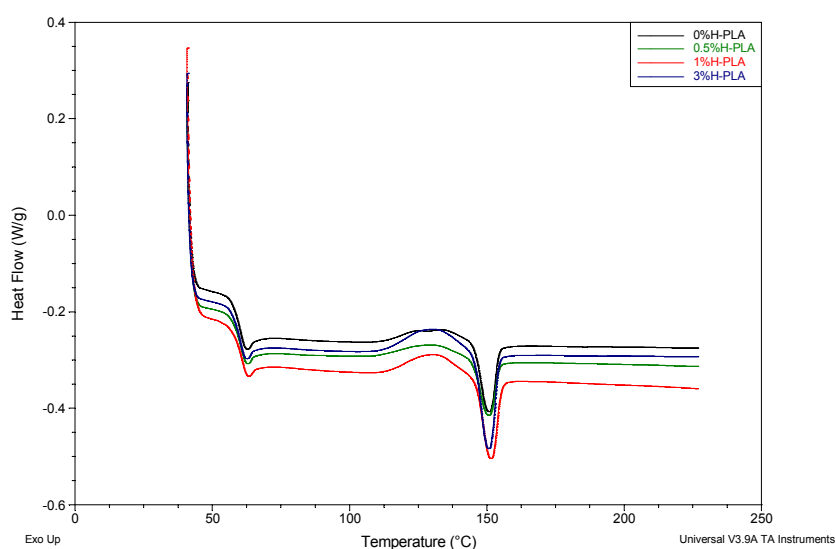
3.3 Rheological Analysis

Rheological analyses were performed in a ROSAND Advanced Capillary Rheometer RH7 to obtain information on property-structure of material and its processability by measuring viscosity as function of shear rate, in the range of 50 -104 s⁻¹.

4 Results

First DSC scan is showed for PLA-HNTs nanocomposites at each percentage of clay in figure 1; while the relative glass transition, crystallization and melting temperatures, their respective enthalpies and the degree of crystallinity of the polymers are reported in table 2. The crystalline level was calculated as the difference between the melting and crystallization enthalpies, considering the melting enthalpy of 100% crystalline polylactide as 93.1 J/gm.

Fig 1: First DSC scansion for PLA-HNT composites



Tab.2: sample ID, T_g , T_c , T_m and X_c

ID	T_g (°C)	T_c (°C)	T_m (°C)	X_c (%)
neat PLA	60.2	133.3	151.5	1.5
0%H-PLA	57.2	121.9	149.0	2.4
0.5%H-PLA	57.9	125.2	150.0	3.5
1%H-PLA	59.1	124.9	150.7	4.2
3%H-PLA	56.4	122.2	149.0	5.3

Generally, the addition of clays is reported to enhance crystallinity and reduce T_c as a consequence of clays' nucleating effect. In the case of the clay used in this preliminary study, there is some evidence of this kind of effect. Crystalline content linear increased with clay percentage because of HNTs ability to act as nucleating agents, but no changes in T_g , T_c and T_m are reported as a consequence of the addition of the clay. It is also interesting to underline that the process itself is able to increase the crystallinity level of the matrix as a consequence of the achieved orientation that is able to increment the fraction of oriented amorphous chains: after film blowing, PLA crystallinity increased of 60%.

Mechanical properties are strongly related to crystallinity level.

Tables 3 summarize the Young modulus, tensile strength and elongation at break of PLA composites both in the take up and blowing direction; while figure 2 and 3 show respectively the stress- strain curve for pure PLA and PLA/HNT composites in the take up and in the blowing directions.

Tab 3: Young modulus, tensile strength and elongation at break of PLA composites in the take up and blowing direction

Take up direction				Blowing direction		
ID	Tensile modulus (MPa)	Tensile strength (MPa)	Elongation at break (%)	Tensile modulus (MPa)	Tensile strength (MPa)	Elongation at break (%)
0%H-PLA	1696±220	24±6	9±3	1788±502	24±4	6±3
0.5%H-PLA	1583±250	25±3	4±1	1667±247	23±5	6±1
1%H-PLA	1856±214	25±1	3±1	1765±150	23±3	3±1
3%H-PLA	1934±176	29±2	5±1	1934±176	34±5	6±2

Fig 2: Stress-strain curve in take- up direction

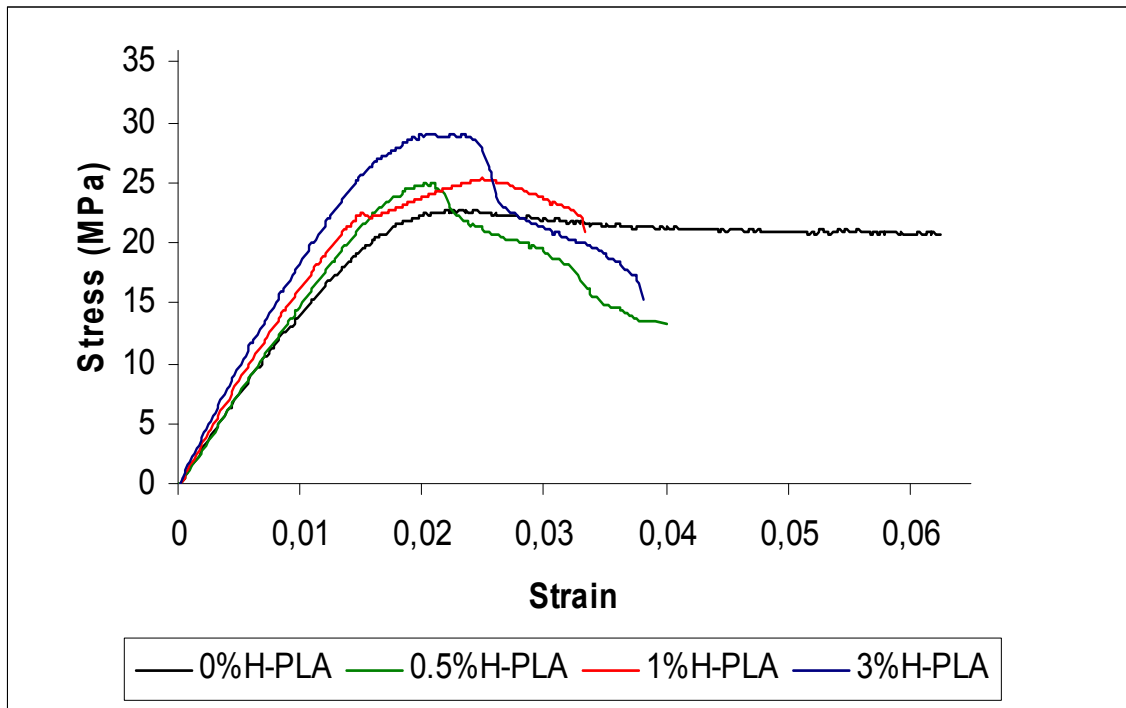
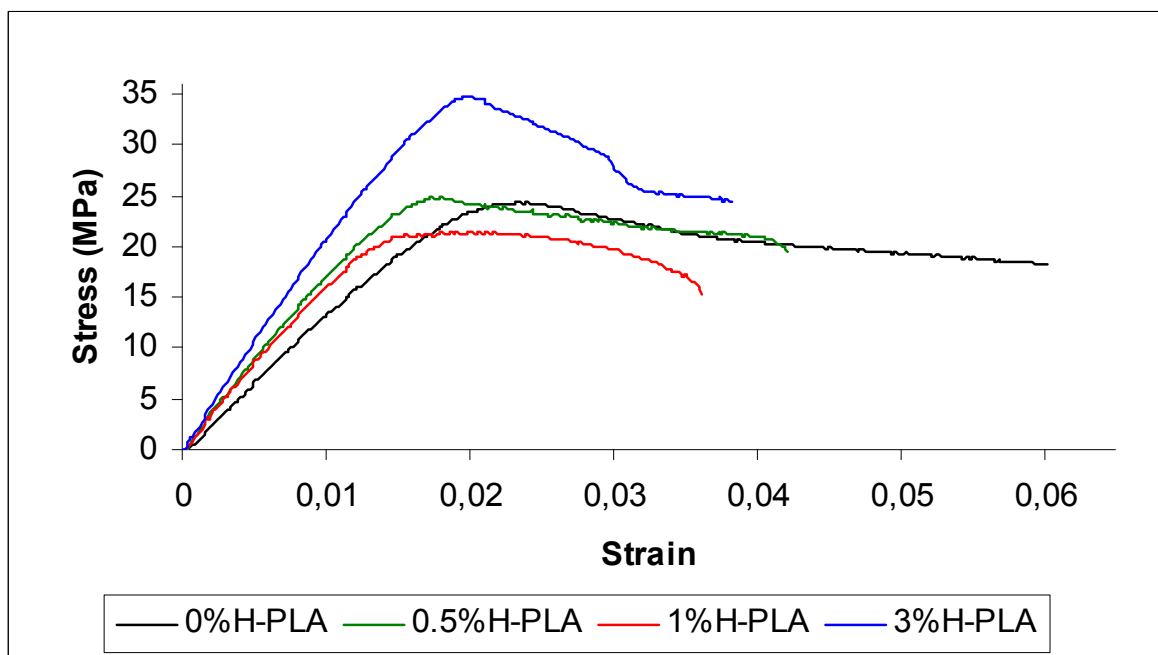


Fig 3: Stress-strain curve in blowing direction



The polymer exiting the tubular die of film blown machine was subjected to a couple of external forces: one associated to the take -up of the film for the collection and the other caused by internal air pressure which forces it to expand in the radial direction.

Mechanical properties of the film will be similar in both TD and BD only if the combination of these two forces gives predominant orientation at 45° [1].

Molecular orientation strongly influences mechanical properties and leads to increase also the strength thanks to the presence of the clay that act as reinforcement. Enhanced mechanical properties and decrease of crystallization temperature are believed to be consequence of the increased fraction of oriented amorphous chains of PLA after stretching.

Introduction of nanoclay is often reported to be a way of improving polymer thermal stability. Increased thermal stability is attributed both to clay's good thermal stability and to the interaction between clay and polymer [2-4].

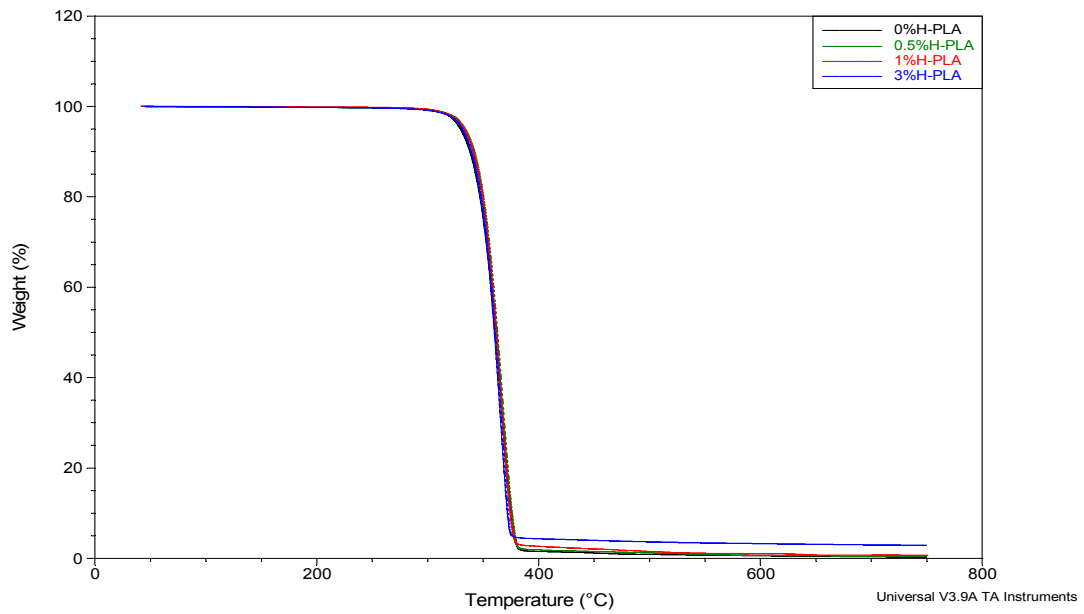
Ogata et al [5] reported that clays seem to retard the deformation of PLA composites' crystalline structure at low temperature, while they can act as deformation accelerator at higher temperature.

Thermogravimetric analyses were conducted both in order to determine if there was correspondence between the nominal and the actual percentile amount of clay and to analyze the effect of the presence of the inorganic filler on the thermal stability of the matrix.

Table 4 shows 10% weight loss temperatures, temperature at the maximum rate of weight losses T_{mwl} and residual at 750°C for pure PLA and PLA-HNTs composites, while their thermogravimetric curves are shown in fig.4.

Clay addition on PLA doesn't lead to any change in PLA thermal stability, probably because of the bad interfacial adhesion between clay and polymer due to the absence of compatibilization between them. Nominal and actual weight percentage of were found to be highly correspondent.

Fig 4: PLA- halloysite composites thermo-gravimetric curves



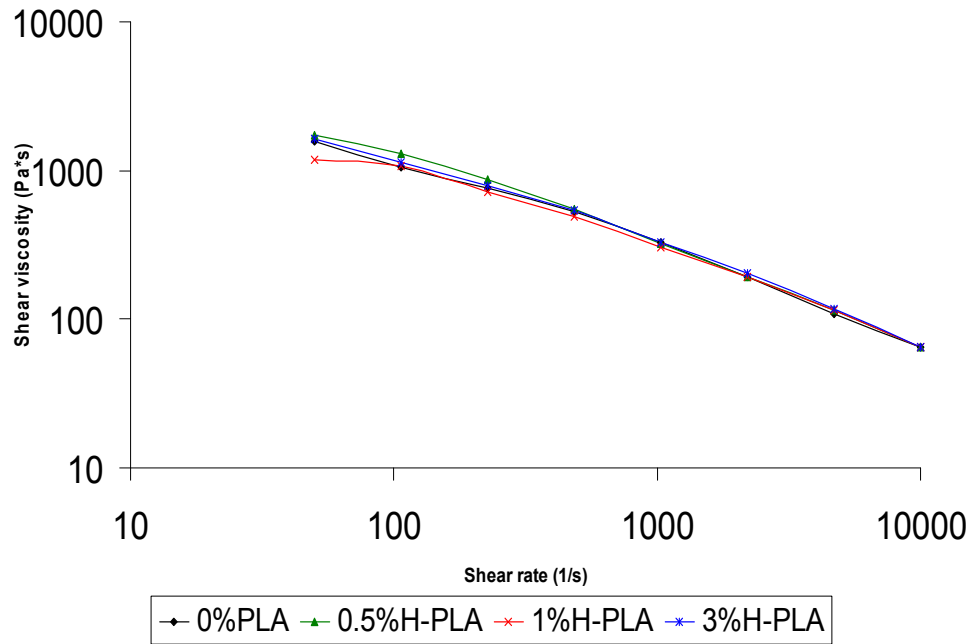
Tab 4: samples ID, onset degradation temperature and residual

ID	T _{-10%} (°C)	T _{mwI} (°C)	Residual at 750°C (%)
0%H/PLA	337.4	364.9	0
0.5%H/PLA	342.2	365.9	0.4
1%H/PLA	341.6	364.9	0.6
3%H/PLA	339.3	364.9	2.8

In figure 5 are reported shear viscosity versus shear rate for extruded PLA and PLA/HNTs composites.

Viscosity of 0%H-PLA, used as reference material, and PLA/HNTs composites decreased with the increasing of shear rate.

Fig 5: shear viscosity versus shear rate



PLA rheological behaviour is not affected by the presence of the clay: no significant variations are reported in PLA composites melt strength neither in their viscosity and shear thinning.

Permeability tests were run on pure PLA and PLA reinforced with 1 and 3% -wt of HNTs. Addition of 1%HNTs on PLA matrix lead to a decrease both in oxygen and carbon dioxide permeability respectively up to 34 and 45% as consequence of increased tortuosity induced by the presence of the clays. Concentrations of clays higher than 1% lead to a strong increase in permeability, probably due to the presence of aggregates leading to the formation of imperfection in the structure. Table 5 shows the Oxygen and CO₂ permeability versus clay percentages.

Tab. 5: Oxygen and CO₂ permeability versus clay percentages

Sample name	Oxygen permeability [(cm ³ (STP)*cm)/cm ² *s*atm]	CO ₂ permeability [(cm ³ (STP)*cm)/cm ² *s*atm]
0%H-PLA	2.61 e ⁻⁰⁹	9.36 e ⁻⁰⁹
1%H-PLA	1.72 e ⁻⁰⁹	5.13 e ⁻⁰⁹
3%H-PLA	1.02 e ⁻⁰⁸	4.94 e ⁻⁰⁸

5 Conclusions

The addition of clay was reported to significant affect crystallinity. Crystallinity increased with the percentile weight of clay during film blowing, but not changes are reported on melting, glass transition and crystallization temperature because of the low interaction between halloysite nanotubes and PLA. Rheological properties were not affected by the presence of the clay as a consequence of the lack of dispersion of the clay and the bad interfacial interaction determined by the absence of compatibilization between clay and polymer. Oxygen and carbon dioxide permeability decrease in presence of 1%-wt of clay, while higher amount of clay, because of the massive presence of agglomerates, lead to an increase of the permeability. Tensile strength at break and Young modulus were found to increase with clay amount in both in the take up and blow direction as a consequence of the orientation process and of the reduced amorphous phase. Similar results were achieved in both directions as a consequence of the 45° predominant orientation of the couple of forces to which the polymer is subject during film blowing.

Bibliography

- [1] Influence of carbon nanotubes on the properties of films of polypropylene prepared by film blowing, F.Iannace
- [2] Zhu ZK, Yang Y, Wang X, Ke Y, Qi Z.J Appl Polym Sci 1999;3:2063
- [3] Petrovic XS, Javni L, Waddong A, Banhegyi GJ. J Appl Polym Sci 2000;76:133
- [4] Fisher HR, Gielgens LH, Koster TPM. Acta Polym 1999;50:122
- [5] Ogata N, Jimenez G, Kawai H, Ogihara T. J Polym Sci, Part B: Polym Phys 1997;35:389

Chapter 8

Conclusions

Conclusions

PLA-sepiolite and PLA-halloysite nanocomposites prepared by melt blending were systematically characterized in terms of mechanical, thermal and barrier properties.

Annealing and unidirectional stretching techniques were used with the aim to improve matrix performances of nanocomposite based films; a preliminary study on the production of PLA-halloysite composites via film blowing has been also considered.

Addition of unmodified clays did not significantly alter PLA properties mainly because of the lack of an adequate filler-matrix interface due to the absence of compatibilizer between polymer and reinforcements that limited clays effect as nucleating agents.

Instead matrix crystallinity, mechanical and barrier properties resulted to be strongly affected by physical aging and orientation. Annealing and orientation are reported to be dominant over clay addition: only slight variations are reported to occur in presence of clay after these treatments.

Fiber-like clays application in unidirectional orientation process led to important improvements in samples properties: different processing conditions will be considered for further investigation in order to additional improve films properties.

Good results were obtained especially after unidirectional stretching: increased crystallinity, improved mechanical properties and reduced water absorption were achieved in presence of only 0.5%-wt of sepiolite. Further investigation will take place to systematically study the effect of different stretching conditions on PLA-sepiolite samples.

More exhaustive information about the achieved results and conclusions are reported below.

PLA annealed composites reinforced with sepiolite and halloysite

In this work, it was demonstrated that good dispersion of clays can be obtained for filler loadings up to 3wt%, especially for sepiolite /PLA composites. These latter formulations are favoured by chemical interaction occurring between PLA and sepiolite and are related to the hydrogen bonding between carbonyl groups of PLA and hydroxyl groups of sepiolite. Sepiolite maintained its geometry throughout the processing regime while the halloysite nanotubes fractured during processing.

Generally samples showed a good transparency especially in the case of sepiolite based ones. An exception was offered by inclusion of halloysite nanotubes in which case higher is the filler concentration more pronounced is the cloudiness of the produced films.

Absence of crystallization peak after annealing treatment for clay percentage higher than 0.5% showed that the clays act as nucleating agent as confirmed by crystallinity measurements. Annealing treatments, as expected, have a strong effect on PLA matrix, leading to a significant increase in crystallinity for both PLA and PLA-composites as a consequence of the reduced free volume of the matrix.

Changes in mechanical properties were not significant in presence of clays. In this case, annealing treatments induced a slight variation in the Young's and yield strength, while its effect on hosting matrix led to a significant enhancement on tensile strength.

Absorption tests showed that the inclusion of sepiolite is able to allow lower values of water absorption with respect to the addition of halloysite nanotubes.

Overall, presence of the fillers in the polymer decreased diffusion coefficients compared to neat PLA by inducing a more tortuous path for the diffusing gas molecules.

Annealing was demonstrated to be an efficient treatment to increase modulus and tensile strength as consequence of reduced free volume and increased crystallinity of the polymeric matrix.

PLA annealed composites reinforced with zeolite and bentonite.

Zeolite – PLA and bentonite-PLA composites properties were strongly influenced by the presence of aggregates even for samples at the lowest percentage of reinforcements as showed by SEM analysis. Cracks initiate and propagate in areas where the aggregates are present. Both zeolite and bentonite composites, during tensile tests, break in the regions of the macroscopically visible aggregate and this effect seemed to be independent from the percentage of clay and annealing treatment. Composites crystallinity increased while T_c decreased with clay percentage both for zeolite-PLA and bentonite-PLA samples. This trend is reported also for annealed samples, but it is enhanced by the physical aging process that lead to much higher crystallinity. Calorimetric results evidenced that annealing treatment can be dominant over clay nucleating ability. Zeolite-PLA and bentonite-PLA composites behavior has been explained in term of lack of dispersion. Also in this case, the formation of aggregates has been attributed to the intrinsic nature of clays. Natural clay zeolite and bentonite were therefore not considered for further investigations as PLA reinforcing agents.

Preliminary studies on drawing conditions

A preliminary study on effects of different temperatures and draw ratios on PLA based film's crystallinity was conducted in order to select the optimal operative production conditions for PLA-clay unidirectional stretched composites preparation. PLA crystallinity percentage was affected by both temperature and draw ratio conditions. In particular, PLA crystallinity level was found to increase with draw ratio, while T_c decreased until it disappears for draw ratio bigger than three as a consequence of the increased fraction of oriented amorphous phase. Effect of temperature was found to affect PLA crystallinity especially at low draw ratio: at draw ratio higher than three it is possible to notice a levelling out of the obtained percentage value of crystallinity that have a limit around 30% of crystalline

Unidirectional stretching of PLA-sepiolite and PLA- halloysite composites

Orientation strongly increased PLA crystallinity and tensile strength. Stretching above T_g turned out in simultaneous crystallization and chain relaxation, which

resulted in increased modulus and toughness. Orientation also affected the chain relaxation of the amorphous PLA, resulting in

- increased crystallinity as consequence of increased fraction of oriented amorphous chains;
- reduction of the crystallization temperature.

Sepiolite addition led to better mechanical properties and increased crystallinity thanks to the synergetic effect of alignment of sepiolite fibers that were also able to act as nucleating agent probably because of the interaction between the polymer and the clay due to the hydrogen bonding between carbonyl groups of PLA and hydroxyl groups of sepiolite. Percentages of clay higher than 0.5% led to the formation of aggregates, reducing mechanical properties and increasing water absorption. Addition of halloysite led to increased crystallinity, while mechanical and water absorption properties were strongly influenced by the failure of halloysite nanotubes during process and formation of aggregates.

Film blowing

The addition of clay was reported to significantly affect crystallinity that increased with the wt% of clay during film blowing, but no changes are reported on melting, glass transition and crystallization temperature because of the low interaction between halloysite nanotubes and PLA. Rheological, oxygen and carbon dioxide barrier properties were not affected by the presence of the clay as a consequence of the lack of dispersion of the filler. Tensile strength at break and Young modulus were found to increase with clay amount in both the take up and blow direction as a consequence of the orientation process and of the reduced amorphous phase. Similar results were achieved in both directions as a consequence of the 45° predominant orientation of the couple of forces to which the polymer is subject during film blowing.

Appendix 1

Instrument description

Haake ptw 24/40

Haake ptw 24/40 is a 24 mm twin-screw extruder line [1]

Technical characteristic, tab. 1 [1]

Screw diameter	24 mm
L/D	40
Screw setup	Variable
Gear ratio	1:2
Rotating direction	Co
Max. Temperature	350°C
Max. pressure	100 bar
Max. Torque	180 Nm
Heating zones	10

Fig. 1, Haake ptw 24/40 [1]



Strand Pelletizer Type CSG 171 T, Collin

Pelletizer Type CSG 171 T consists of a granulating unit with a pair of draw-in rolls, guide unit, stationary cutter and rotating fly cutter [2]. This instrument switches off immediately when the front door is opened [2].

Fig.2, Strand Pelletizer CSG 171 T [2]



Film Blowing Unit BL50 T

The take-off unit is centrally positioned on the substructure with the collapsing frame, which is attached to the central pillar and whose height can be adjusted. Electrical and pneumatic systems are located in the bench-top housing with the fan for cooling off the film bubble. The pressure between the nip rolls is controlled pneumatically [2].

Technical characteristic, tab. 2 [2]

Nip roll diameter	50mm
Nip roll width	200 mm
Max. lay flat width	170 mm
Max. bubble diameter	110 mm
Adjustable take-off height, above die	350 - 750 mm
Max. tensile force	250 N
Take-off speed	1 - 12 m/min

Fig. 3, Film Blowing Unit BL50 T [2]



Single-Screw Extruder E 20 T, Collin

Barrel and the screw are made of nitrided steel. The barrel is heated by three heating zones, two of which operate with air cooling. A quick-release hopper facilitates material changes and cleaning. The unit is equipped with a water-cooled feed section [2].

Technical characteristic, tab. 3 [2]

Screw diameter (mm)	20
Screw length (mm)	25
Drive power kW	1,5
Screw speed 1/min.	18 – 180
Maximum throughput kg/h	4
Connected load kW	7,4
Central height of screw mm	355

Fig. 4, Single-Screw Extruder E 20 T



Flat film take - off unit CR72T, Collin

Combined calender flat-film system is made of a three-roll unit with a central fixed roll, an upper adjustable smoothing roll and a lower cooling roll. The polishing roll can be moved pneumatically. Adjusting the gap it is possible to produce smooth sheets, to calendar films or to produce laminates. Rolls surfaces are chromium plated and polished.

Rolls are of double-jacket design for exact temperature control using fluid heating-cooling units [2].

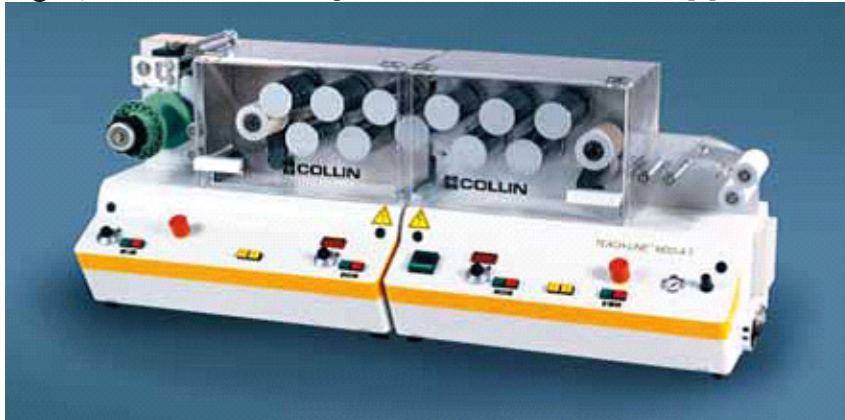
Fig.5 Flat film take - off unit CR72T



Mono-Axial Stretching Units MDO-AT and MDO-BT, Collin

By mono-axial stretching the physical properties of polymers can be drastically changed, widening the range of applications: mechanical properties, like tear strength, optical behaviour and barrier effect against vapor or gases can be changed. A modular system has been developed for the mono axial stretching of film, strap or monofilament consisting of cooling systems for the primary product, holding back godet MDO-AT, different types of heating zones, and take-off godets with winder, Type MDO-BT.

Fig. 6, Mono-Axial Stretching Units MDO-AT and MDO-BT [2]



Extruder ZK 25, Collin

Technical characteristic, tab. 4 [2]

Screw diam.	25 mm
Screw length	18 x D (3 x 6 D)
Drive power	2,5 kW
Screw speed	5 - 200 rpm
Screw torque	2 x 44 Nm

Fig.7 Extruder ZK 25[2]



Bibliografy

[1] www.asi-team.com/asi%20team/haake/haake%20data/HAAKE_Polylab_OS.pdf

[2] www.drcollin.de